Politecnico di Torino

Corso di Laurea Magistrale in Ingegneria Energetica e Nucleare
'Renewable Energy Systems'
A.a. 2020/2021
Sessione di Laurea: Ottobre 2021

A coupled system for electrochemical capture and conversion of CO_2 into syngas

Relatori:
Prof. Fabrizio Pirri
Prof. Massimo Santarelli
Dr. Adriano Sacco

Candidato:
Angelo Pettigiani

Sommario

Abstract 3
1. Climate change 4
1.1 Greenhouse effect 5
1.2 CO_2 gas data 10
2. The mitigation challenge 18
2.1 Policies 22
2.2 Age of fossil source 24
2.3 Future ideas 28
3. CO_2 Capture 31
3.1 Emissions 32
3.2 Compression – Transportation 33
3.3 Final uses 35
3.3.1 A new idea 37
3.4 Purpose of the thesis 39
4. Theoretical CO_2 capture phase 42
4.1 Thermodynamic 43
4.2 Results 50
4.3 Discussion 54
4.4 Energy penalty 59
5. Electrodialysis system 61
5.1 Operation 62
5.1.1 Instrumentation 68
5.2 Optimization 69
5.2.1 Effect of current 70
5.2.2 Effect of flow rate 72
5.2.3 Effect of electrolyte concentrations 74
5.3 Results 76
6. Continuous CO_2 capture 82

6.1 Operation 82
6.2 Optimization 84
6.2.1 Interpolation 88
6.2.2 Typical test 89
6.2.3 Stability test 93
6.3 Flue gas simulation 94
7. CO_2 reduction 97
7.1 Electroreduction cell 97
7.1.1 Parameters 100
7.1.2 Functioning test 102
7.2 Coupled system 103
Conclusions 110
Ringraziamenti 114
Bibliography 115

Abstract

As the 21st century progresses, the problem of global warming becomes more and more pressing on our planet. In this regard, the proposed thesis sets itself the initial objective of highlighting this phenomenon to the reader, probing the numbers, the relations between temperature and climate-changing gas emissions (GHG) and the effects of humanity, which prompted the concentration of CO_2 in the air over 400 ppm. Subsequently, the concept of problem mitigation is proposed to the reader, analyzing different aspects such as the carbon lock-in, the policies currently in place to limit the temperature increase beyond 2°C, and the possible solutions. In particular, one of the possible solutions is investigated, namely the capture of CO_2 - the most present greenhouse gas in the environment. It consists in removing this gas either from the exhaust gases resulting from combustion or from the atmosphere. the experimental part of the thesis is divided in three parts. Firstly, the thermodynamics governing the process is analyzed, which requires a minimum energy in the order of 5-6 kJ per mole of CO_2 captured by exhaust gases and 20-21 kJ per mole of CO_2 if captured from the atmosphere. The second part is constituted by the study and experimentation of an electrochemical capture system, based on the electrodialysis of $NaHCO_3$, which releases CO_2 and produces NaOH, being able to capture the CO_2 present in a gaseous mixture regenerating the solution itself and allowing continuous operation over time. A simulated exhaust gas with CO_2 concentration equal to 16% was employed as input, obtaining CO_2 with purity up 98% as output. The continuous operation of the system was verified for up to 8 consecutive hours. The operation parameters have been optimized it, with a flow of 6 ml/min of CO_2 captured compared to 20 ml/min in the inflow. Furthermore, from the capture system, it is also possible to obtain valuable by products such as H_2 and O_2 In the last part of the work, the system was coupled with a CO_2 electroreduction device to produce syngas. The latter consists of a mixture of CO (2.2%) - deriving from the reduction of CO_2 - and H_2 (78.3%)- deriving from the water splitting of the water present in the system- capable of being reused as fuel or as a platform for other molecules. In this way, it has been possible to develop a new system, consisting in a loop capable of capturing CO_2 from combustion processes (avoiding contributing to global warming), and of directly transforming it into another reusable substance, with an efficiency of 7.3%, through a directly coupled system.

1. Climate change

Climate change is a set of natural phenomena that occur on our planet in a cyclical way over time and involve the variation of the climatic conditions present. These phenomena may be due to changes in the behavior of the Sun, the Earth's orbit, volcanoes, terrestrial magnetism, and the amount of greenhouse gases. These aspects are studied by the physical, astronomic, and geological disciplines. In general, these phenomena involve the variation of terrestrial temperatures and, therefore, create periods of glaciation, drought or flood. However, these changes, barring sudden events such as a meteorite fall, are slow and observed over the centuries, not creating a sudden problem for the Earth's population, which is able to adapt.

The problem today is that these climate changes occur too quickly, leading to the well-known problem of 'Global Warming', i.e. the phenomenon of average rise in terrestrial temperatures. This leads to an increase, both in frequency and intensity, of phenomena such as hurricanes, fires and floods as well as the growth of sea level caused by the melting of glaciers and the desertification of places, due to the increase in temperature and the absence of rainfall. This causes problem for biodiversity, due to abnormal migrations, food shortages and hard living conditions [1].

Thanks to the research of scientists, who over the years have had to fight against a sense of 'indifference' of the population and politicians, who have often seen this problem as distant in time or even non-existent, it is possible to affirm that this situation is largely due to the human species, which, since the time of the industrial revolution, has started to emit a large amount of greenhouse gases, contributing substantially to the rise in temperatures and to the problems mentioned above. Although climate change exists in its own right, studies have revealed a very strong correlation with anthropological activities that are somehow connected with the emission of climate-altering gases that modify the Earth's heat balance too quickly compared to the natural one.

1.1 Greenhouse effect

In particular, we focus on the factor of climate change, which is not only formally influenced by human activity, but is also the one predominant in this historical period: the greenhouse effect.

The atmosphere already performs the function of the greenhouse effect in a spontaneous and natural way, without which we could not maintain temperatures suitable for life. However, the so-called greenhouse gases influence its behavior, amplifying this effect. In fact, the solar radiation incident on the planet is partly re-emitted in the form of infrared radiation and, if the greenhouse gas component is too high, these radiations are unable to escape from the atmosphere causing an increase in temperatures. it is possible to observe this behavior in figure 1.1, in which natural behavior and that amplified by human behavior are compared [2].

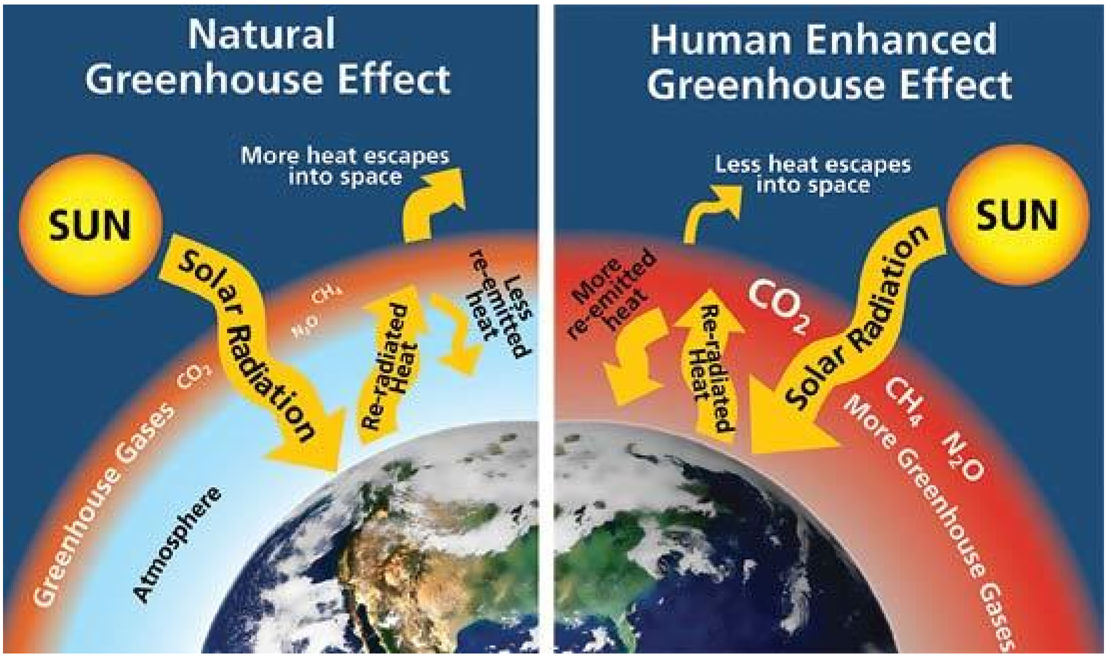

Figure 1.1- Greenhouse effect. Source: climatechange.lta.org

The term 'greenhouse gas' refers to different gases capable of producing the same effect, albeit with different intensities. In particular, this category includes carbon dioxide (CO_2), methane (CH_4), nitrous oxide (N_2O), sulfur hexafluoride (SF_6) and other compounds as hydrofluorocarbons (HFC) and perfluorocarbons (PFC). To classify the different gases and characterize their behavior, different aspects must be considered:

- Concentration: based on the concentration of the gas analyzed in the environment, there will be different influences on the greenhouse effect.
- Global Warming Potential (GWP): it quantifies the ability of the gas to behave as a greenhouse gas over time with respect to CO_2, whose value is set to 1, regardless of the time over which the analysis is carried out. It mainly depends on two factors, i) the radiative forcing, which quantifies the containment force of infrared waves based on its spectrum, and ii) the residence time in the environment, which depends on the type of gas and quantifies the average lifetime in the substance in the 'environment. The latter is the reason why when we talk about GWP it is necessary to specify at what time interval the analysis consists [3].

By multiplying these two factors it is possible to calculate the 'Carbon Dioxide Equivalent' (CO_2e), that is the index that specifies how much CO_2 corresponds to a certain emission of a greenhouse gas. This factor is important to define a sort of 'overall danger' of greenhouse gases, which depends not only on its power over time but also on its quantity in the environment or on the quantity emitted, since many gases are particularly dangerous but not very present and vice versa. Table 1.1 shows the current and the pre-industrial concentration values of the gases, the percentual increase, their residence time, their GWP at 100 and 500 years and the CO_2e based on the reported concentration for both the GWPs. It is obvious that if the quantity emitted of a gas with a high GWP were equal to that of CO_2, the last index would lose its usefulness as the hazard could be observed considering only the GWP, but if the real quantities are considered, a true comparison can be obtained between the different gases, considering their CO_2e value on the basis of the quantity actually present [4].

	Pre-industrial concentration [ppm]	Recent concentration [ppm]	Percentual increase [%]	Lifetime [years]	GWP_{100} [-]	GWP_{500} [-]	CO_2e (GWP_{100}) [ppm]	CO_2e (GWP_{500}) [ppm]
CO_2	280	399.5	42.7	100-300	1	1	399.5	399.5
CH_4	0.7	1.834	162.0	12.4	28	7.6	51.4	13.9
N_2O	0.27	0.328	21.5	121	265	153	86.9	50.2
SF_6	0	0.0000086	> inf	3200	23500	32600	0.2	0.3

Table 1.1: Greenhouse gases. Source: Intergovernmental Panel on Climate Change Fifth Assessment Report

From this table it is possible to observe that CO_2 has the lowest GWP at 100 and 500 years, while substances such as SF_6 have high GWP and are considered compounds with a high environmental hazard. Furthermore, CO_2 has a long residence time compared to other substances, therefore in the calculation of the GWP the ability to block radiation is lower than other substances with a shorter residence time and higher GWP. For the substances like SF_6, in which the residence time is longer than the time considered for GWP calculation, it can be noted that the GWP at 500 years is higher than the one at 100 years. This happens because the substance has not yet begun its decay and therefore its effect is still present. On the other hand, for the other substances the index decrease because of the residence time causes the gas to disappear. Finally, it should be emphasized that, despite the aspects listed above, CO_2e, calculated on the basis of the actual concentration, is lower than that of CO_2 for all gases. Therefore, given that CO_2 is the most present substance in the environment and has a longer residence time than the others, it can be said that it is, at the moment, the most impacting climate-altering substance. Furthermore, it is also the climate-altering substance most emitted by humans together with methane as it is possible to see observe in the table 1, in which these two substances have the greater increase in concentration from the pre-industrial age up to now. It is however necessary to keep the emission level of substances with high GWP under control, because their eventual increase could irreversibly contribute to the temperature increase.

Given the fact that CO_2 is the substance we need to worry about most in this historical period, there are many studies that certify the link between the current lifestyle of the population and the increase in average temperature due to greenhouse effect. In this sense, thanks to the analyses carried out by 'NOAA's National Centers for Environmental Information' it is possible to observe, in figure 1.2, the direct analogy that exists between temperature increase and CO_2 concentration increase [5].

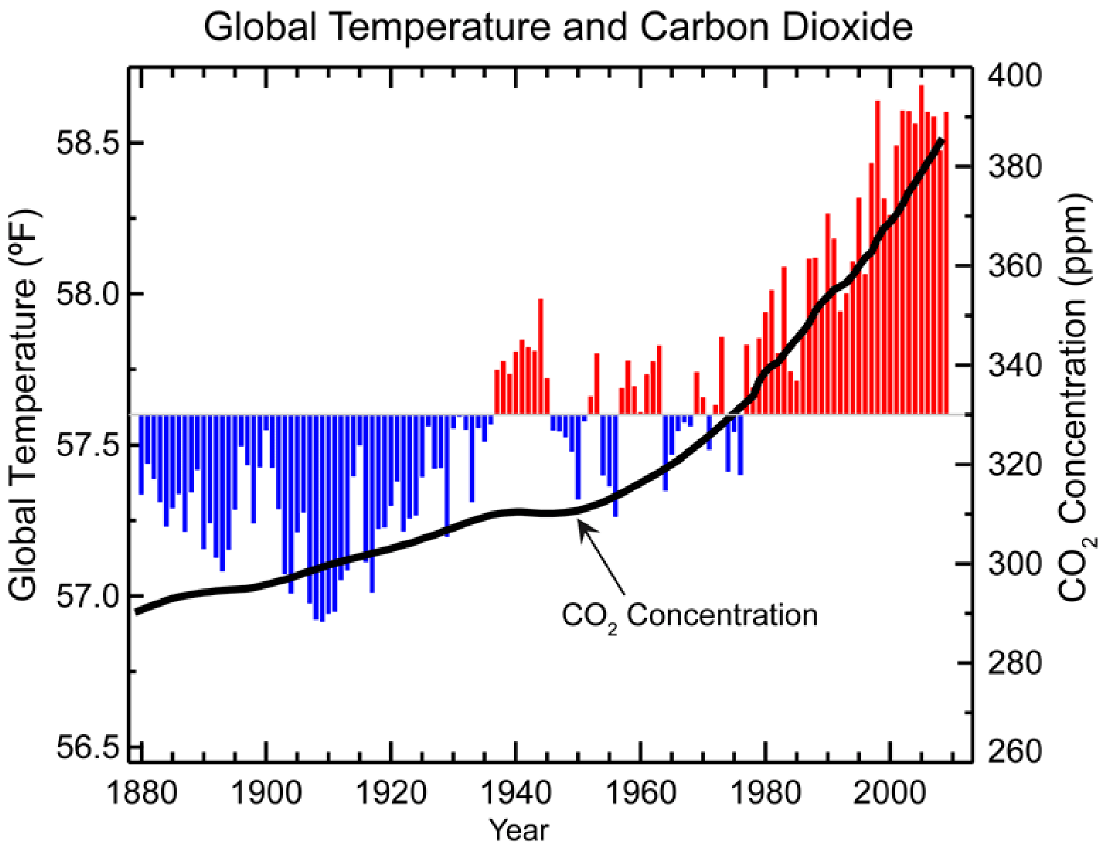

Figure 1.2- T versus CO_2 concentration. Source: NOAA's center

From the previous graph it is observed that the average temperature has increased, leading to the birth of those problems discussed above. The trend is on the rise, especially since the post-war period in which many developing countries have begun to contribute substantially to emissions.

Still considering the studies carried out by this center, it is observed, in figure 1.3, that there is a correlation between the average temperature and the variation in the type of human activity on the planet. Furthermore, the graph highlights the difference between natural and artificial contributions; in fact, as previously said, the greenhouse effect exists naturally, but in this way it would have led to a stable temperature in the short term, preventing the onset of problems. The average temperature assumed in the case of natural influence alone is what we consider as an ideal reference in current and future scenarios. It is important to underline that these values are valid only for our time, as the timing of the natural greenhouse effect is very dilated and difficult to observe in 100-200 years [5].

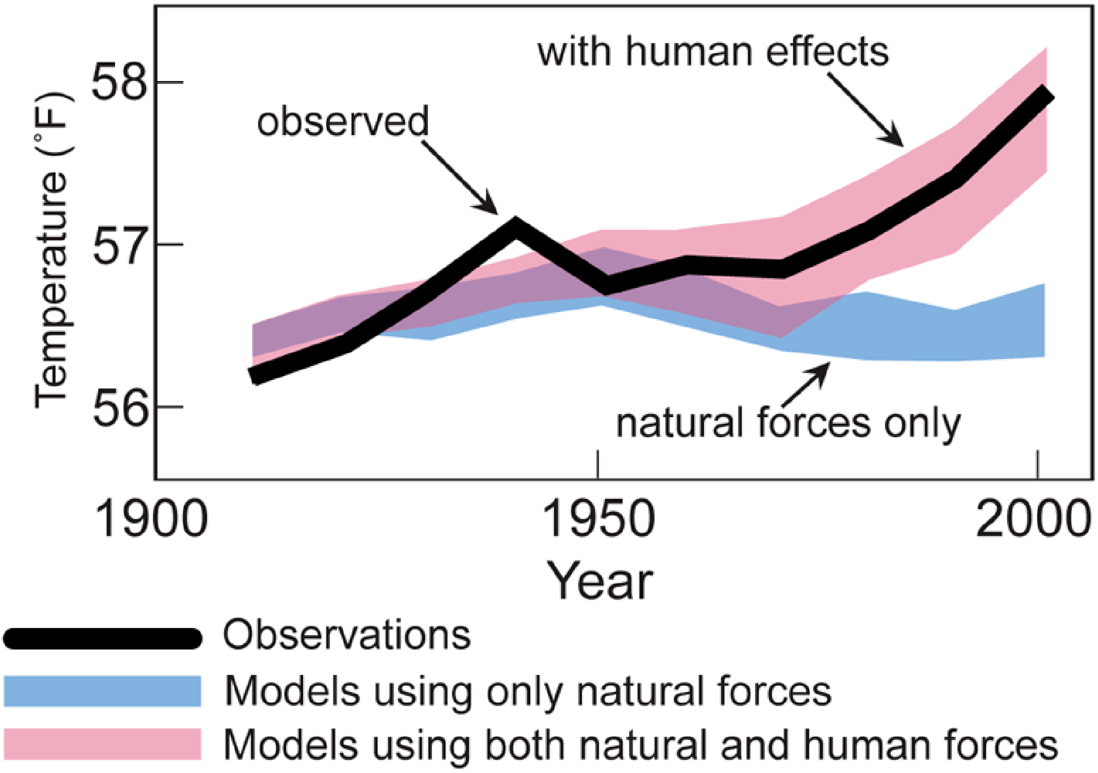

Figure 1.3 – Temperature versus years. Source: NOAA's center

Consequently, based on the information provided in this chapter, we can focus our attention only on carbon dioxide, confidently stating that it is the main anthropological cause of the greenhouse effect from the pre-industrial era onwards.

1.2 CO_2 gas data

Carbon dioxide, or CO_2, is a molecule made up of one carbon and two oxygen atoms. It is essential for many vital mechanisms of the plant and animal kingdoms, such as photosynthesis and respiration. It is therefore necessary for life, but in the right quantities to guarantee the above-mentioned processes. On the contrary, in too high concentrations, it produces a strong greenhouse effect that prevents the right balance of these mechanisms. Furthermore, the greenhouse effect is a global issue because it is wide distributed and subject to fluid dynamics transport phenomena tending not to settle. The oceans also participate in the CO_2 balance, containing a high quantity of CO_2 in the form of carbonate and bicarbonate ions, contributing to the general equilibrium of the quantity of CO_2 in the air, as the dissolution reaction is reversible. There is, therefore, a cycle of CO_2 in the Earth system - figure 1.4, which includes the aspects of natural emission, capture and regulation [6].

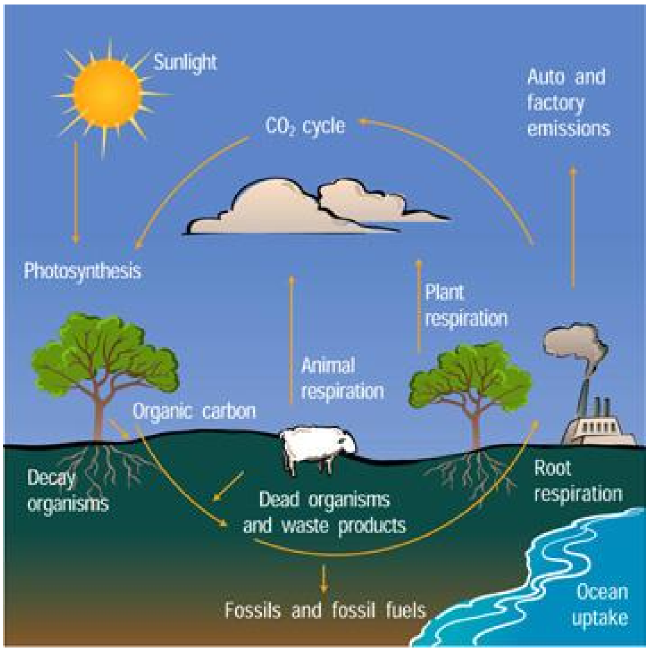

Figure 1.4 - CO_2 cycle. Source: UCAR - Center for science education

As mentioned above, CO_2 is not the most dangerous greenhouse gas, but it is one of those with the longest residence time and highest concentration. In fact, CO_2 is produced through natural processes such as volcanic eruptions, geysers, dissolution of carbonate rocks, spontaneous and artificially driven fires such as the combustion of fossil resources, for the production of energy, cement, metal alloys, and uncontrolled deforestation. In fact, this cycle is strongly influenced by human behavior, as human activities influence many aspects of the cycle [7].

Being a minority component of the atmosphere, it is measured in ppm (parts per million) compared to the amount of air present on the planet. It is estimated that the concentration in the pre-industrial age was 280 ppm, while in 2018 it was 399.8 ppm, which is an increase of about 43%. In absolute terms, human CO_2 emissions have gone from about 3 Gt in 1900 to about 7 Gt in 1950, to then currently surpass 30 Gt as shown in figure 1.5, where it is possible to observe the trend of total annual emissions.

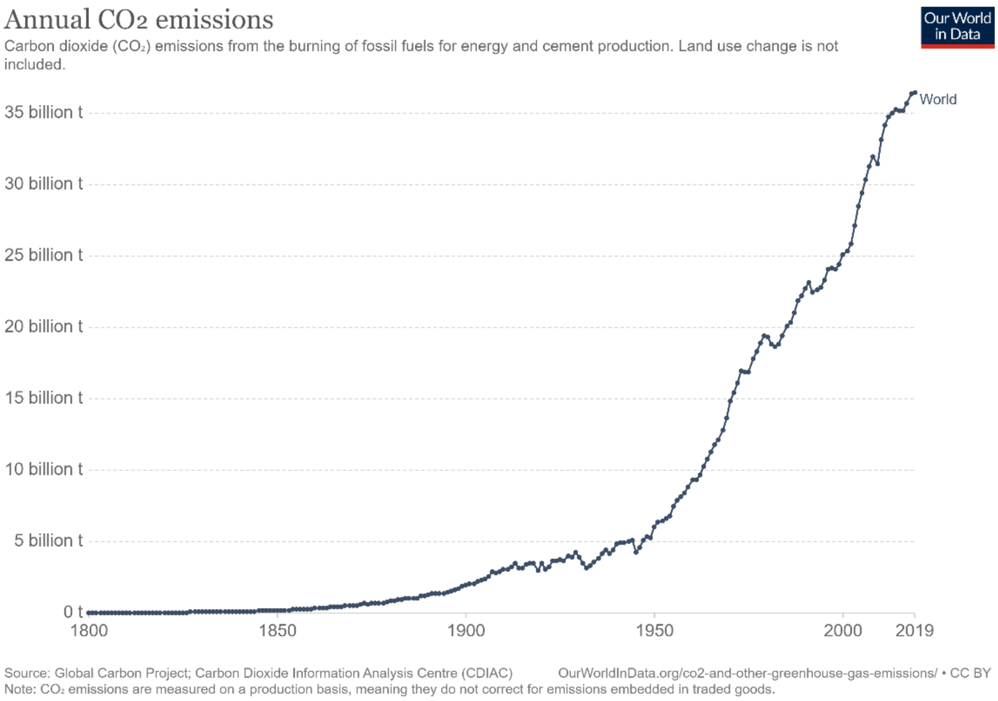

Source: Global Carbon Project; Carbon Dioxide Information Analysis Centre (CDIAC) OurWorldInData.org/co2-and-other-greenhouse-gas-emissions/ • CC BY
Note: CO_2 emissions are measured on a production basis, meaning they do not correct for emissions embedded in traded goods.

Figure 1.5 - Absolute CO_2 emission. Source: Our World in Data

Considering the current emissions, over 30 Gt, it is estimated that every year about half of the gas fails to enter the natural cycle of CO_2 through a positive feedback, now saturated, effectively becoming part of the earth's atmosphere. From this it is possible to calculate the yearly increase of CO_2 concentration in the environment through some calculations and the reported assumptions [8]:

$$CO_2[ppm/year] = \frac{CO_2 emission\ [kg/year] * Non\ absorption\ factor\ [-] * 10^6\ [ppm]}{Volume\ of\ atmosphere\ [m^3] * CO_2\ density\ [kg/m^3]} \tag{1.1}$$

In this calculation, we assume an atmosphere thickness of 8 km and a terrestrial radius of 6371 km – volume of 4.09E9 km^3, CO_2 density - calculated at 0 °C and P_{atm} - equal to 1.96 kg/m^3 and emission equal to 30 Gt per year with a non-absorption factor of 0.5 Furthermore, it is also assumed that the rest of the atmosphere remains the same, even though there are actually more factors at play. From eq. 1.1 we get 1.9 ppm/year.

Therefore, assuming to maintain these conditions, there would be an increase in the CO_2 concentration equal to about 2 ppm per year, which would lead to about 560 ppm of CO_2 in the atmosphere in 2100, 40% more than the current quantity.

Now, various aspects concerning the artificial emission of CO_2 will be analyzed, in order to frame the situation more clearly. First of all, we observe the emission of greenhouse gases in the various locations on the planet showed in figure 1.6, through the percentage breakdown of total annual emissions by country [9]:

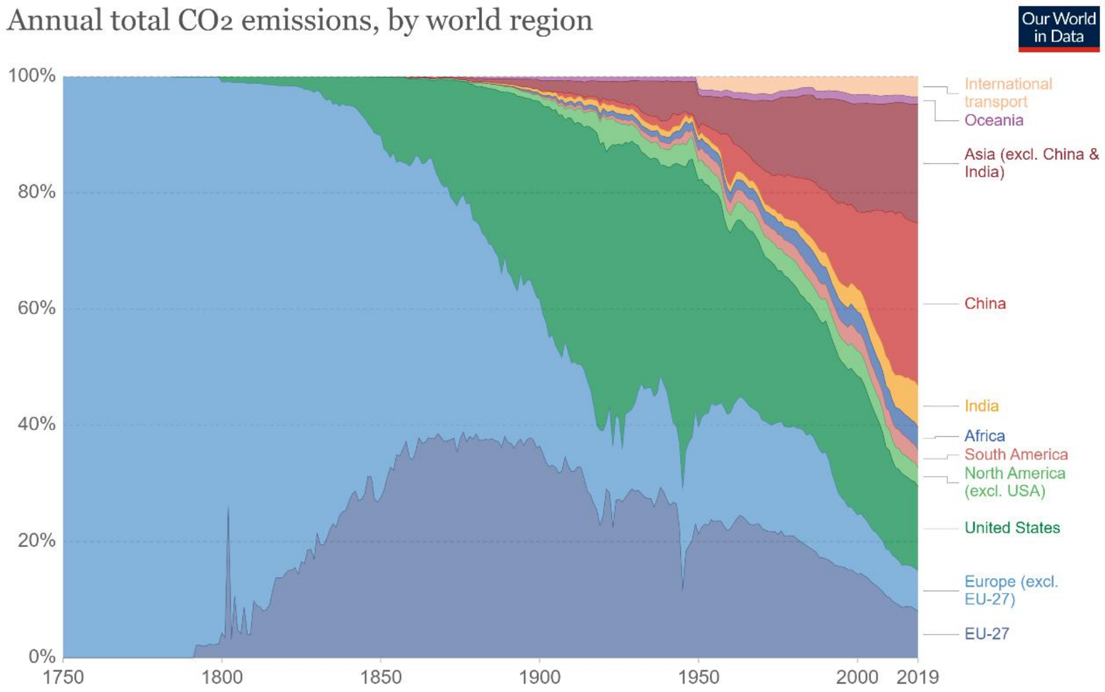
Annual total CO2 emissions, by world region

Source: Our World in Data based on the Global Carbon Project OurWorldInData.org/co2-and-other-greenhouse-gas-emissions • CC BY
Note: This measures CO_2 emissions from fossil fuels and cement production only – land use change is not included. 'Statitistical differences' (included in the GCP dataset) are not included here.

Figure 1.6 – Relative Regional CO_2 emissions. Source: Our World in Data

Thus, in addition to the already known trend of emissions over time, it can be seen that over time the territories that emit more CO_2 have changed. Previously it was the so-called developed countries, Europe and North America, that emitted more, due to an energetically expensive lifestyle. To date, the countries that most pollute are the developing ones, such as the countries of Asia, China and India. Starting from this, we then have the curve of cumulative emissions over time, in figure 1.7, which can provide an idea of the countries that have actually polluted the most over the course of the years.

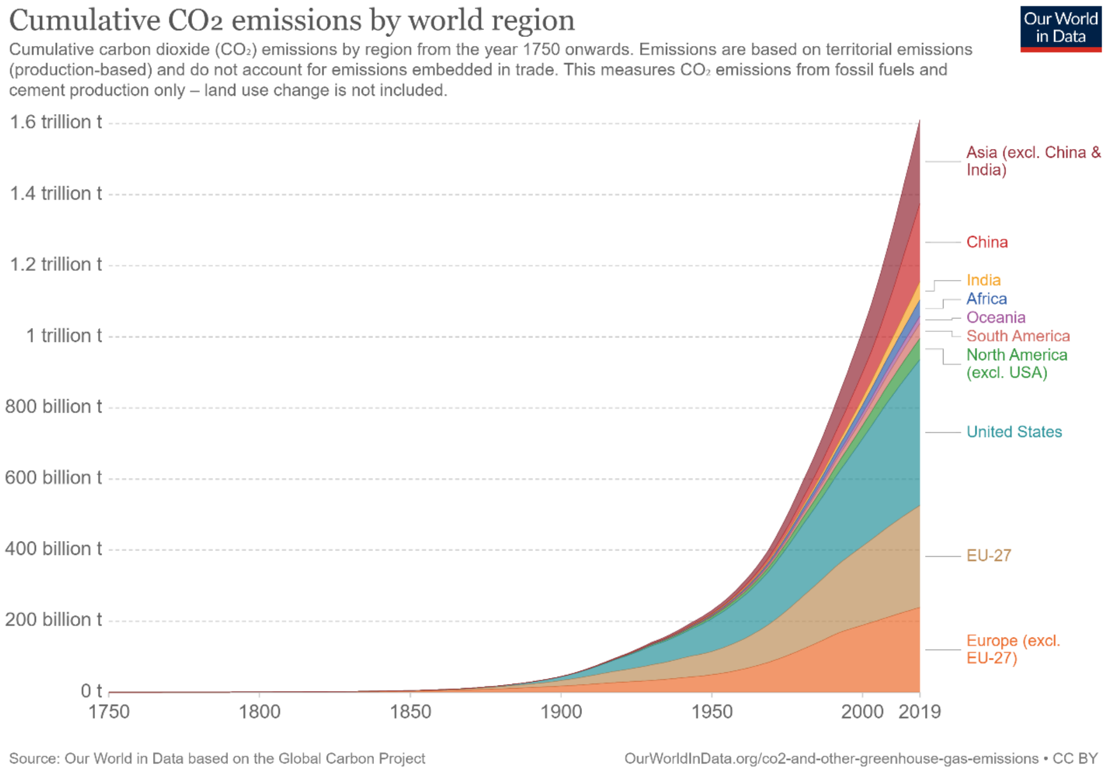

Figure 1.7 - Cumulative emissions during the history. Source: Our World in Data

From the previous images, it is observed that up to the decades of the early 1900s emissions were almost exclusively the prerogative of Europe and North America. Over the years they have been gradually exceeded, in percentage of annual emissions, by developing countries, until today the latter are the largest emitters. Furthermore, their growth has been so fast that in a short time they have cumulatively emitted about the same amount of CO_2 as the historical countries. However, it is important to underline that the emissions for developing countries are from a certain point of view 'forced', since in general the least expensive production technologies, useful for developing quickly, are also the most polluting, such as coal-fired thermoelectric plants. Furthermore, it must also be considered that the population of certain areas of the world is much higher and denser than that of Europe, which is another reason why emissions are higher. Finally, with globalization and international trade, a substantial part of the needs of states are produced in other countries and then exported to countries that consume, but which therefore do not participate in the counting of emissions. Taking this aspect into account, we move from an approach based on production to one based on consumption. In this case the amount of CO_2 is therefore counted to the states that consume the good, instead of those which produce it. We can see this aspect in the figure 1.8, which shows the quantity of CO_2 embedded in global trade, that is the quantity that is ideally exchanged together with the exported (negative value) or imported (positive value) product [10].

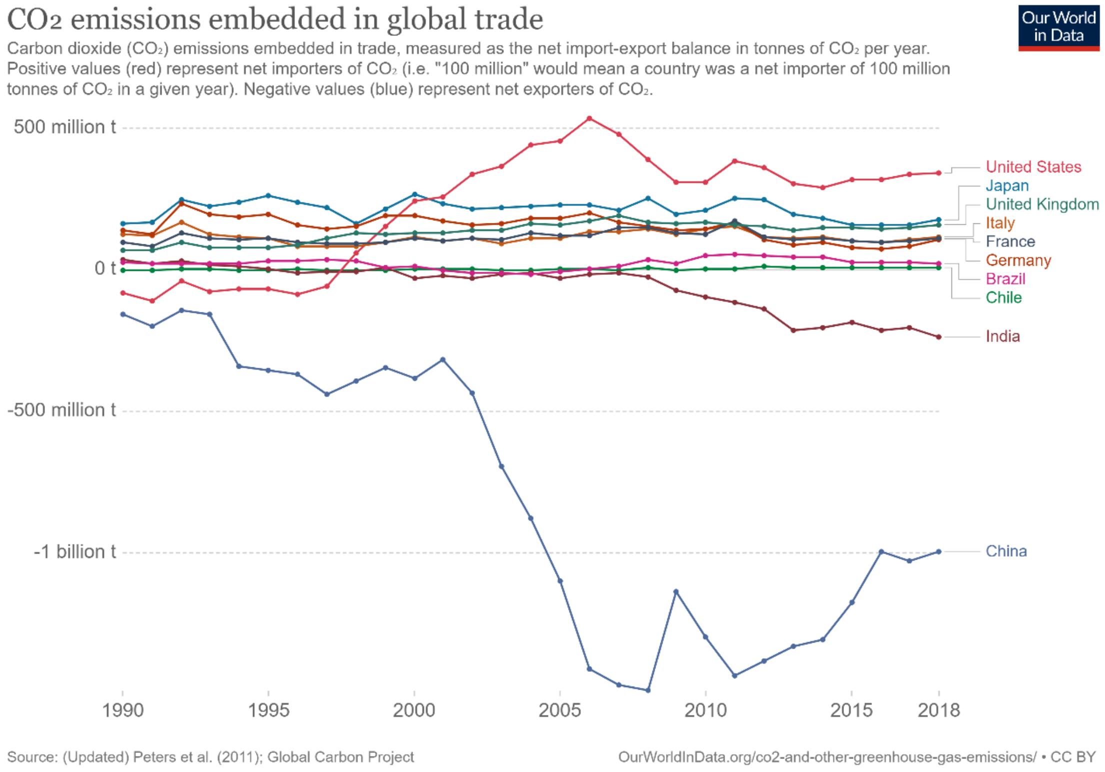
CO2 emissions embedded in global trade

Carbon dioxide (CO₂) emissions embedded in trade, measured as the net import-export balance in tonnes of CO₂ per year. Positive values (red) represent net importers of CO₂ (i.e. "100 million" would mean a country was a net importer of 100 million tonnes of CO₂ in a given year). Negative values (blue) represent net exporters of CO₂.

Source: (Updated) Peters et al. (2011); Global Carbon Project

OurWorldInData.org/co2-and-other-greenhouse-gas-emissions/ • CC BY

Figure 1.8 - Consumption-based emissions. Source: Our World in Data

The values shown in the previous figure should be added, with their sign, to the values based on the productive approach to allow for a global vision of a country. In fact, for example, China and India emit a lot of CO_2 also for other countries that consume their products, while countries like Japan or the USA import many products, resulting in actually having higher emissions. There are also countries, such as Chile, which have a zero net of exported-imported CO_2, as they either produce and consume all their needs independently or the imports-exports are the same.

Now, considering that, as mentioned, CO_2 emissions are mainly caused by the combustion of fossil fuels, we analyze the quantity of each fossil source used and its relative emission factor during combustion. The latter depends on many factors such as the chemical and quantitative composition of the substance and the physical state, which affects the quality of combustion. It is more convenient to analyze the quantity of fossil fuel used and not the emissions caused by it, as in this way it is possible to separate the quantity of fuel used (in figure 1.9) from the emission factors of the substance (table 1.2). The emission factor of interest shows the quantity of CO_2 emitted per unit of energy produced, as it is of our interest to refer to the quantity of energy that is produced - and therefore consumed - and not the quantity of fuel used. This is because fuels produce more or less energy for the same weight. In this sense, the table also shows the lower calorific values (LHV) which determine the link between the energy produced and the mass of the substance, necessary to obtain the factor of interest.

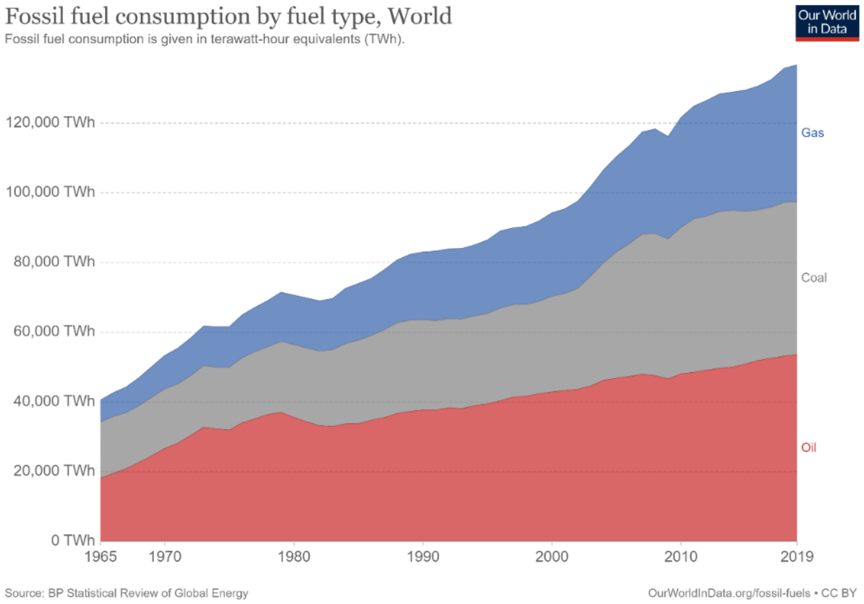

Figure 1.9 - Fossil fuel consumption by fuel type. Source: Our World in Data

	Emission Factor	*LHV*
Natural Gas	201362.4 [tCO_2/TWh]	35.25 [GJ/Stm^3]
Oil	275875.2 [tCO_2/TWh]	41.02 [GJ/t]
Coal	340354.8 [tCO_2/TWh]	24.85 [GJ/t]

Table 1.2 - Emissions factor. Source: Ministero dell'Ambiente IT

From the table and the graph, which present average values regardless of the by-products, it can be observed that although coal is the substance with the lowest LHV, it is historically one of the most used, due to its ease of extraction and low cost. Historically, coal and, above all, oil are easily stored and therefore easily usable and marketable, as the usage values attest. From the point of view of emissions, on the other hand, coal has the highest emission factor per unit of TWh, therefore of energy requirements. Oil has an intermediate value, while gas is the cleanest fossil source.

Ultimately, it is necessary to observe which sectors have the highest emissions, to understand what the solutions could be and on which sector they could be applied. The subdivision observable in figure 1.10 is made taking into account the global and non-local values, which could be slightly different. In turn, the various sectors within them collect different sub-sectors with different emission rates, which are added together [11].

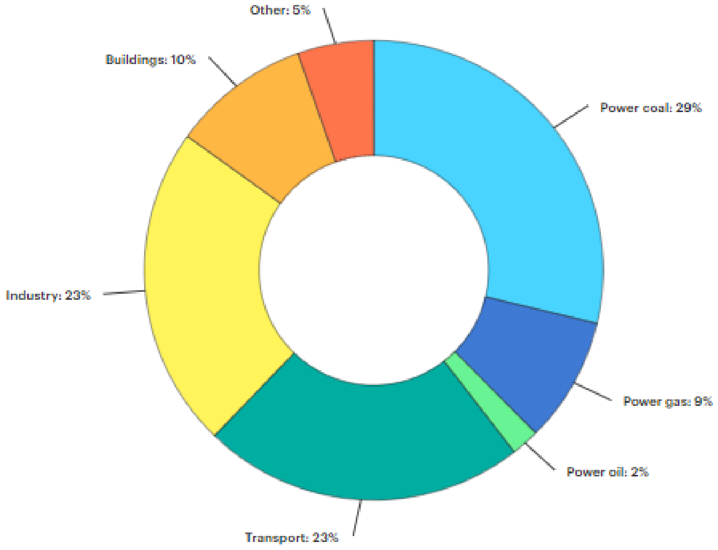

Figure 1.10 - CO_2 emission by sector. Source: IEA statistics

These emissions are produced by the combustion of fossil fuels, such as coal, gas and oil. This percentage subdivision considers the emissions produced by the combustion of the gases analyzed in the previous paragraph. It is noted that the most important sectors are those of electricity generation, transport - maritime, land, air - and industry, in particular the cement and steel industry. A not insignificant part is due to buildings, generally for the production of heat for space heating. In conclusion, although the production of electricity and the consumption of coal are the main sources of CO_2, there are many alternatives, spanning many fields, on which to act to control emissions.

2. The mitigation challenge

After the considerations made in the first chapter on the greenhouse effect, we can focus the attention on only the CO_2 emissions, thus leaving out the other climate-altering gases. This because CO_2 is the most present and lasting greenhouse gases. We will consider only the emissions due to the combustion of fossil fuels, that is the most important and controllable artificial source.

Given the scientific studies and physical evidence of climate change, a global policy aimed at mitigating the problem of temperature increase has been underway for some decades. The Intergovernmental Panel on Climate Change (IPCC) - the United Nations body for assessing the science related to climate change - has confirmed and published the results of several years of studies linking different indices such as temperature, population and GDP, with the increase of anthropological emissions of greenhouse gases [12]. In particular, the IPCC produced scenarios representing the evolution of temperatures in the current century based on present and forecast emissions. These scenarios, called RCP (Representative Concentration Pathways) reproduce the temperature trend based on the cumulative radiative forcing value expected in the next few years, i.e. the ability to block greenhouse gas radiations mentioned in the first chapter. According to this approach, the more the CO_2 concentration value is expected to increase, the more the forcing increases and the more the RCP value and therefore the temperature increases [13]. In the last, report produced in 2015, it is possible to find the most up-to-date data on the scenarios - figure 2.1 - for different values of RCP - table 2.1.

Scenarios	*Features*
RCP 2.6	mitigation scenario (very high emissions reduction -rising of 2°C)
RCP 4.5	stabilization scenario (large reductions)
RCP 6.0	stabilization scenario (mild reductions)
RCP 8.5	high emissions scenario (business as usual)

Table 2.3 - RCP. Source 'IPPC'

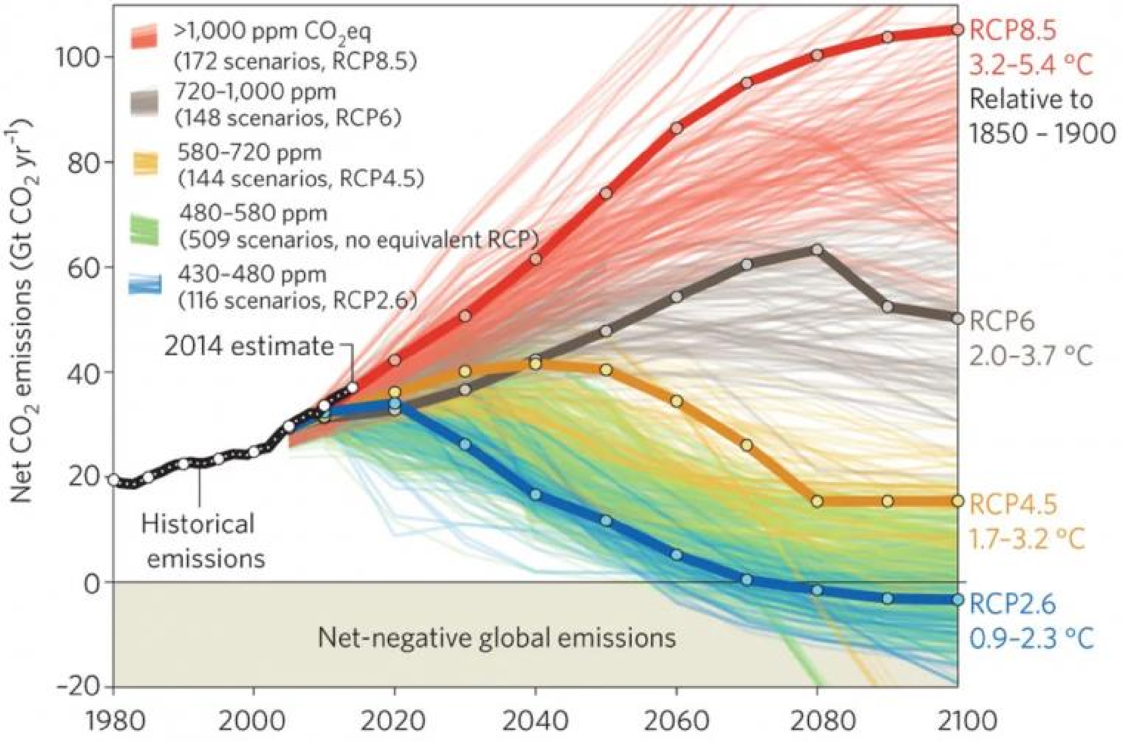

Figure 2.11 - CO_2-Temperature Scenarios in time. Source 'Fuss et Al. Betting on negative emissions.'

Temperatures, as observed in figure 2.1, are expected to increase in the coming years between 0.9 °C and 5.4 °C, depending on the model used. Furthermore, it must be considered that despite the increase in emissions, the Earth is a physical system which, even considering the increase in emissions, after a first transitory phase, will reach an equilibrium phase, in which both the concentration of CO_2 and the temperature will stabilize. However, this increase does not seem to be compatible with the current world standard of human, animal and plant life, predicting a worsening of living conditions, an increase in environmental disasters and the disappearance of many forms of life [1]. Figure 2.1 also shows the net CO_2 concentrations predicted in these scenarios, from which it is possible to extrapolate the maximum concentration tolerable by the atmosphere in order to remain below a certain global temperature threshold. To reinforce this fact, again in the latest IPCC report, a new concept of cumulative quantity of CO_2 emitted, called the

'CO_2 budget', was introduced, compatible with a certain increase in temperatures - figure 2.2 [14].

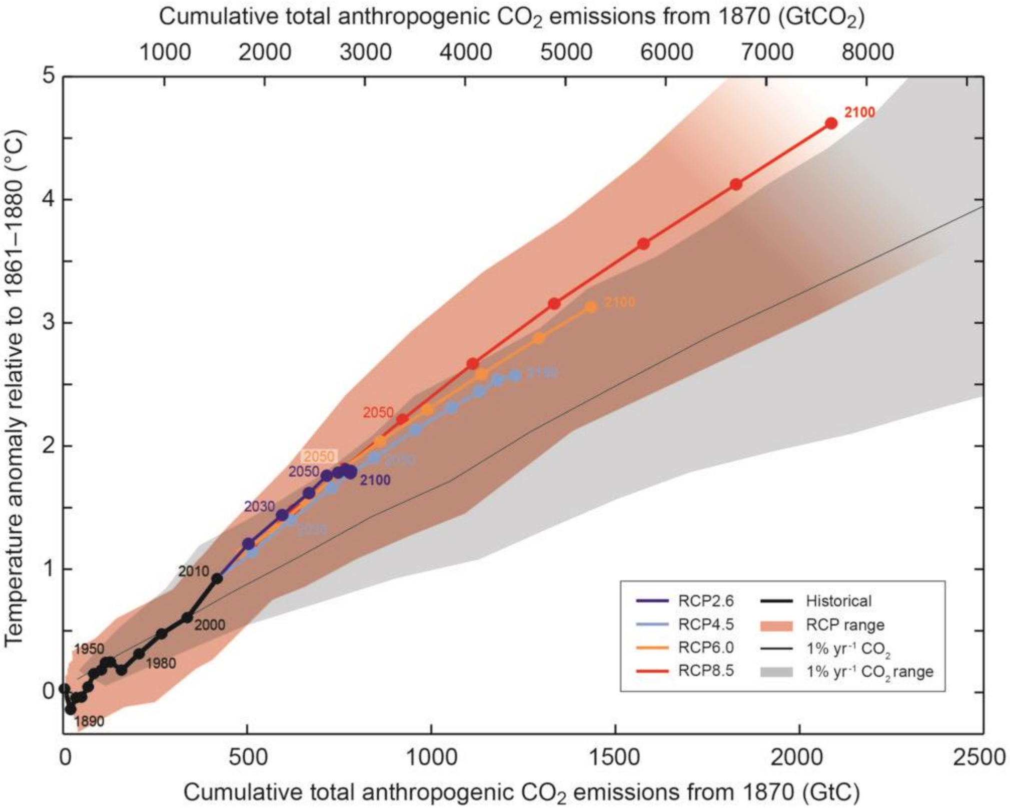

Figure 12.2 - Cumulative CO_2 emissions vs Temperature. Source: 'IPCC'

As expected, large CO_2 budgets correspond to strong rises in temperatures. It is important to remember that it is the absolute quantity of CO_2 that creates a problem, (due to its lifetime in the environment) and not the instantaneous emission rate. For this reason, it is possible to express the containment measures in the form of maximum total CO_2 issuable in a given time interval. This because there is a quasi-linear correspondence between the CO_2 budget and the temperature increase.

2.1 Policies

As mentioned in the previous section, thanks to the emission scenarios and the expected CO_2 budget it is possible to formulate an answer to the problem. The first phase of this process begins in 1992 with the 'United Nations Conference on Environment and Development' held in Rio de Janeiro with the definition by the United Nations of the 'United Nations Framework Convention on Climate Change (UNFCCC) 'for the reduction of GHGs and the containment of the increase in temperature. This treaty is not binding, it was ratified in 1994 with the achievement of 50 signatory countries and every year the parties participate in a discussion, called 'Conference of Parties (COP)'. However, it allows the adoption of specific protocols, which define mandatory limits for the signatory countries, such as the Kyoto Protocol, defined in 1997 at COP3. The latter foresaw that in the period 2008-2012 greenhouse gas emissions would be reduced by 5% overall compared to 1990. The ratification, which was to count at least 55 countries responsible for 55% of emissions, took place in 2005 and to date has 175 countries, which account for 61.6% of emissions [15].

Subsequently, in 2015 the COP21 was held and the Paris agreement was signed. With this agreement, the objective was to maintain the temperature increase compared to the pre-industrial era of at least 2 °C. There is particular interest in limiting this increase to 1.5 °C, which would guarantee risks and effects of minimal climate change. With this agreement, each participating country had to have its own non-binding plan to achieve the objectives. The ratification took place in 2016 with 183 signatory countries that must present a 'national climate action plans (NDC)' in which their objectives and methods of achievement are collected [16].

In particular, the EU has published the 'European Green Deal', which sets the goal of reducing emissions by 40% compared to 1990, increasing the share of renewable energy by 32% and improving by 32.5% energy efficiency, all by 2030. In December 2020, it updated its plan, raising the emission reduction target to 55% [17].

Starting from the proposed policies, the goal is therefore to limit the temperature increase to 1.5 °C and to focus on limiting emissions by 55% by 2030, which are the primary objectives. Indeed, the aspects of the Green Deal are mutually dependent and intersected. Numerically, if we consider the same data used in the first chapter, we have an annual increase of about 2 ppm of pollution if we assume an emissions trend equal to 30 Gt per year. In reality, it is already bigger. From figure 2.1, if we consider an expected temperature increase of up to 2 °C, by 2100, we can assume that the maximum concentration of ppm in the air must be between 430 and 480 ppm [18]. Given the current concentration of 400 ppm, it is observed that the increase in sustainable concentration is at 50 ppm - considering 450 ppm as a maximum. This, considering a constant non-absorption factor equal to 0.5, allows us to calculate, with the following formula, the total issuable CO_2 budget from now until 2100:

$$CO_2 budget\ [Gt] = \frac{\Delta CO_2[ppm] * Volume\ of\ atmosphere\ [m^3] * \ CO_2\ density\ [kg/m^3]}{Non\ absorption\ factor\ [-] * 10^6\ [ppm]} \tag{2.1}$$

With the assumptions made in chapter 1, we obtain a CO_2 budget equal to 800 Gt (eq. 2.1). Considering this result, we can say, albeit in an approximate manner, that by 2100 the planet will only be able to emit more than 800 Gt of CO_2. Given that the current issue is around 30 Gt per year, there are less than 30 years left before exceeding the threshold level indicated. At this point, it is clear that the solution is to reduce emissions. However, there are more catastrophic scenarios, that consider only negative trend for the environmental aspect involved in the climate change, where the tipping point has already been passed. This means that even by completely canceling emissions, today it would not be possible to stop the rise in temperatures below 2 °C, compromising the health of the planet in certain contexts [19]. In any case, if this has not yet happened, this process will take place in the coming decades if the right measures are not taken.

2.2 Age of fossil source

As pointed out earlier, the obvious solution is to reduce emissions in some way. However, starting from the industrial revolution, we enter an age that can be called the 'age of fossil fuels' because the whole society has developed through the use of these fuels and still continues to do so. In fact, it is unthinkable to suddenly stop CO_2 emissions, for a series of reasons, which can be grouped into two macro-aspects:

- Technological: many energy-intensive sectors are not yet able to replace many applications of fossil fuels due to the lack of adequate technologies, such as difficulties in the combustion of hydrogen. Many technologies, on the other hand - despite being in an advanced state of development - still do not have a sufficient economy of scale capable of lowering the cost.
- Economic: for decades it has been the cost of fossil fuels that has marked the path of the world economy, due to the exclusive ownership of resources, geopolitical interests and the quantity used / sold. The cost is therefore in most cases still affordable, effectively blocking alternative sources and measures to contain emissions.

There is also a sort of energy 'inertia', that is the fact that the coal and especially natural gas power generators are of recent construction, as shown in the figure 2.3.

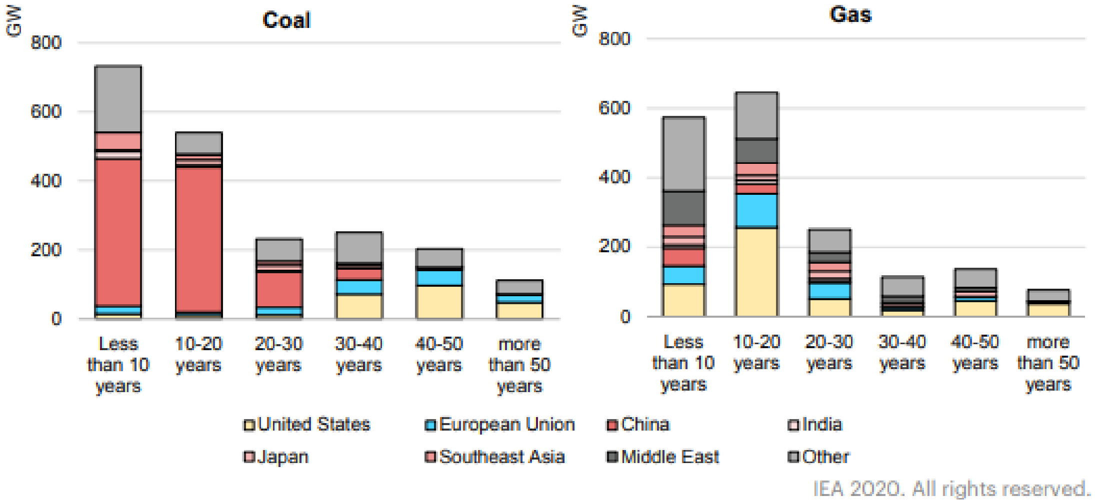

Figure 2.13 - Age structure of existing coal and gas power capacity by region. Source: IEA Statistics

This prevents the host countries from blocking them to not incur in waste of investments and penalties. In fact, the plants are built with an investment of at least a few decades, about 30-40 years. These investments concern not only the economic aspects, but also the environmental ones for land, water and atmospheric pollution, and the emission of greenhouse gases. The latter are estimated during the design of the system: on the basis of the planned operating hours of the system, it is possible to calculate the amount of CO_2 that will be emitted during the life of the system. This quantity is called 'Committed CO_2'. During operation lifetime, CO_2 is emitted at an annual rate, as in the figure 2.4a. While, considering a certain instant of life, the emissions can be divided into released and remaining, as in the figure 2.4b. The first considers the emissions that are released into the environment during working hours; the second considers the difference between the committed and released CO_2, i.e. the quantity that the plant will theoretically still emit by the end of its life. [20].

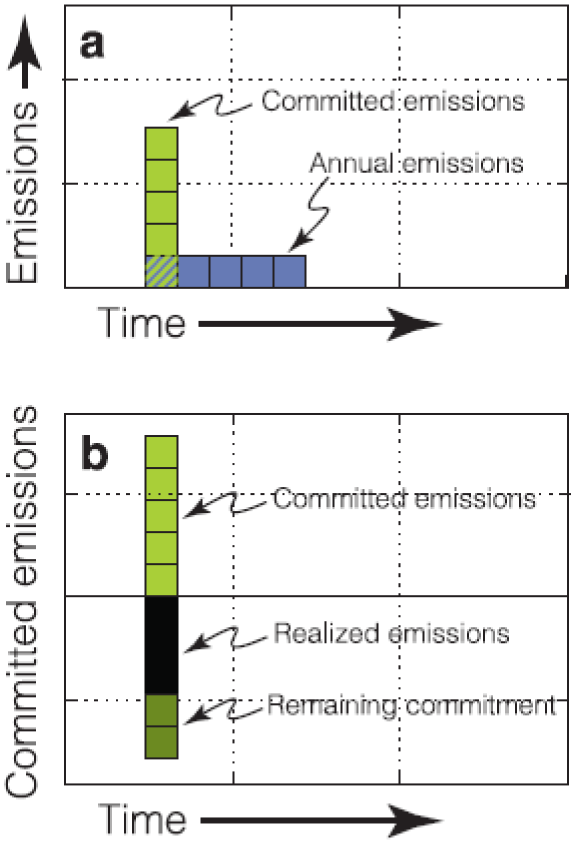

Figure 2.14 - a) Committed and annual emissions. b) Realized and remaining emissions.

Source: Davis et Al. Commitment accounting of CO_2 emissions

Thanks to this approach, assuming no longer investing in fossil fuels, it is possible to estimate how many emissions there will still be and for how long, before the decommissioning of all existing plants – like in figure 2.5. This analysis assumes that there are five different scenarios based on the life of the plants, between 20 and 60 years, in which the committed CO_2 is also higher as the annual emission rate is always the same. The future annual emissions and their duration are therefore assumed for each scenario, in the event that it is decided to stop designing from a certain point onwards.

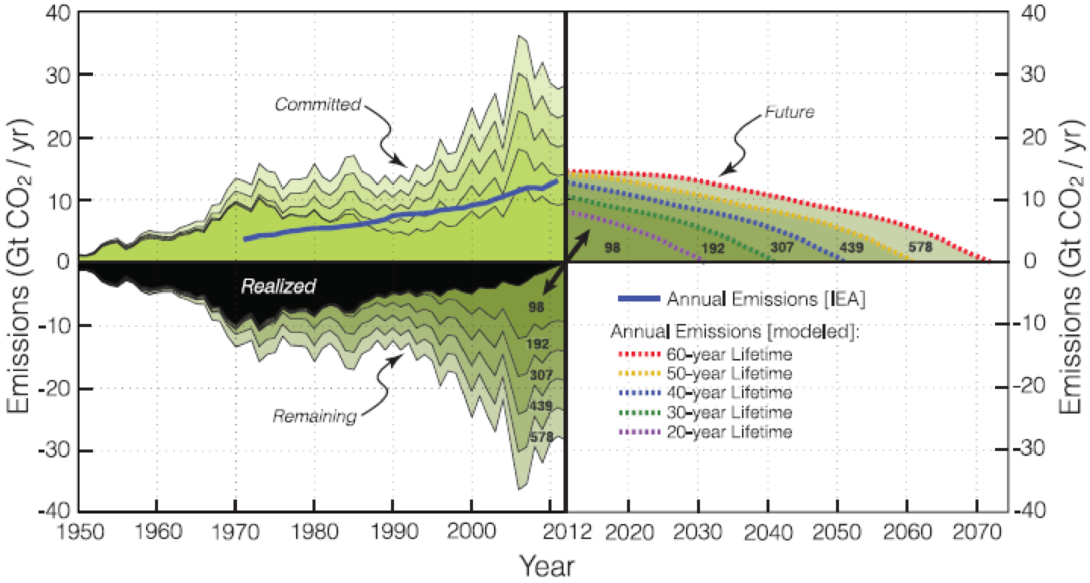

Figure 2.15 - Future emission from committed plants. Source: Davis et Al. Commitment accounting of CO_2 emissions

As predicted, figure 2.5 shows that even if the construction of new plants is stopped, there will still be future emissions. In particular, newer construction plants will emit still for many years over time. Furthermore, the long-term plants built only in recent years have issued only a small part of their committed part, which must be completed after the contracts are stipulated. It causes the so-called 'Carbon Lock-In', that is, a situation in which, even in the best of cases, one is forced to continue to emit CO_2 in the coming years due to past decisions [21]. This is shown in figure 2.6, in which the red part is the scenario considering to stop new investments. Instead, the grey part are the different IPCC scenarios, that will contribute to the carbon lock-in.

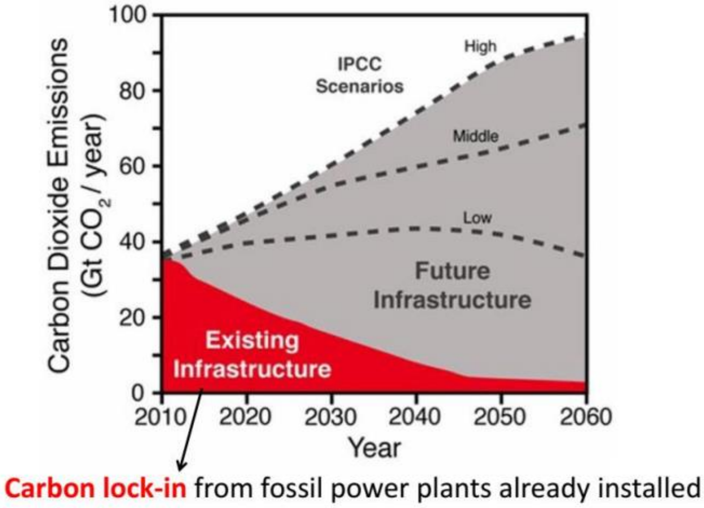

Carbon lock-in from fossil power plants already installed

Figure 2.16 - Carbon lock-in. Source: https://www.envipark.com/wp-content/uploads/2019/11/SETHI-CCS-e-NET.pdf

These concepts confirm the difficulties described in the course of the chapter with regard to reducing emissions. They are constrained by the current productive and economic situation.

2.3 Future ideas

The international agency IEA Statistics has produced a scenario based on the need to limit the temperature increase to 2 °C, considering a CO_2 budget from 2019 to 2070 equal to 800 Gt. Thanks to this scenario – figure 2.7 - we can observe that all the sectors responsible for emissions (at least in a proportional manner) are involved in the reduction. The graph shows the total annual emissions expected with the increase in mitigation measures. Furthermore, the cumulative CO_2 value that that sector expects to emit until 2070 is reported within each sector [22].

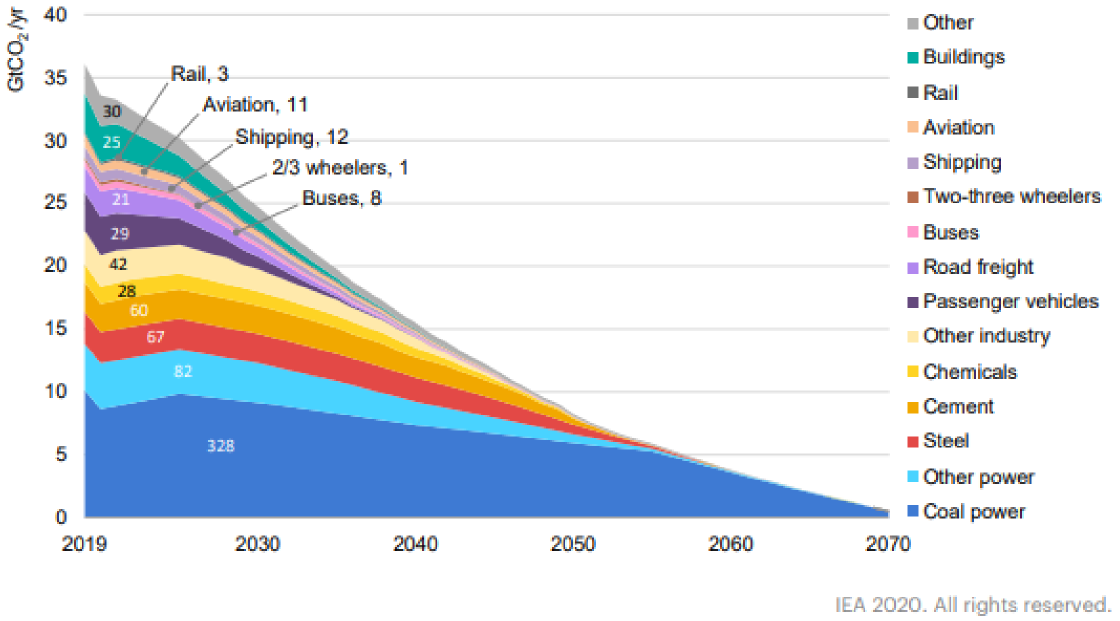

Figure 2.17 - Global CO_2 emissions from existing energy infrastructure by sub-sector, 2019-70. Source: IEA Statistics

All emitting sectors will be part of this process, known as 'decarbonization'. Obviously, the production sectors do not all work in the same way, because the mitigation methods are many and different from each other according to the needs. Therefore, having confirmed the need to reduce emissions, we can have several solutions:

- Energy efficiency: the idea is to save energy both during its consumption and during production itself. This solution, in addition to being environmentally advantageous, is also economically advantageous as waste is reduced. However, it is necessary to reach a trade-off between reducing consumption and social well-being. This is because consumption can be reduced, but the quality and quantity of the services currently offered must not be undermined, as this would not be socially welcome [23].
- Renewable sources and electrification: the idea is to replace fossil sources with renewable sources, such as solar, wind and hydroelectric, thus going to use 'carbon-free' energy sources. The energy scenarios envisage the improvement of electricity grids to cope with this change, since fossil sources are for the most part

directly linked to the production of direct energy and are often not temporally controllable. This process has already begun, but it has many technical difficulties, because they are not 'comfortable' to use. It has also economic difficulties because they are not yet convenient compared to fossil sources. Furthermore, it collides with the lock-in phenomenon which prevents its development. It is also important not to forget to consider the Life Cycle Assessment (LCA) of the technology, as the construction and decommissioning phases could be highly polluting [24].

- Capture with storage and reduction: the idea is to divide the CO_2 present in the exhaust gases or in the environment through a process called 'capture'. Subsequently, it is planned to store the CO_2 waiting to be used for other purposes or to transform it directly into another product that can be used immediately. This idea allows to continue to use fossil sources, reducing the impact on the environment. However, it is economically disadvantageous because it requires the use of energy-intensive systems without obtaining advantages.
- Increase of green areas and intelligent agriculture: the idea is to increase green areas and fight the deforestation phenomenon, because the vegetation naturally stores CO_2 and releases oxygen. Smart agriculture means the reduction of greenhouse gas emissions - especially CH_4 - by farms and the implementation of a sustainable supply chain of plant and organic products [25].

All of these processes have pros and cons. All have environmental advantages and generally have economic disadvantages. This is because to reduce the emissions of a process that generates energy it is always necessary to spend more energy, lowering the yields of the systems. Therefore, from now on the analysis will proceed considering the environmental need to reduce emissions, neglecting the economic disadvantages. The subsequent analyses will be based on the fact that this process is mandatory and must cost as little as possible in energy and economic terms.

3. CO_2 Capture

In general, the term Carbon Capture or CO_2 Capture refers to the set of processes aimed at separating CO_2 from a gas stream and consequent storage or and/reuse. More specifically, the complete process is called 'CO_2 capture, utilization and storage' (CCUS) or 'CO_2 capture and storage' (CCS), in which storage is carried out directly, without using the gas produced [26]. This solution is seen as a temporary one, before the disappearance of fossil fuels. In fact, while waiting for the carbon lock-in to run out and for renewable sources to replace fossil ones, there is still a need to reduce CO_2 emissions. This process, if done considering the capture of CO_2 from the atmosphere, could also be useful for a possible target of negative net emissions. It is made up of several phases, as outlined in figure 3.1.

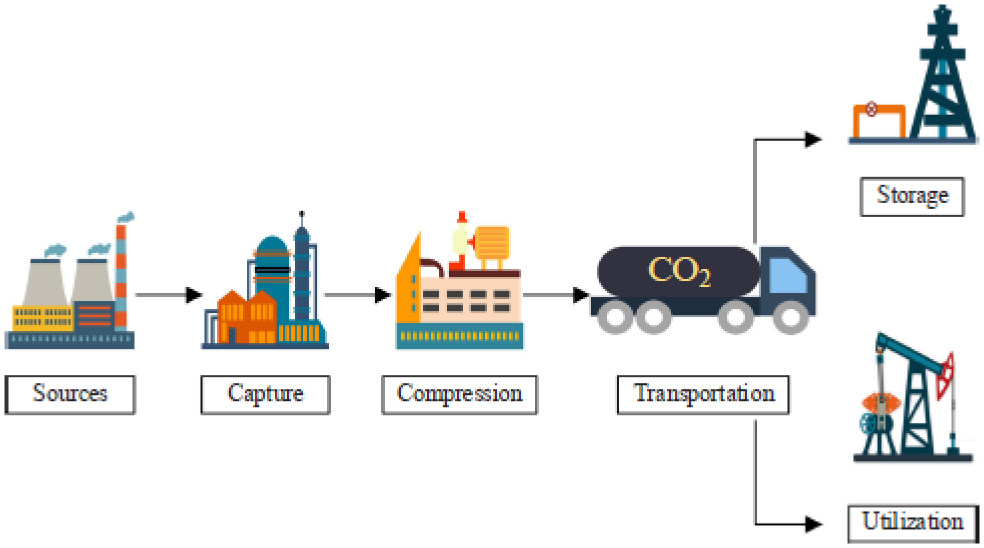

Figure 3.18 - CCUS supply chain scheme. Source: Zhang et Al. "An Optimization Model for Carbon Capture Utilization and Storage Supply Chain: A Case Study in Northeastern China."

From this block diagram, we can identify the different phases of the process which will be analyzed in the rest of the chapter: emissions, compression - transport, end uses. It was decided to dedicate a separate chapter to the capture phase, both because it is the central part of the study, and because it is interesting to start from the needs and constraints of the final uses to better design the capture process.

3.1 Emissions

CO_2 emissions, already extensively discussed in the previous chapters, are the beginning of the problem. In our case, the objective is to reduce CO_2 emissions from combustion, which depend on the type of fuel used, the purpose of the plant and its efficiency. We can find them in exhaust gases, mixed in the atmosphere and dissolved in ocean water. The aim is to reduce the concentration of CO_2 from the atmosphere to avoid the greenhouse effect, so we will focus our work on capture from exhaust gases and the environment. We neglect capture from water due to the different technologies used and the natural storage phenomenon described above. In particular, we will assume to work with the three types of sources shown in table 3.1, which contain different amounts of CO_2.

Source	*CO_2 quantity [%]*
Natural Gas	4
Coal	12
Air	0.04

Table 3.4 - Concentration of CO_2. Source: Wilcox et Al. Assessment of reasonable opportunities for direct air capture.

We consider applying the capture process to two types of exhaust gases, deriving from natural gas and coal, considering only the emissions from fixed plants, thus neglecting mobile emissions such as those from transport. Also, we want to apply it to the air around us. This last process does not prevent CO_2 from being emitted, but captures the one already present in the environment, regardless of the source produced. These data will take on practical value in the next chapter, which will deal with the capture part.

3.2 Compression – Transportation

Before analyzing the final uses it is necessary to underline the weight of the compression and transport process in the total process. They are linked because CO_2 is transported - and also stored - at temperatures and pressures different from the ambient one. So it needs to be compressed.

Considering large power plants, CO_2 emissions constitute a large volume of gas, which can be transported through a pipeline system or through large tanks, which can travel by land or by sea. This need for transport derives from the fact that for the moment the most followed routes for the use of CO_2 - which will be discussed in detail in the next paragraph - are storage and use for oil recovery. Hence, this product needs to be moved. The transport takes place immediately after the compression, which transforms the gas into an ideal physical phase for the process. It is important to estimate the energy required for the compression, because after the capture phase it represents the most energetically expensive process, reducing the economic advantages of the CCUS. In order to calculate the energies required for the various transport processes, the Mollier diagram should be used [27].

However, to simplify the calculation, we will apply the concept of ideal gas. We will thus calculate the ideal minimum work, which corresponds to the isothermal compression of an ideal gas. In this way, we will underestimate the work needed. However, this assumption is legitimized by the fact that we are interested in highlighting the minimum cost that this compression has on the yield of the plant.

To calculate the energy required for compression, the first principle of thermodynamics is used, exploiting the formula for ideal gases subjected to isothermal compression:

$$w \, [\frac{kWh}{kg_{CO2}}] = R \, [\frac{J}{mol * K}] \, * \, T \, [K] \, * \, ln(\frac{P_{out}}{P_{in}}) \, [-] \, * \, \frac{1}{\mu} \, [\frac{kmol}{kg}] * \frac{1}{3600} \, [\frac{kWh}{kJ}] \tag{3.1}$$

Where R is the universal gas constant, T the reference temperature, Pin and Pout the inlet and outlet pressures and μ the molar mass of CO_2.

Transportation through pipe networks takes place under conditions of high pressure, which allows the movement of the gas. The high pressure allows, first of all, to maintain a high density regardless of the temperature. However, the temperature must be kept above a certain level to remain in a supercritical regime in which the gaseous and liquid phases do not differ. This situation avoids the presence of two phases and therefore the flow to flow regularly. In addition, a high density allows for smaller piping and lower pressure drops. On the other hand, the mechanism of transport through tanks often also consists in refrigerating the fluid as well as increasing the pressure. In this way the density is further increased allowing to transport a greater quantity of CO_2 for the same volume. The gas under these conditions is similar to LPG, which is already transported in this way over long distances. In any case, to obtain the minimum necessary compression effect, it is assumed to have a pressure of at least 150 bar [28]. Considering starting from an initial condition of 1 bar and 20 °C and following an ideal transformation - isothermal - the value obtained is 0.077 $\frac{kWh}{kg_{CO2}}$ (eq. 3.1).Considering a coal plant, with an emission factor equal to 340354.8 $\frac{t_{CO2}}{TWh}$ - see table 1.2 - and a realistic efficiency of 40%, the energy cost of the power produced with respect to the CO_2 emitted is obtained with the following formula:

$$Energy\ cost\ [\frac{kWh_e}{kg_{CO2}}] = (Emission\ factor\ [\frac{t_{CO2}}{TWh}]\ )^{-1} *\ plant\ efficiency\ [\frac{kWh_e}{kWh}\ ] \tag{3.2}$$

By replacing the data we get an energy cost equal to 1.17 $\frac{kWh_e}{kg_{CO2}}$. Considering that the energy required for compression is electricity, we can consider a figure-of-merit that is the energy penalty - and therefore economic - that a coal plant must incur to treat its CO_2 emitted. The following formula is used:

$$Energy\ penalty\ [-]\ =\ \frac{Treatment\ cost\ [\frac{kWh_e}{kg_{CO2}}]}{Energy\ cost\ [\frac{kWh_e}{kg_{CO2}}]} \tag{3. 3}$$

In which the treatment cost is the compression cost or, as we will see in the following chapters, the capture cost. By replacing the values, we can state that the 0.077 kWh needed to compress 1 kg of CO_2 corresponds to 6.56% - energy penalty (eq. 3.3) - of the energy that a coal plant produces for every kg of CO_2 emitted. This phenomenon lowers the yield of the plants, making them less advantageous. Also, only gas compression is considered here, but the capture penalty will also be added in the next chapter. The aim is to keep the penalty close to the ideal one as much as possible.

3.3 Final uses

In this last page we consider the final uses that can be done with the captured CO_2, so that it is no longer harmful to the environment. The most widely used and best-known methods will be briefly described in the following analysis. While, in a following analysis, a process still under development will be exposed, to which its own section will be assigned.

- Storage: called also sequestration, is the last step in the CCS process, where CO_2 is stored after being captured. The purpose is basically to store the CO_2 to prevent it from mixing with the air. It is expected to last even more than a century, until it is possible to make another sustainable use of this CO_2. Generally, we tend to put this CO_2 in deposits depleted of fossil fuels, as they represent a space already present and often able to prevent the gas from escaping. In fact, the fundamental aspect of this type of storage is the presence of a highly impermeable layer called 'cap rock', which prevents the gas from escaping pushed by its pressure. It is certainly convenient that there are also no lateral losses, both in order not to contaminate the adjacent areas, and because if the interest is to reuse the CO_2 this would be a loss. Typically, this gas is injected into a supercritical state. Therefore, it should be compressed even if there was no need to transport it, resulting in the same energy cost described above. Technically, the reverse process used to extract natural gas is used, placing it in the empty basin and then sealing the inlet.

CO_2 can be also stored in deep saline formation, already used for some chemicals. They are characterized by large volumes and many porous rock formations, but have not yet been thoroughly studied [29].

- Methanation: through this process CO_2 is used as the basic molecule for the production of synthetic methane. It reacts with hydrogen to produce methane in reactors called methanators. This process is integrated with electrolysers for the production of hydrogen in a process called 'power to gas', that involves exploiting renewable sources for the creation of methane.
- Water purification and oxygen production: the integration process with bacteria and algae is being studied. This implies the use of CO_2 and dirty water - nourishing for plants - to purify the latter and also release oxygen. The process takes place in a reactor called 'photo-bio reactor' which with the help of sunlight repeats the process of photosynthesis. The algae and bacteria that are created can be reused later as biomass in a virtuous circle.
- Enhanced oil recovery (EOR): this technique consists of using gases, including CO_2, to help extracting oil out of the field. When the pressure in the liquid is low or the reservoir is at the end of its life, this process is used to collect what remains. It consists of injecting gas into the field, pushing the oil towards the exit. This process can take place by injecting pure CO_2 or mixed with water and depending on the temperature and pressure conditions there is a variation in the viscosity of

the oil, helping its flow. It must be considered that a part of the CO_2 is stored in the reservoir instead of oil while a part returns to the surface with it, but can be easily separated and reintroduced. The advantage of this technique is that CO_2 is stored and at the same time exploited to extract oil, making the process profitable and highly exploited [30].

3.3.1 A new idea

The end uses described in the previous paragraph are the best known and most used today. There is a new idea recently developed that we can always categorize as an end use. This is the prototype of an artificial leaf, studied by the Italian Institute of Technology in the Turin office [31]. The idea of this prototype is to treat the captured CO_2 by reducing it into reusable compounds with added value, both in the energy and industrial fields. The energy required for the process is produced in a renewable way through photovoltaic energy. The device as a whole is shown in the figure 3.2.

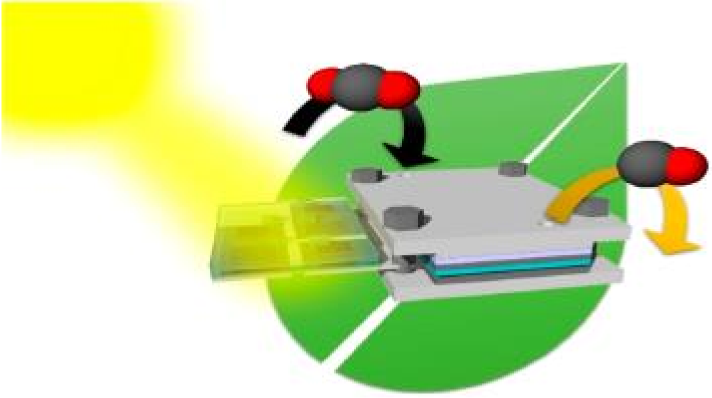

Figure 3.2 - Artificial leaf. Source: ACS Sustainable Chem. Eng. 2020, 8, 7563−7568

The process combines the possibility of storing solar energy in the form of chemical energy with the possibility of converting, with this energy, CO_2 into a reusable chemical product. In this way the CO_2 is directly treated and reused without the need to store it. The idea artificially takes up the natural phenomenon of photosynthesis. In fact, the process consists in producing electricity with sunlight through the use of photovoltaic panels. In this way, not only is CO_2 reused, but it is also done in a sustainable way. These photovoltaic cells are of the 'dye sensitized solar cell' (DSSC) type, which also allow to work with indirect or artificial light. [32]. The energy produced in this mode is used by a reactor for electrolysis of CO_2 into other chemical compounds. The reaction that takes place in the cell is the reduction of CO_2 (CO_2RR), which, based on the potential applied, produces carbon monoxide (CO) as main product. Other minor co-product are the formic acid (HCOOH) and the hydrogen (H_2). This last one is obtained because the reactions are carried out in water-based electrolyte and the electrolysis reaction can happen. These molecules have a non-negligible calorific value and are reusable for combustion. Ideally, a virtuous circle could be created in which these products are burned, and the CO_2 produced is reused. Furthermore, these products are often used in industry for the production of chemicals. The most interesting molecule in this context is CO, which is a platform molecule in many chemical processes and is easily burnable. The most innovative part of the device is the integration between the two processes. In fact, electricity is not produced on one side and then used in the reduction cell, but the photovoltaic cell and the reduction cell directly share an electrode. This makes the process faster and less prone to electrical losses, thanks to the direct connection. Furthermore, this should allow for some constructive convenience. In this way, the working curves of the two phases overlap and the intersection point is the working point of the system as a whole. This device is still being improved, in order to optimize the overall efficiency of the system by finding the correct operating point without one of the two parts acting as a bottleneck.

From a practical point of view, the prototype works at ambient pressure, so the use of resources for CO_2 compression would be avoided. In addition, it works at room temperature, saving energy even in this context. It must be considered that the energy used for the reduction comes from a solar source, therefore it is free. Furthermore, the process benefits economically from the reuse of the gases produced. Although, for the moment, this is still minimal due to the cost of the prototype itself. Anyway, despite the economical point of view, this technology is helpful to fight against the climate change. Therefore, it is of common benefit to develop the idea trying to maximize the return while keeping costs as low as possible.

3.4 Purpose of the thesis

In this chapter, the CO_2 capture phase has been omitted. However, all the analyzed systems require a flow of CO_2. The latter must either be produced on purpose – through inexpensive and not environmentally useful process - or captured and separated from the rest of the gases. This artificial leaf prototype currently uses a stream of CO_2 stored in a pre-loaded cylinder for testing. The final idea is to couple to this system also one for the capture of CO_2 from the environment or exhaust gas. In this way, at the entrance of the pre-existing prototype, it will be possible to have a flow of CO_2 which has been prevented from being in the environment, thus reducing the greenhouse effect. Furthermore, this will occupy the last piece for the creation of the virtuous circle envisaged by the idea of the artificial leaf. Figure 3.3 shows this concept just mentioned. Considering the reduction prototype integrated with the functioning photovoltaic system, net of optimizations still necessary, only the capture element is missing. This figure also shows the division of storage and capture paths, which however can also be connected. However, due to the shortcomings of the storage technologies, it was decided not to consider the storage phase in the process. So, we can think to use immediately the products.

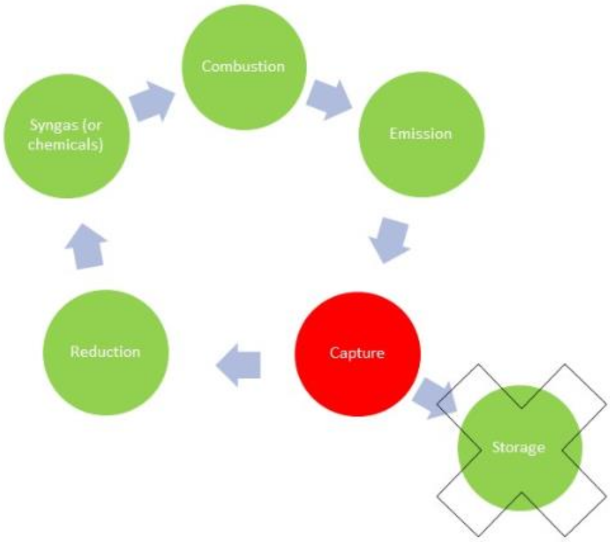

Figure 3.3 - CO_2 virtuous cycle.

The aim of the final work is not only studying a CO_2 capture method that can be coupled with the artificial leaf, but focuses on the final production of syngas, that is a mixture of CO and H_2. This means that the global process will no longer just have to capture and reduce CO_2, but also produce an important quantity of hydrogen, in addition to that already produced from the reduction system, for this reusable blend. This mixture can be used again as a fuel for the production of energy, both in classical processes such as internal combustion [33], and in flameless processes, such as fuel cells. Furthermore, it can also be used in processes such as gas-to-liquid (Fischer-Tropsch processes [34]) or biological fermentation [35], where the gas mixture is treated and new hydrocarbons or molecules are produced for the chemical industry. In this framework, considering the leaf as a starting point, the idea is to study a system that is able to capture and concentrate the CO_2, necessary for the reduction cell, and at the same time produce H_2 for the final syngas. The CO_2 will have to come from exhaust gases or from the environment in order to reduce greenhouse gas emissions. The capture and reduction cells must be coupled with each other, allowing the captured CO_2 to flow directly into the reduction cell. Furthermore, as for the leaf, the capture cell will also have energy supplied by a renewable energy source, possibly photovoltaic energy. In the end, in this way, we will have that the capture cell will supply CO_2 to the reduction cell, which will main produce CO. The hydrogen produced in the capture cell will join in the final syngas.

In this thesis we will start to implement this idea. First of all, in the following chapter the energy required for the capture phase will be dealt with from the thermodynamic point of view, a common aspect for both the described paths. Later, in chapter 5, the functioning of an electrochemical capture system will be experimentally analyzed, replicating a system present in the literature and trying to optimize it. We will simulate the capture from an exhaust gas mixture. This system, in addition to capturing CO_2, will also make it possible to produce an important amount of hydrogen. In the next chapter, the sixth, we will show the current modifications to the pre-existing capture system to make the system compatible with coupling and the energy results obtained. In the last chapter, a first experimental solution of a coupled capture-reduction system will be proposed, which in this phase will still be powered by a classical source. At the end of the work, we will have a system able to both capture the CO_2 and produce a syngas. All experimental tests were carried out with the 'CO_2 reduction' research team at the Italian Institute of Technology in Turin (CSFT @ POLITO).

4. Theoretical CO_2 capture phase

From this chapter on, we will focus on the actual capture of CO_2. Our aim, in particular, is to study a procedure that can be integrated with the idea of the artificial leaf, in order to have the complete process in a single machine. The idea involves, as analyzed in the previous chapter, to capture the CO_2 and convert it directly into a reusable product. In this chapter we will focus on the theoretical evaluation of the phenomenon.

First of all, let's consider capturing CO_2 only in gaseous conditions. Therefore, the capture can be done considering separating from the rest the CO_2 present in the exhaust gases or in the atmosphere. This process needs to consume energy, as for the compression process. The latter cost has been eliminated by considering working at ambient pressure with a direct utilization of the captured CO_2. This condition is not only a theoretical approximation, but it is a situation obtainable in the experimental phase, as will be observed later. On the other hand, in the case of capture it is not possible to approximate the working condition to a situation in which the CO_2 is not separated from the other gases present in the mixture and all the mixture containing climate-altering gases is directly treated. Therefore, while not considering a compression phase, it is necessary to separate the CO_2 for several reasons:

- Presence of toxic gases and harmful substances: some substances, mainly present in larger quantities in the exhaust fumes, are toxic or harmful for existence and for the technologies available. It is necessary to avoid treating toxic gases for living beings, as these could create potentially dangerous mixtures especially for professionals. In the initial mixture there may also be substances harmful to the technologies in use. In fact, some substances such as powders could clog or damage the ducts of the device. Other substances, on the other hand, could be harmful to the components of the device, corroding it or preventing correct operation, as in the phenomenon of component deactivation. These substances could also create problems for the catalysts, causing them to work under non-optimal conditions.

- Presence of non-climate-altering gases: large quantities of non-climate-altering gases are present in the exhaust gases, but especially in the environment. These, while non-toxic, could be harmful to certain systems. Furthermore, treating a large amount of gas unnecessarily would lead to avoidable subsequent waste of resources. In this way it is also possible to have technologies of smaller dimensions and costs, which treat only the strictly necessary quantity.

Hence, we have many reasons to separate the CO_2 without treating the entire full stream. Furthermore, many problems are more related to capture from exhaust gases, others to capture from the environment. The choice of the source from which to capture is a fundamental aspect, both from the technological point of view - instrumentation, gas cleaning, dimensions - and energy. Subsequently, the energy differences between these two processes will also be dealt with, in order to have an overall picture.

4.1 Thermodynamic

This paragraph describes the thermodynamic methodology used to theoretically calculate the work required to capture CO_2 regardless of the source.

First of all, it must be emphasized that the following analysis will consider the separation of CO_2 into a two-component mixture - i.e. air plus CO_2. This assumption facilitates the analysis and is likely, since in general it can be considered to have a fixed composition of two gases: a climate-changing agent - CO_2 - and a non-climate-changing agent - air or exhaust gas - which do not change their composition during the process.

Another parameter to consider is the composition of this mixture, which depends on the starting gas. As seen in table 3.1 of paragraph 3.1, depending on the source on which it is decided to act, there is a different initial concentration of CO_2. This affects the work required to separate it from the remaining component. In our calculations we consider a variation between 0% and 14% of initial CO_2 in the exhaust gases, while we consider a variation between 200 ppm and 900 ppm of CO_2 in the ambient air. This is because the capture from exhaust gas can take place considering combustion of methane, with CO_2 equal to about 4%, or from coal, with CO_2 equal to about 12%. For the environment, on the other hand, the current standard concentration is equal to 400 ppm, but could rise or fall by a few hundred based on climate change. Furthermore, the CO_2 in the environment is not constant over the entire earth's surface but can change where there are areas of greatest emission [36].

Thus, there will be one inlet flow A - flue gas or ambient air - and two outflows. They will be a stream B with CO_2 at a higher concentration, ready to be either transported or used in one of the final uses, while the other stream C will be the waste stream with possibly the residual CO_2, which will go into the environment [37]. The process is schematized in figure 4.1.

Figure 4.19 - CO_2 separation scheme. Source: Bains et Al. 'CO_2 capture from the industry sector'

Other fundamental parameters for the final result are the final purity and the percentage of capture [38]. The first, the final purity, consists of the desired CO_2 concentration - in molar terms - at the end of the process. This means that the separation may not be complete, leading to a final stream that is composed of CO_2 - more than the concentration of the initial stream - but not necessarily 100%. The second concept, the capture percentage, consists of the amount of CO_2 that is intended to be captured - in molar terms - from the initial amount. One can think of capturing all the CO_2 present in a given stream or only a part, if sufficient. In addition to the latter case, the situation will also be analyzed in which the objective is to have a CO_2 concentration of 300 ppm in the discarded flow that will go into the environment. This concentration is the ideal one considering we want to keep the pre-industrial trend.

In our analysis we will analyze four cases for both exhaust gas capture and ambient air capture. In each of these we will analyze the variation of a certain parameter keeping the others constant:

1. Initial CO_2 percentage change; constant outlet purity and capture percentage.
2. Capture percentage variation; constant outlet purity and initial CO_2 percentage.
3. Outlet purity variation; constant initial CO_2 percentage and capture percentage.
4. Initial CO_2 percentage change; constant outlet purity and fixed amount of CO_2 in the waste stream.

Thermodynamically we consider first of all the principle of conservation of mass. This applies to the total flow and to the two components. We considering always to have mixtures of ideal gases. Considering a two-component flow with an inert gas (other) and CO_2 and considering $\dot{m}_i$ the mass flow rate for the i-th stream, we have the global mass balance equation:

$$\sum_{i=A}^{C} \dot{m}_i \left[\frac{kg}{s}\right] = 0 \tag{4. 1}$$

The mass flow rate $\dot{m}_i$ is given by the product of the molar flow rate $\dot{n}$ and the molar mass MM_i, as shown by the following equation:

$$\dot{m}_i \left[\frac{kg}{s}\right] = \dot{n}_i \left[\frac{mol}{s}\right] * MM_i \left[\frac{kg}{mol}\right]$$

(4. 2)

We assume the absence of chemical reactions in this phase of theoretical study. In fact, we consider a simple gas mixture separation process. So, for this, we obtain that the conservation equation of mass is valid in molar terms:

$$\sum_{i=A}^{C} \dot{m}_i \left[\frac{kg}{s}\right] * \frac{1}{MM_i} \left[\frac{mol}{kg}\right] = \dot{n}_i \left[\frac{mol}{s}\right] = 0$$

(4. 3)

Always considering the absence of chemical reaction and assuming the term y the mass fraction, we can write the mass balance equations for the components of the total flux:

$$\sum_{i=A}^{C} \dot{m}_i \left[\frac{kg}{s}\right] * \ y_{i,CO_2}[-] = 0$$

(4. 4)

$$\sum_{i=A}^{C} \dot{m}_i \left[\frac{kg}{s}\right] * \ y_{i,OTHER}[-] = 0$$

(4. 5)

Considering the relationship between mass and molar streams and assuming the term x_i the molar fraction, we can expose the abovementioned equations for the components in molar terms:

$$\sum_{i=A}^{C} \dot{n}_i \left[\frac{mol}{s}\right] * \ x_{i,CO_2}[-] = 0$$

(4. 6)

$$\sum_{i=A}^{C} \dot{n}_i \left[\frac{mol}{s}\right] * \ x_{i,OTHER}[-] = 0$$

(4. 7)

Generally, as a matter of convenience, calculations will develop in molar terms. Indeed, most scientific papers treat CO_2 capture budgets in these terms. Moreover, once a certain time interval has been set, the previous equations are also valid in absolute terms, that is, without considering their instantaneous value. In molar terms it is also possible to express the concept of percent capture, with the following equation:

$$percent\ capture\text{:}\ \frac{captured\ moles\ of\ CO_2\ in\ outlet\ flow}{total\ moles\ of\ CO_2\ in\ inlet\ flow} = \frac{\dot{n}_B \left[\frac{mol}{s}\right] * \ x_{B,CO_2}[-]}{\dot{n}_A \left[\frac{mol}{s}\right] * \ x_{A,CO_2}[-]}$$

(4. 8)

Similarly, it is possible to express the concept of the outlet purity in molar terms with the following equation:

$$outlet\ purity\text{:} \frac{captured\ moles\ of\ CO_2\ in\ outlet\ flow}{total\ moles\ in\ outlet\ flow} = \frac{\dot{n}_B \left[\frac{mol}{s}\right] * x_{B,CO_2}[-]}{\dot{n}_B \left[\frac{mol}{s}\right]} = x_{B,CO_2}[-]$$

(4. 9)

Now, after analyzing the mass conservation principle, we will analyze the theoretical energy necessary to have the CO_2 separation from the incoming stream. The theoretical minimum work is the net change in the potential work of the system, that is the exergy [39]. To have the minimum work, we consider that the incoming flow undergoes an isothermal and isobaric transformation, in which only splitting takes place. Furthermore, we consider the system as adiabatic. Thus, the minimum work W_{MIN} necessary for the separation is given by the net difference of the exergy of the flows Ψ_i in the system, as shown in the following equation:

$$W_{MIN}[J] = \Delta\Psi_i[J]$$

(4. 10)

Considering the previously made assumptions, the change in work potential equals the change in Gibbs free energy. Considering *R* the universal gas constant, *T* the temperature of the system, n_i the number of moles of the flux and *x* the mole fraction, we obtain the following equation for calculating the minimum work:

$$W_{MIN}[J] = R[\frac{J}{K * mol}] * T[K] * (\sum_{i=A}^{C} n_{i,CO_2}[mol] * ln\, x_{i,CO_2}[-] + \sum_{i=A}^{C} n_{i,OTHER}[mol] * ln\, x_{i,OTHER}[-])$$

(4. 11)

Thermodynamically, the formula expresses the variation that the partial pressures of the components of the initial mixture undergo. In fact, the only process that theoretically needs work is the partial pressure variation. This is because if the flow were simply split maintaining the same initial conditions for both flows, the work would be null. The partial pressure variation consists of a compression or expansion that the affected gas undergoes. If the partial pressure rises, the gas is compressed and it needs energy. If the partial pressure drops, the opposite phenomenon occurs, producing energy. The partial pressure of the components changes as the purpose is to change the concentration of gases in the outgoing streams, with respect to the incoming one. CO_2, which is generally concentrated, increases its partial pressure and therefore requires energy. The system must, however, take into account the behavior of all the gases present in the system, therefore both CO_2 and the inert gas.

It is possible to normalize the necessary work by referring it to the input moles n_{INLET} through the following equation:

$$W_{MIN,MOL}[\frac{J}{mol}] = \frac{W_{MIN}[J]}{n_{INLET}[mol]}$$

(4. 12)

Also, it is possible to normalize the necessary work with respect to the moles of CO_2 captured. In this way it is possible to compare the results of different cases based on the set capture conditions - such as outlet purity and percent capture - without considering the amount of flow. This can be calculated through the following equation:

$$W_{MIN,CO_2MOL}[\frac{J}{mol_{CO_2}}] = \frac{W_{MIN}[J]}{n_{OUTLET\ CO_2\ CAPTURED}[mol_{CO_2}]}$$

(4. 13)

It needs be remembered that the signs of the flows, both for the conservation of mass and for the calculation of energy, must be consistent with the reference system adopted at the time of the calculations.

As mentioned above, the aim is to capture CO_2 while minimizing the work required. This is because the process must be done for environmental reasons and therefore it is convenient to use the least necessary work. Since in reality it is thermodynamically impossible to obtain a process with efficiency equal to 1, the real work needed will always be greater than the minimum ideal work. This concept is expressed with second-law efficiency through the following equation:

$$\eta[-] = \frac{W_{MIN,CO_2MOL}[\frac{J}{mol_{CO_2}}]}{W_{REAL,CO_2MOL}[\frac{J}{mol_{CO_2}}]}$$

(4. 14)

This equation to tend towards one must be maximized. This means that since the term W_{MIN,CO_2MOL} is fixed and it is the minimum to aim for, the denominator W_{REAL,CO_2MOL} must be minimized by trying to use less energy-intensive processes. Furthermore, it must be remembered that the two terms of the report must correspond to the same conditions of use, such as outlet purity, percent capture and temperature.

4.2 Results

This part shows the results obtained by applying the methodology described in the previous paragraph. The results show the work per unit of CO_2 captured required under the study conditions. Cases 1., 2., 3. and 4. were studied, as described below. For all cases the following assumptions were made:

Parameter	*Value*
$R\left[\frac{J}{K*mol}\right]$	8.314
P[Pa]	101325
T[K]	298
n_{INLET} *[mol]*	40.895

Table 4.5 - Parameters for theoretical CO_2 work calculation

For each case, the situations of capture from exhaust gases – e.g., 1.a - and directly from the environment – e.g., 1.b - have been studied. The applied methodology is the same, but the CO_2 concentration at the entrance changes by several orders of magnitude. This was done in order to compare the two possibilities of CO_2 capture from an energy point of view.

- 1. In this case we consider having 100% outlet purity - i.e. pure CO_2 at the outlet - and having a percent capture equal to 50% - i.e. capturing half of the available CO_2. Furthermore, for the capture from exhaust gases - table 4.2a - we consider a range of CO_2 input - $x_{A,CO2}$ - concentration between 0% and 18% in molar terms. For direct capture from the environment - table 4.2b - we consider to vary between 0 ppm and 900 ppm.

$x_{A,CO2}$ [%]	W_{MIN,CO_2MOL} $[\frac{kJ}{mol_{CO_2}}]$
0	0
2	10.441
4	8.711
6	7.694
8	6.968
10	6.402
12	5.938
14	5.543
16	5.199
18	4.894

Table 4.2a - Case 1a: capture from flue gas

$x_{A,CO2}$ [ppm]	W_{MIN,CO_2MOL} $[\frac{kJ}{mol_{CO_2}}]$
0	0
100	23.581
200	21.863
300	20.859
400	20.146
500	19.593
600	19.141
700	18.759
800	18.428
900	18.136

Table 4.2b - Case 1b: direct capture from ambient

- 2. In this case we again consider the outlet purity set at 100%, while the percent capture varies from 0% to 100%. This means that the system goes from a condition in which it captures nothing to one in which all available CO_2 is captured. In this way it is possible to observe the progress of the work with respect to the quantity captured and it is possible to compare the difference between the work required, with the same percent capture, in case of flue gas - table 4.3a - and in case of capture from the environment - table 4.3b. For the case of capture from exhaust gas, an initial amount of CO_2 equal to 4% was set, as for the combustion of natural gas. While for the capture from the environment the quantity of 400 ppm of CO_2 has been set, the current concentration value.

Percent capture [%]	W_{MIN,CO_2MOL} $[\frac{kJ}{mol_{CO_2}}]$
0	0
10	8.099
20	8.232
30	8.376
40	8.535
50	8.711
60	8.910
70	9.140
80	9.416
90	9.774
100	10.403

Table 4.3a - Case 2a: capture from flue gas

Percent capture [%]	W_{MIN,CO_2MOL} $[\frac{kJ}{mol_{CO_2}}]$
0	0
10	19.514
20	19.652
30	19.801
40	19.965
50	20.146
60	20.350
70	20.585
80	20.866
90	21.229
100	21.863

Table 4.3b - Case 2b: direct capture from ambient

- 3. In this case, as in case 2, we consider the same initial CO_2 quantities: 4% for capture from exhaust gas - table 4.4a - and 400 ppm for capture from environment - table 4.4b. We set the value of the capture percentage at 50%, as in case 1. The value of outlet purity varies from 0%, a situation in which nothing is captured and the incoming flow is not split, and 100% in where the final stream of interest is pure CO_2. In the range there is the situation in which the final flow of interest is not composed only of CO_2, but also of a portion of the inert gas that makes up the initial mixture. This parameter usually depends on the desired CO_2 stream composition after capture, based on usage.

Outlet purity *[%]*	W_{MIN,CO_2MOL} $[\frac{kJ}{mol_{CO_2}}]$
0	0
10	1.165
20	2.725
30	3.788
40	4.620
50	5.328
60	5.966
70	6.571
80	7.174
90	7.822
100	8.711

Table 4.4a - Case 3a: capture from flue gas

Outlet purity *[%]*	W_{MIN,CO_2MOL} $[\frac{kJ}{mol_{CO_2}}]$
0	0
10	12.096
20	13.948
30	15.102
40	15.978
50	16.711
60	17.367
70	17.984
80	18.596
90	19.251
100	20.146

Table 4.4b - Case 3b: direct capture from ambient

- 4. In the latter case, as in case 1, the outlet purity value was set at 100%. The initial CO_2 values vary as in case 1: between 0% and 18% for capture from flue gas - table 4.5a - and between 0ppm and 900 ppm for the environment - table 4.5b. In this case, unlike case 1, the percent capture has not been set at a percentage value but has been set so that 300 ppm of CO_2 are present in the discarded and directed flow into the environment, equal to the CO_2 value in a pre-industrial environment. In this way, a theoretical scenario is imagined in which CO_2 is to be captured so as not to modify the concentration of CO_2 already present in the environment. This scenario can be evaluated for both capture cases as the treated air comes in any case from the environment, as air is used during combustion.

$x_{A,CO2}$ [%]	W_{MIN,CO_2MOL} $[\frac{kJ}{mol_{CO_2}}]$
0	-22.576
2	11.990
4	10.315
6	9.310
8	8.586
10	8.015
12	7.543
14	7.139
16	6.784
18	6.467

Table 4.5a - Case 4a: capture from flue gas

$x_{A,CO2}$ [ppm]	W_{MIN,CO_2MOL} $[\frac{kJ}{mol_{CO_2}}]$
0	-22.576
100	-21.215
200	-20.567
300	0
400	19.725
500	19.412
600	19.141
700	18.902
800	18.688
900	18.493

Table 4.5b - Case 4b: direct capture from ambient

4.3 Discussion

In this last paragraph we will discuss the results obtained, first case by case and finally collectively.

- 1. In this first case we can observe that for the same quantity captured - in proportion - and the final purity of the stream, the higher the initial concentration, the less work per unit of CO_2 is required. This is valid for both capture methods.

We can see these trend for the capture in the chart 4.1.

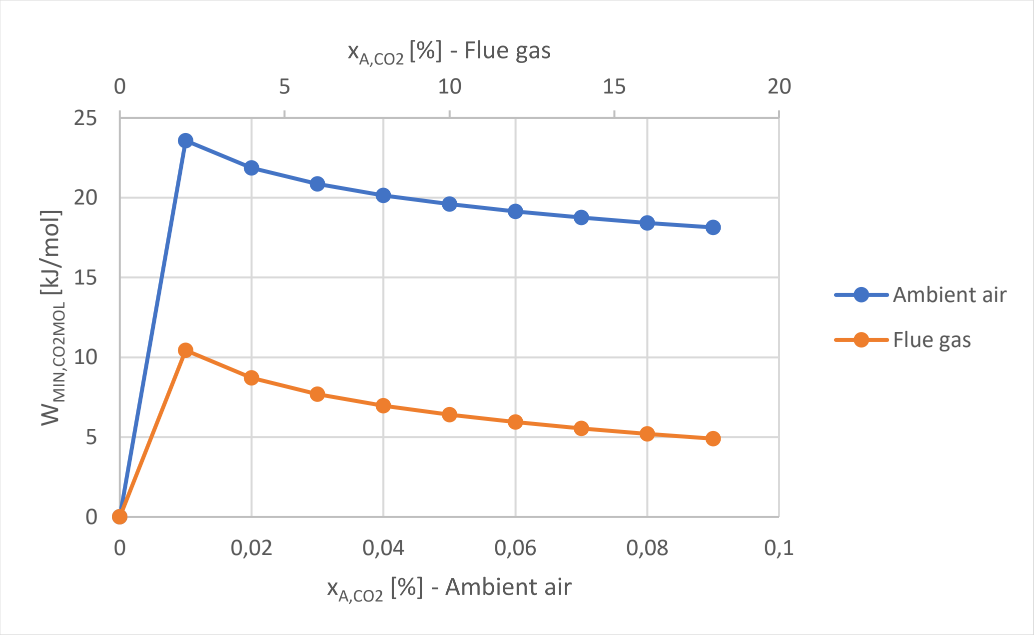

Chart 4.1: Capture work with variation of the initial concentration for ambient gas

This happens because the more CO_2 is present, the easier it is for the system to find and separate it. It is therefore obtained that the capture from exhaust gases is less energetically expensive than that from the environment. Paradoxically, to have an energetic advantage in capturing from the environment, concentrations in ppm should be higher, which however are not environmentally friendly. It should also be emphasized that in absolute terms, to capture the same amount of CO_2, if this were the goal, it would be necessary to treat a greater amount of air in the case of capture from the environment as the concentration is lower. As explained in the thermodynamic section, the physical process is governed by the partial pressure of CO_2, which starts from a certain initial value and must be brought to a certain final value according to the working conditions. In this case, the higher the initial partial pressure, the less work is required.

- 2. In this second case, the capture percentage varies. In both cases, regardless of the initial concentration, the higher the quantity captured, the higher the work required. This is because the more the percentage to be captured increases, the more expensive it becomes to separate all the molecules. This happens because to obtain the necessary work value it is necessary to consider all the flows and not just that of CO_2. The difference between capture from flue gas and from environment is due to the fact that the initial concentration is different therefore the initial partial pressure is different. As in the first case, the capture from the environment turns out to be more expensive and needs to deal with larger incoming flows. We can see the trend in the chart 4.2.

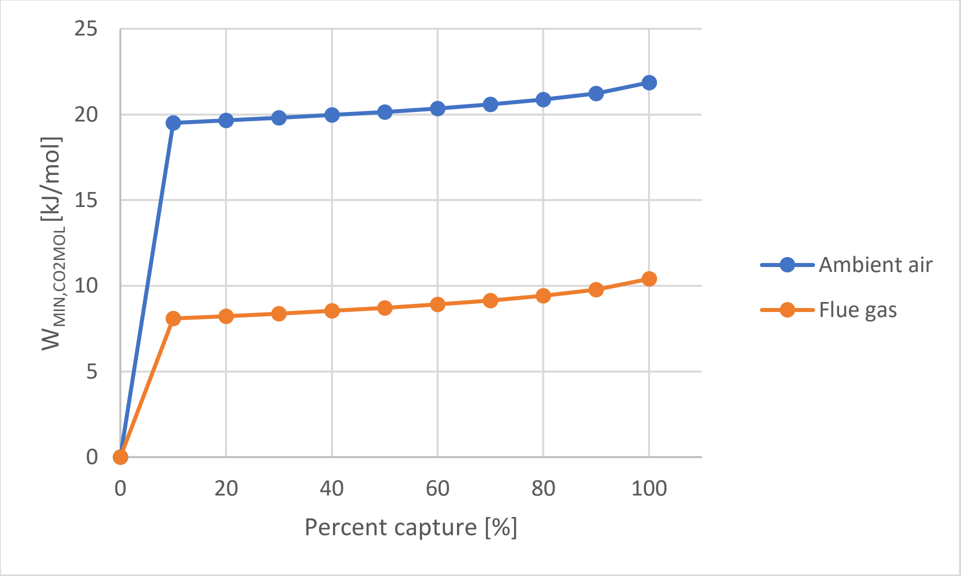

Chart 4.2: Capture work with variable percent capture

- 3. In this case, the final purity and therefore the desired final partial pressure vary. In fact, the purer the final flow, the higher the need for necessary work. The same effect is observed between capture from the environment and from flue gas, with the latter having a higher partial pressure and therefore a lower required work. We can see the trend in the chart 4.3. The calculations are carried out while maintaining a fixed capture rate, therefore the phenomenon described in case 2 does not affect here.

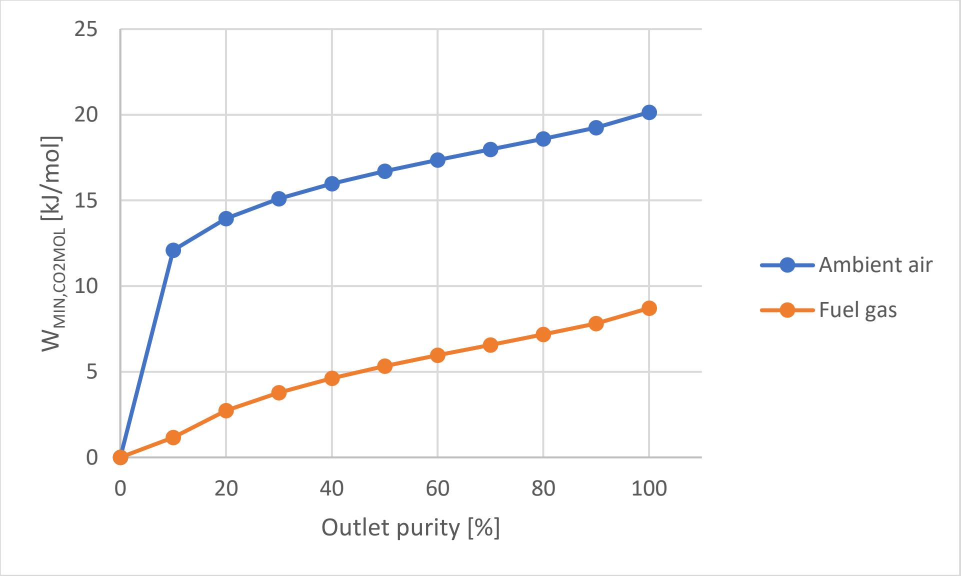

Chart 4.3: Capture work with variable output purity

- 4. In the latter case, the particularity of wanting a quantity of CO_2 fixed in the flow discharged into the environment leads to negative working values in the event that the inlet concentration is lower than the required discharge 300 ppm. This is because in such a situation it would be necessary to inject CO_2 into the system instead of capturing it. For concentration values greater than 300 ppm, however, the behavior is exactly the same as in the other cases: the higher the initial concentration, the lower the work. Coherently, for initial concentration of 300 ppm the work is zero because we have not to capture or inject CO_2. We can see the complete phenomenon in the chart 4.4 for both the capture cases.

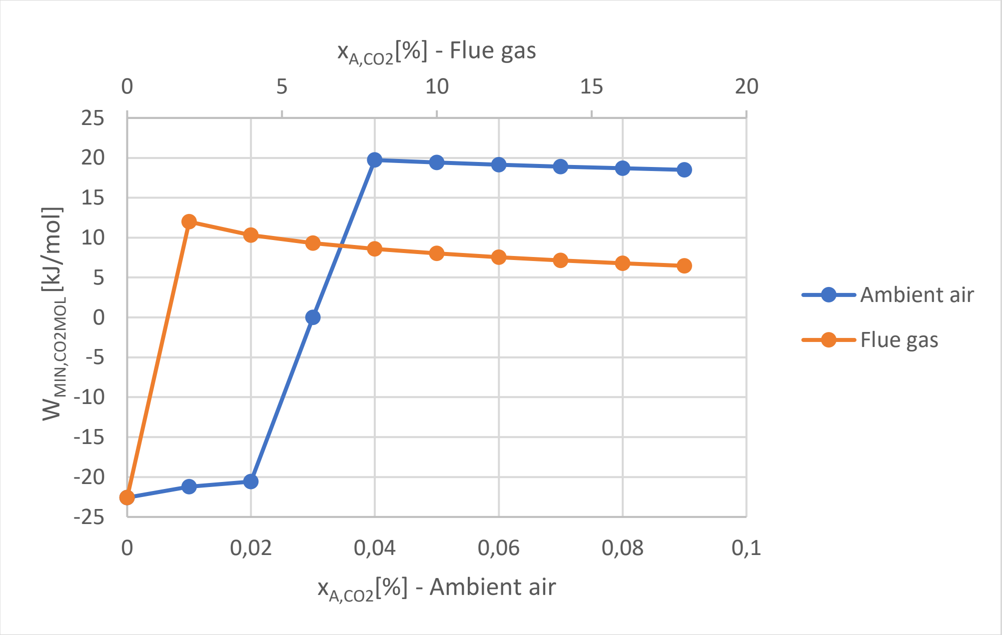

Chart 4.4: Capture work in case of fixed output for variable CO_2 input

This solution is generally not used, as it is preferred to consider capturing all the available CO_2 or capturing a predetermined amount for one's own purposes.

From a general point of view, we can say that the higher the initial concentration of CO_2, the less work required for the capture with equal percentage of capture and purity at the outlet. This means it is more cost effective to capture CO_2 from exhaust gases. The capture percentage shows that if the environment tolerated minimal quantities of CO_2 it would be possible to use processes with lower capture percentages and therefore with less work. Likewise, the lower the purity of the outgoing CO_2 stream, the less energy will be needed. However, at the present time, the end uses almost all foresee the use of pure CO_2 flows, both because, as previously mentioned, costs are avoided later, and because some applications are not able to treat non-pure CO_2 flows. In particular, this also happens for the artificial leaf, which treats an incoming pure CO_2 stream.

However, in some situations the capture from the environment could be favorable because it can be done anywhere. Also, it is generally not necessary to treat the air before it flows into the system, which must be done for exhaust gases due to pollutants. From an energetic point of view, the comparison with direct capture is always inconvenient. It could be convenient in some situations if working in conditions of low output purity, around 5%, and low capture percentage. In case of outlet purity of 5% and percent capture of 50% we have to use about 10 $\frac{kJ}{mol_{CO_2}}$ of work to capture from the ambient (300 ppm). This value is comparable with the value of capture from flue gas produced by methane combustion (2-4% of CO_2 in the gas) but with an output purity of 100%. This last solution is being studied, in fact there are analyzes in favor of the use of flows of this type through technologies that exploit microalgae [38].

In the following chapters we will assume to work with streams for the capture of high incoming CO_2 - as exhaust gas - to use less energy. Furthermore, the goal for purity at the outlet is to reach 100% for integration with the artificial leaf. The capture percentage should be as high as possible to verify the effective functioning of the system. Finally, as the technology is under development, it is necessary to work with easily observable CO_2 concentrations for reasons of simplicity of application.

4.4 Energy penalty

As seen for the compression phase, also the capture phase represents a source of penalties on the efficiency of the plant or on the yield of the fossil fuel used. This is why it is necessary to use a renewable source for the capture phase in order not to increase the CO_2 released into the environment or the energy needed to capture it. To calculate the penalty represented by the capture phase, we consider to proceed in the same way as in paragraph 3.2 for the compression phase. We directly assume the same energy cost calculated in that paragraph, equal to 1.17 $\frac{kWh_e}{kg_{CO2}}$ if we consider producing electricity from a coal plant with the same efficiency and the same emission factor. Now, considering to capture the CO_2 to send it to the artificial leaf, we need to have a pure CO_2 flow (100% outlet purity). Furthermore, we consider to capture all the CO_2 produced per unit of energy produced - as was done for compression - so that the capture percentage is equal to 100%. Assuming that the CO_2 concentration in the flue gas is 16% and carrying out the same operations done previously, we obtain that the work per mole of CO_2 captured is equal to 6.81 $\frac{kJ}{mol_{CO_2}}$. This value will be our reference for the future second-law efficiency calculations. Now, can convert the energy from kJ to kWh_e and MJ and we can refer the obtained values to the CO_2 mass unit with the following formulas:

$$w\left[\frac{kWh_e}{kg_{CO_2}}\right] = w\left[\frac{kJ}{mol_{CO_2}}\right] * \frac{1}{3600}\left[\frac{kWh_e}{kJ}\right] * \frac{1000}{\mu}\left[\frac{mol_{CO_2}}{kg_{CO_2}}\right] \tag{4. 15}$$

$$w\left[\frac{MJ}{kg_{CO_2}}\right] = w\left[\frac{kJ}{mol_{CO_2}}\right] * \frac{1}{1000}\left[\frac{MJ}{kJ}\right] * \frac{1000}{\mu}\left[\frac{mol_{CO_2}}{kg_{CO_2}}\right] \tag{4. 16}$$

By substituting the data in the eq. 4.15 and 4.16, we obtain, respectively, an energy need of 0.043 $\frac{kWh_e}{kg_{CO_2}}$ and 0.155 $\frac{MJ}{kg_{CO_2}}$. Considering that the energy used for the capture phase is electricity, we can say that 0.043 kWh of energy to separate one kg of CO_2 correspond to the 3.66% of energy that a coal plant produces for every kg of CO_2 emitted. This is the minimum energy penalty that can be incurred and, as in the case of compression, it is necessary to stay as close as possible to these values in order not to further lower the efficiency of the systems. Overall, considering both capture and compression, there is a minimum penalty of about 11%.

5. Electrodialysis system

After presenting the theoretical aspects of CO_2 capture, we will experiment with one of the possible solutions. As anticipated in the previous chapters, our aim is to couple the capture of CO_2 with the artificial leaf, also promoting the production of hydrogen. Before presenting the solution used, it is necessary to group together the reasons that led us to choose the solution to use:

- Ambient pressure: the reduction cell works at ambient pressure; therefore, it is not necessary to have gas under pressure at the exit of the capture phase, saving energy.
- Ambient temperature: in order not to use thermal sources and to work in the same environment with the photovoltaic cells and the reduction cell, it is necessary to adopt a solution that works at room temperature.
- No presence of toxic agents: for reasons of safety and social impact of the artificial leaf, we prefer to work with solutions that use non-toxic substances.
- Use of renewable sources: to ensure the carbon neutrality of the process it is necessary to use a renewable source as an energy source.
- Coupling with the artificial leaf: the capture phase, as mentioned, must be coupled with the artificial leaf, so electrochemical solutions that resemble the CO_2 reduction process are preferred.

This process, which involves the capture and release of CO_2 in conjunction with the production of hydrogen, is well connected with the electrochemical process of electrodialysis of a salt. In fact, the latter meets our requirements: it works at ambient pressure and at room temperature, does not use toxic solvents and can be powered with a renewable source. Furthermore, the electrochemical process is easier to integrate with that already present in the leaf. To put this into practice, we took up the experiment done by Nagasawa et Al. [40]. In this way, in addition to capturing CO_2, we can also produce hydrogen.

Last but not least, the solution chosen for the capture must minimize its energy cost as much as possible to be competitive with other existing solutions. In fact, as seen in paragraph 4.4, it is necessary to get as close as possible to a penalty of about 4%. In this sense, an analysis will be carried out in the following paragraphs.

5.1 Operation

The process used by Nagasawa consists of two phases: adsorption step and stripping step. Chemical adsorption, if present, consists in the capture of CO_2 by a solution that has a good affinity with the CO_2 itself. The stripping phase consists in the regeneration of the sorbent - to be reused for the capture phase - and in the simultaneous release of CO_2 in concentrated form. This last phase is generally the most energetically expensive and, in our case, it takes place through an electrochemical reaction and not through heat or pressure treatments. The substance used for the absorption is sodium bicarbonate ($NaHCO_3$) which can dissociate in Na^+ and HCO_3^- ions. Starting from the bicarbonate ion, to release CO_2 it is necessary to produce carbonic acid by adding H^+ ions. Then, further lowering the pH of the working ambient thanks to the presence of H^+ ions, the carbonic acid dissociated in water and gaseous pure CO_2. Globally, we have the following reactions – and concentration relations:

$$NaHCO_3 \rightleftarrows Na^+ + HCO_3^- \gg [NaHCO_3] = [HCO_3^-]$$

$$HCO_3^- + H^+ \rightarrow H_2CO_3 \gg [HCO_3^-] = [H_2CO_3]$$

$$H_2CO_3 \rightarrow H_2O + CO_2 \gg [H_2CO_3] = [CO_2]$$

Considering to work with an aqueous solution, the bicarbonate ions become from the dissociation of the salt used - $NaHCO_3$ – in solution, which has a slight basicity and, once it once has reacted and produced H_2CO_3, releases CO_2 when in contact with acidic substances. Hence, it is necessary to provide H^+ ions and simultaneously separate the metal ions from the bicarbonate ones; anions and cations have to be put away in order to have not a recombination. This last process, called electrodialysis, is the energetically expensive part of the overall process, i.e. the stripping and regeneration phase. Electrodialysis consists of a process in which, once a potential difference is applied to the two ends of the cell, the positive and negative ions of the salt migrate, favored by the presence of anionic and cationic membranes that allow the passage of only a certain ion. The process for the production of H^+ ions instead consists in the electrolysis of water, favored by the presence of a bipolar membrane. The cell arrangement can be four- or five-chamber and can use anion-only, cation-only, or both membranes depending on the direction of the ions. The arrangement chosen is the one presented as most advantageous by Nagasawa. It consists of a four-chamber cell - as shown in the figure 5.1, in which the acidification of the solution occurs in the two central compartments with the release of CO_2 in gaseous form. While in the outer two, the production of H^+ ions, necessary for acidification, but also of OH^- ions, necessary to retain the metal ions produced by electrodialysis, takes place. In particular, the cell used consists of the following parts:

- Cathode electrode: negative electrode that attracts positive ions. It is composed of a platinum foil.
- Chamber 2: an aqueous solution based on $NaHCO_3$ circulates in this chamber, in which it has the sole purpose of increasing the electrical conductivity to move the ions. In this compartment, with the help of the bipolar membrane alongside, there is the presence of H^+ ions which allow the production of hydrogen. In the Nagasawa case study this result was only a consequence of the need to have OH^- ions in the adjacent chamber. In our case, this hydrogen produced is seen as a further product of the process, which is used for the production of syngas, as per the initial objective.

- Bipolar membrane BPM: this membrane carries out the water electrolysis producing H^+ and OH^-. The protons flow to chamber 2 and the hydroxyl ions to flow to chamber 4.
- Chamber 4: this chamber is the solvent regeneration compartment. In fact, the OH^- ions arrive in this chamber from the bipolar membrane and the Na ions from the cationic membrane that divides this chamber from chamber 3. In this compartment the two ions can combine to form sodium hydroxide (NaOH), which is able, eventually, to capture CO_2 forming sodium bicarbonate. The latter is ready to restart the capture circuit. In this chamber NaCl – as electrolyte - is circulated, so as to allow good ionic conduction and to act as a buffer of Na^+ ions.
- Cathode Membrane CM: This membrane allows the passage of only one type of ions, the positive ones - in this case Na^+. They will only move from chamber 3 to chamber 4.
- Chamber 3: this is the feed compartment. A sorbent solution of $NaHCO_3$ is introduced into this chamber. This solution, after the electrodialysis process, will release sodium ions that go towards chamber 4. The bicarbonate ion will react with the H^+ ions coming from the right bipolar membrane to form H_2O and CO_2, releasing the latter in gaseous form. This chamber is therefore the one which releases the captured CO_2 in concentrated form.
- Bipolar membrane BPM: it works exactly like the previous one, releasing H^+ ions towards chamber 3 and OH^- ions towards chamber 1.
- Chamber 1: this chamber works in the same way as chamber 2, except that it accepts OH^- ions instead of H^+ ions as in chamber 2. In this way, an excess of OH^- ions remains in chamber 1, which allow the release of O_2 into the environment. Despite oxygen is a by-product of the reactions present, it can be seen as a positive aspect, as in the overall process CO_2 is captured and O_2 is released.

- Anode electrode: positive electrode that attracts negative ions. A potential difference or current is applied between this electrode and the cathode electrode which allows the system to work.

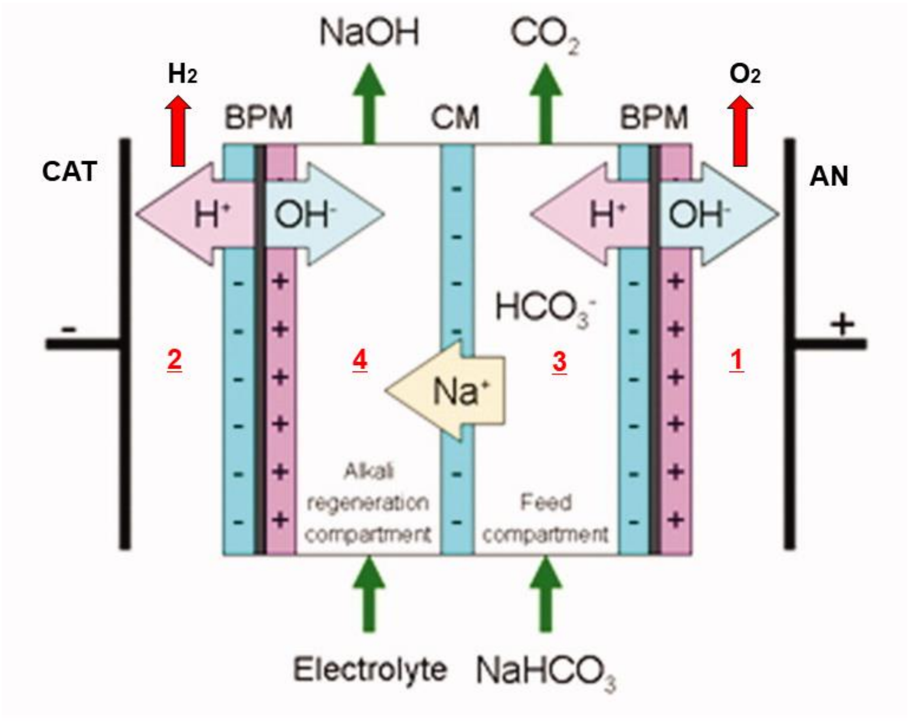

Figure 5.20: Basic configuration of the flow cell used (adapted from [40]).

From an operational point of view, the experiments were carried out using a laboratory cell mounted according to the described scheme. Each chamber has an inlet and an outlet, with a flow moved by a pump. The recirculated volume of solution, for every compartment, was 50 mL. In this first experiment, the outlet of each compartment was connected to the inlet of the same chamber, so as to ensure a continuous rewinding. The tests, lasting three hours, consist in applying a fixed current to the cell, while returning the voltage, based on the internal resistance. To measure the effectiveness of the process, the pH inside the cell 4 is measured: it is neutral at the beginning and then gradually becomes more basic with the continuous formation of NaOH. We can see the setup in the figure 5.2.

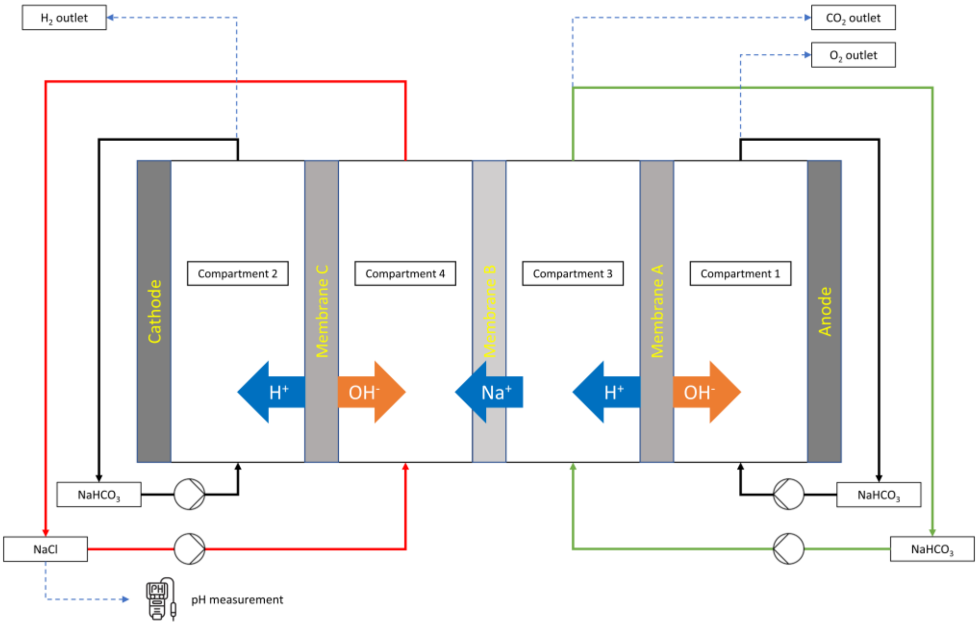

Figure 5.21: Setup of the electrodialysis system

In this case, the CO_2 to be captured is that present in the sodium bicarbonate, as there is no external input of CO_2 that regenerates the salt. To measure the quantity of CO_2 captured, it is sufficient to measure the concentration of OH^- ions present at the end of the measurement, compared to the initial ones, in the flow container of chamber 4. Considering the concentration of OH^- we can say that it, net of losses of non-measurable recombination, is equal to the concentration of CO_2 released. This is because the concentration of OH^- ions is equal to the concentration of Na^+ ions present to form NaOH. In turn, the concentration of the Na^+ ions present derives from the electrodialysis process that took place in chamber 3, so the concentration of Na^+ ions is equal to that of the HCO_3^- ions present in chamber 3. This can be observed through the following formula:

$$Na^+ + OH^- \rightarrow NaOH \gg [OH^-] = [Na^+]$$

$$NaHCO_3 \rightarrow Na^+ + HCO_3^- \gg [Na^+] = [HCO_3^-]$$

Considering the reactions shown at the beginning of the chapter, we can therefore state that the final concentration of CO_2 released is equal to that of the bicarbonate ion, which in turn is equal to that of the measured OH^- ion. Moreover, the final concentration of CO_2 released is equal to the concentration of the produced H^+ ions, in the same way of OH^- ions. This is affirmable since the stoichiometric coefficients of the reactions are all equal to 1. To measure the concentration difference of OH^- ions, the pH of the solution is measured, and then the following formulas are used:

$$pH = 14 - pOH$$

$$pOH = -Log[OH^-]$$

$$\Delta[OH^-] = [OH^-]_{FIN} - [OH^-]_{IN} = 10^{-pOH_{FIN}} - 10^{-pOH_{IN}} = 10^{pH_{FIN}-14} - 10^{pH_{IN}-14}$$

(5.1)

From this we have the difference Δ of OH^- ions, which is equal to the concentration of CO_2 $[CO_2]$ released in moles per liter of the initial solution in which the pH is measured:

$$\Delta[OH^-] = [CO_2]$$

(5.2)

Considering a certain volume Vol, that is the volume of the recirculated flow, we can obtain the number of moles obtained with the following formula:

$$CO_2mol[mol_{CO_2}] = [CO_2]\left[\frac{mol_{CO_2}}{l}\right] * Vol[l]$$

(5.3)

From the energetic point of view, the theory foresees that the necessary work is 0.8 $\frac{MJ}{kg_{CO_2}}$, equal to 35.2 $\frac{kJ}{mol_{CO_2}}$, for this system, based on alkaline carbonate solution [40]. The energy penalty for the theory value is 18.9% (eq. 3.3) and the second-law efficiency, with respect to the thermodynamic energy value (0.155 $\frac{MJ}{kg_{CO_2}}$), is 19.4% (eq. 4.14). However, the real work will be higher due to losses and irreversibility. During the experiment, a constant current is applied all the time, while the potentiostat used returns the voltage between the two electrodes of the cell. From the voltage V, the current density j and the area A, considering average values, it is possible to calculate the average power applied with the following formula:

$$P[W] = j\left[\frac{A}{m^2}\right] * V[V] * A[m^2] \tag{5.4}$$

From this, considering a time t of the experiment, it is possible to calculate the energy used with the following formula:

$$E[J] = P[W] * t[s] \tag{5.5}$$

Finally, having obtained the real energy used and the amount of CO_2 captured in the same period, it is possible to calculate the work w required for the capture per unit of CO_2 with the following formula:

$$w[\frac{J}{mol_{CO_2}}] = \frac{E[J]}{CO_2mol\left[mol_{CO_2}\right]} \tag{5.6}$$

5.1.1 Instrumentation

To build the system, an "ElectroCell, Micro Flow Cell" electrochemical reactor, with electrodes having an area of $0.001m^2$, was used. The bipolar membranes are fumasep FBM (FumaTech), while the proton membrane is Nafion Membrane N117 (Sigma-Aldrich). The catalysts, placed at both ends, are of Platinum. For the recirculation of the solution inside the four chambers of the cell a peristaltic pump Peri-Star Pro (WPI) is used. The current is provided by a source measure unit 2635A (Keithley), that also permit to perform the voltage acquisition. The control and measurement of the gas mixtures entering - N_2 and CO_2 - and exiting - CO_2, H_2 and O_2 - from the system are made by EL-FLOW select (Bronkhorst) mass flow controllers/meters. The reagents $NaHCO_3$, 99.5% (Sigma-Aldrich) and NaCl, 99.5% (Sigma-Aldrich) were used for the solutions, dissolving them in distilled water. The gases used are taken from Nippon Gases Rivoira cylinders. In figure 5.3 it is possible to see the exploded diagram of the flow cell used. Specifically, it is composed of gaskets (yellow rows) to prevent the escape of gases and liquids, of the frames that constitute the chambers, of the membranes, and of the electrodes. In figure we can see also the pathway of fluids inside the cell.

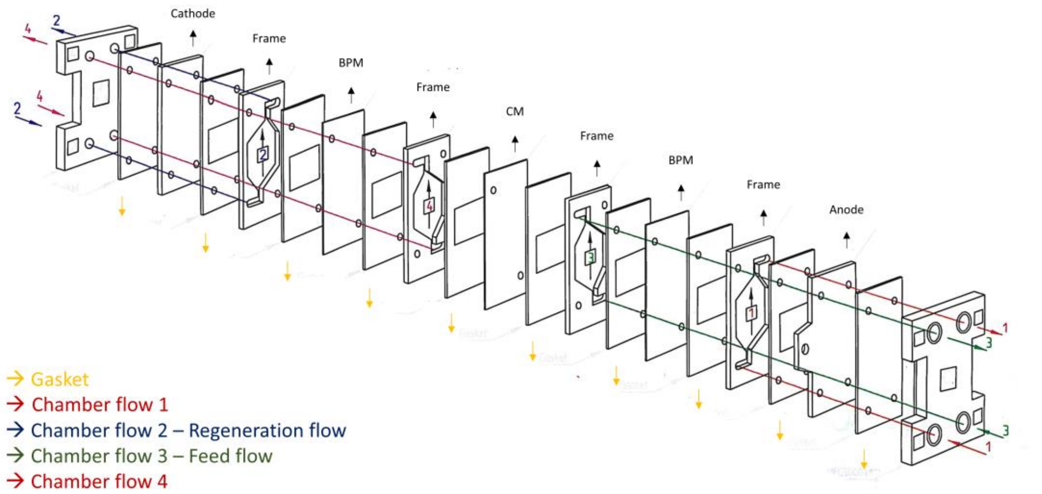

Figure 5.22:Exploded scheme of Micro Flow Cell

5.2 Optimization

Before calculating the figures-of-merit described in the previous paragraph, we performed an optimization of the system parameters. The purpose of this optimization is to find a trade-off between the amount of CO_2 captured, the energy and the chemicals used. To carry out the analysis we repeated the same experiment several times by varying the characteristic of interest while keeping the other variables constant. The factors that have been made to vary are:

1. Current density applied to the cell
2. Speed of movement of the flow by pump
3. Concentration of $NaHCO_3$ and NaCl.

The starting point of these factors are taken from the work of Nagasawa: 170 mA (corresponding to a current density of 17 $\frac{mA}{cm^2}$), 0.1M NaCl and 0.8M $NaHCO_3$. For the speed of the pump, since our equipment does not allow to follow the value of the existing work, we have assumed 10 $\frac{ml}{min}$ as starting point. In the next subsections the results of the three cases mentioned above are shown and discussed. It is necessary to remember that, in general, the pH has a logarithmic trend, so at the beginning it rises very quickly and then settles over time, even if the reactions continue to take place. Furthermore, the voltage is not immediately constant, as there is always a transient at the beginning. After a few minutes it stabilizes, even if some sporadic peaks may be present due to a few brief interruptions in flow.

5.2.1 Effect of current

In this first case, four tests were made, with currents equal to 85 – 170 – 255 – 340 mA. The following graphs show the results for pH over time - figure 5.4 - and for voltage V over time – figure 5.5. The following table - table 5.1 - shows the average voltage values obtained and the final pH values for each experiment.

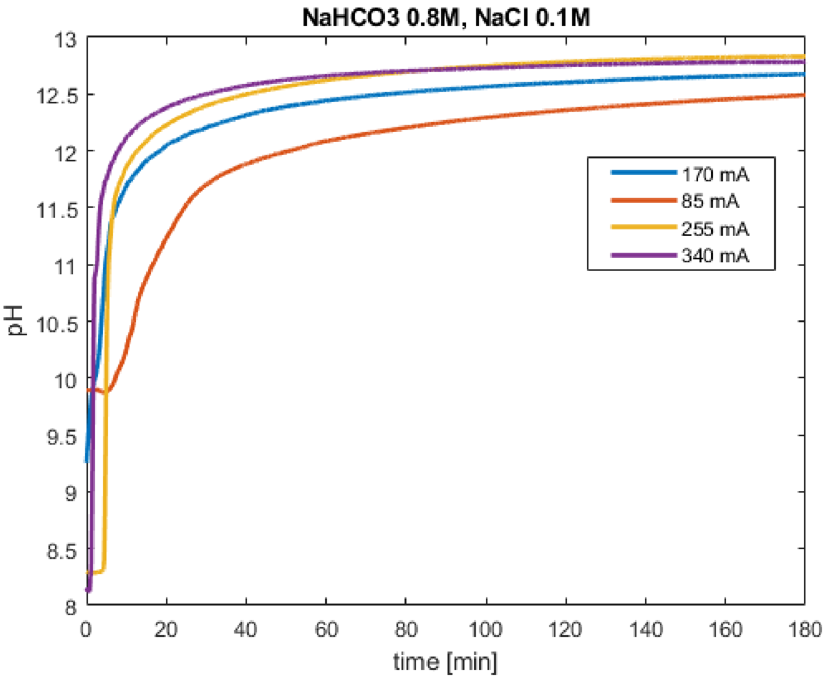

Figure 5.23 - pH versus time: current variation

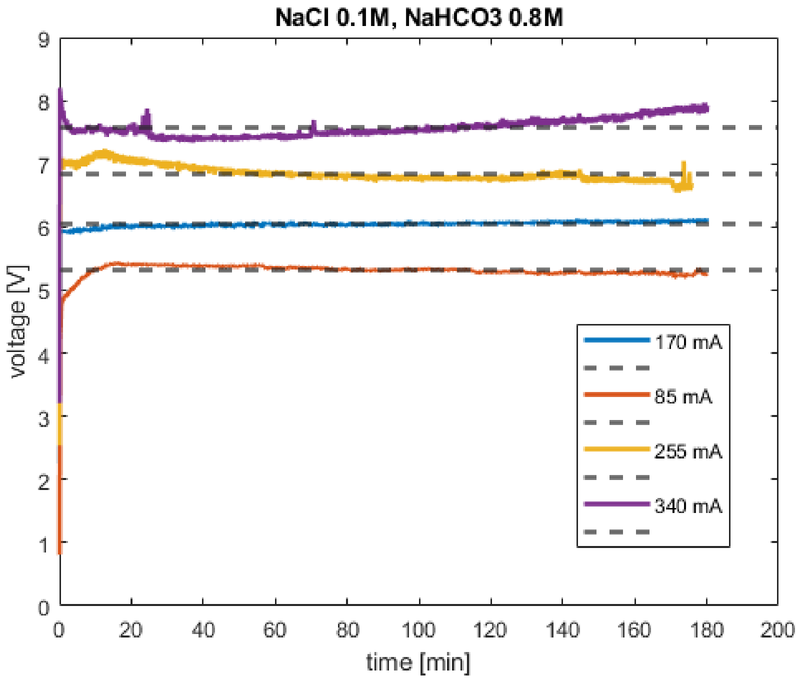

Figure 5.24 - Voltage versus time: current variation

Current [mA]	*Voltage [V]*	*pH [-]*
85	5.31	12.49
170	6.12	12.67
255	6.84	12.83
340	7.57	12.78

Table 5.1 - Summary values: current variation

From the graphs we can obviously see that for an increase in the current there is an increase in the voltage. The pH also increases with increasing applied current, but for currents equal to 255 and 340 mA there is no longer a substantial difference, highlighted by the superimposition of the curves. Therefore, a current equal to 255 mA will be considered as optimal, which guarantees the best result - higher pH - with less energy.

5.2.2 Effect of flow rate

In this case, only the speed of the fluid was varied thanks to the pump, to observe the final pH - figure 5.6 and if there were differences in the voltage value returned - figure 5.7. Table 5.2 shows the summarized results.

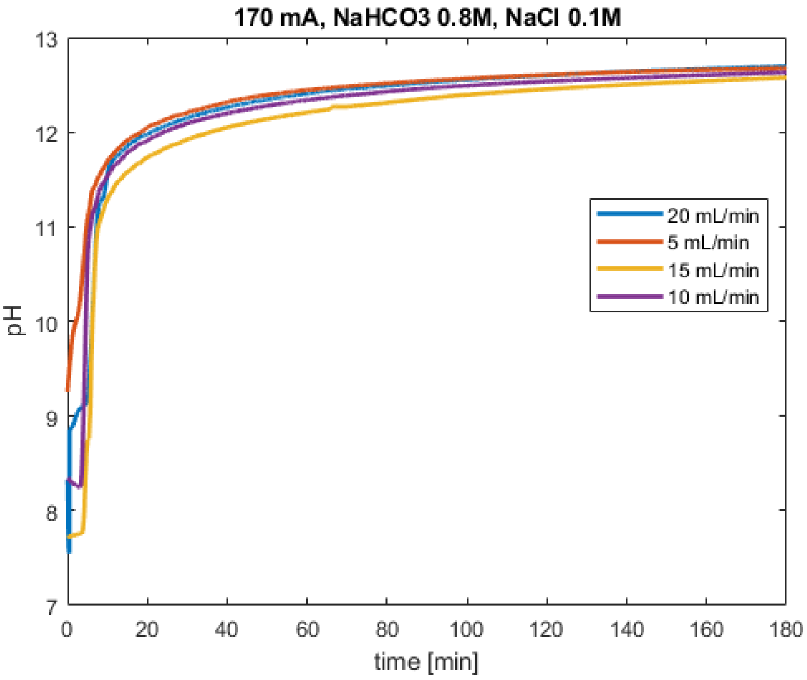

Figure 5.6 - pH versus time: flowrate variation

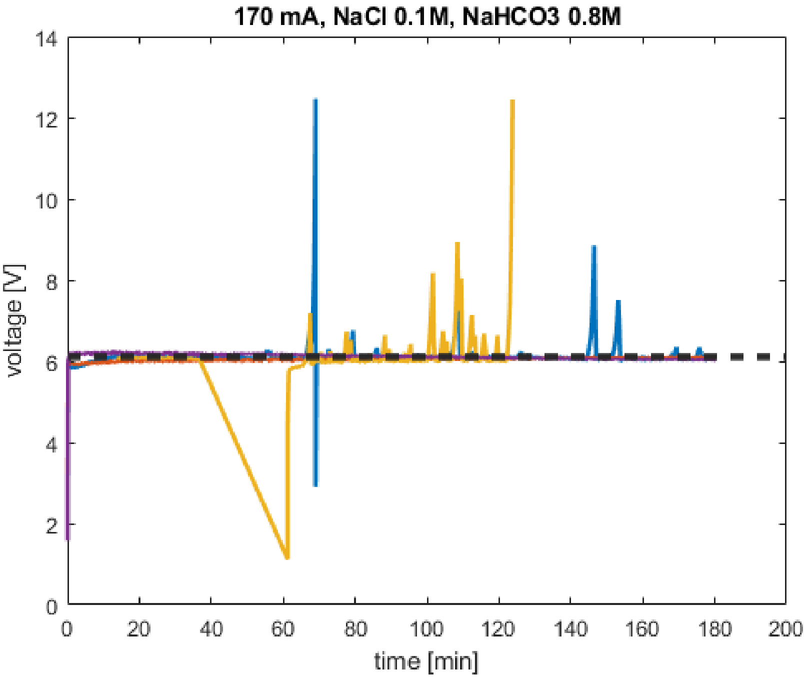

Figure 5.7 - Voltage versus time: flowrate variation

Flowrate $\left[\frac{ml}{min}\right]$	*Voltage [V]*	*pH [-]*
5	6.04	12.67
10	6.12	12.63
15	6.16	12.57
20	6.13	12.69

Table 5.2 - Summary values: flowrate variation

From the results, we can see that the flow does not substantially impact the final result. The voltage remains constant, while the pH varies slightly without a definite trend. However, to have a sufficient pressure at the outlet it is convenient to maintain an average flow of 10 $\frac{ml}{min}$. With higher speed the problem was that the pump tubes tended to break.

5.2.3 Effect of electrolyte concentrations

In the latter case, the concentrations of the solutions were varied - the concentration of NaCl with 0.1M, 0.2M and 0.5M values, while that of $NaHCO_3$ with 0.8M and 1.2M values. As in the previous cases, the pH - figure 5.8 - and the voltage - figure 5.9 were evaluated. In table 5.3 the final results can be seen.

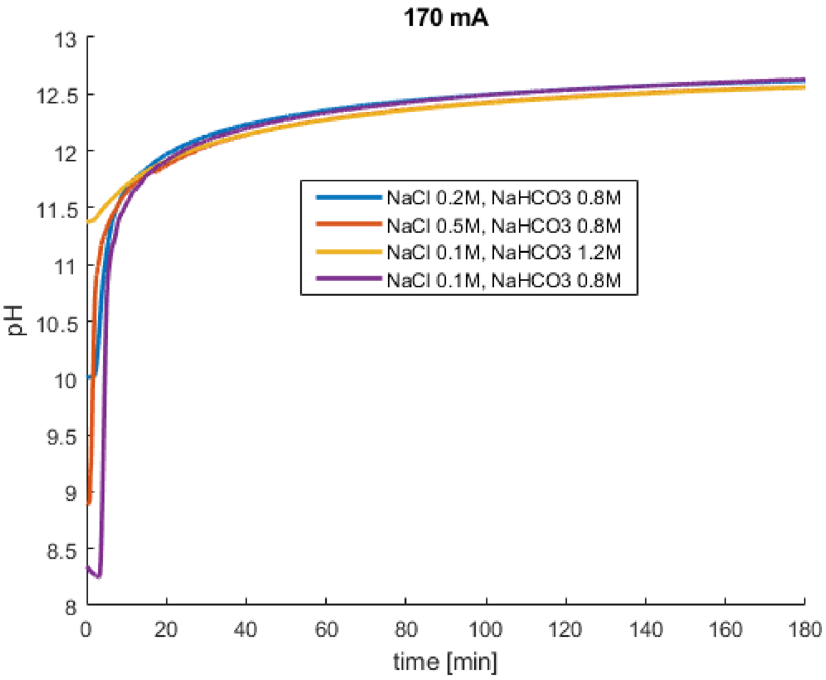

Figure 5.8 - pH versus time: concentrations variations

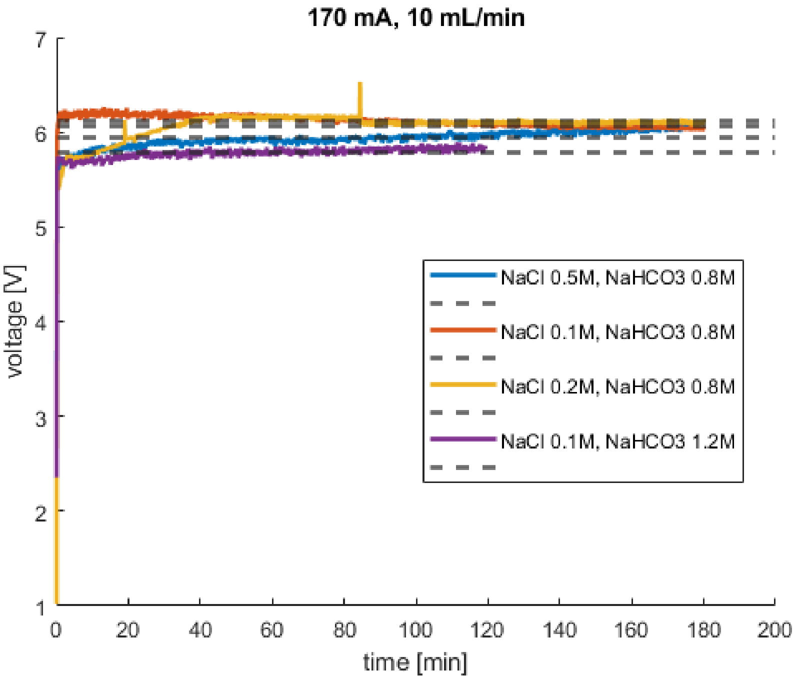

Figure 5.9 - Voltage versus time: concentrations variations

NaCl [M]	*$NaHCO_3$ [M]*	*Voltage [V]*	*pH [-]*
0.1	0.8	6.12	12.67
0.2	0.8	6.07	12.63
0.5	0.8	5.93	12.57
0.1	1.2	5.78	12.69

Table 5.3 - Summary values: concentrations variations

For voltage, the trend seems to show lower values in case of higher concentrations. This is because if the salt concentration is greater, the resistance of the solution is lower and the voltage drops. From the point of view of the pH there are no substantial differences. However, there are minimal differences that allow us to say that the system works better with low concentrations, equal to 0.1M for NaCl and 0.8M for $NaHCO_3$.

At the end of the optimization analysis, we can summarize with table 5.4 the values of the test chosen as the best. These values have been chosen considering a trade-off between the energy used - considering, with the same current, the voltage - and the CO_2 produced - considering the pH.

Current [mA]	Voltage [V]	Flowrate [mL/min]	NaCl [M]	$NaHCO_3$ [M]	pH [-]
255	6.84	10	0.1	0.8	12.83

Table 5.4 - Results of the best optimization

From the results it is observed that the only parameter to vary, compared to Nagasawa's work, is the current, which in this case increases. This is due to the fact that a higher current increases the number of electrons available to react, thus reducing, in proportion, the internal losses of the cell.

5.3 Results

From the values obtained from the optimization - table 5.4 - it is possible to calculate the parameters described in paragraph 5.1. First of all, the concentration of released OH^- ions is 0.0676 $\frac{mol}{L}$ (eq. 5.1) - considering an initial neutral pH, equal to 7 - which is equal to the concentration of CO_2 released. Now, considering that, as mentioned, the quantity obtained is equal to the concentration of CO_2 released, it is possible to calculate the quantity of moles of CO_2 released, equal to 0.00338 mol_{CO_2}(eq. 5.3), considering a volume of fluid equal to 50 mL, as presented in paragraph 5.1. Next, we consider the current I as the product between the applied current density J and the area of interest and we calculate, considering the average voltage V obtained, the instantaneous power applied by the potentiostat, that results in 1.744 W (eq 5.4). Then, considering to work for a time equal to 3 hours – 10800 s - the energy used by the process is 18.84 kJ (eq. 5.5). Finally, it is possible to calculate the specific energy per unit of mole of CO_2 captured in this process, that is 127 $\frac{MJ}{kg_{CO_2}}$ (eq. 5.6).

Now, it is possible to compare the result obtained with theory. The theoretical energy needed to capture CO_2 from systems working with alkaline carbonate solution is equal to 0.8 $\frac{MJ}{kg_{CO_2}}$ - as already reported in paragraph 5.1. The latter value consists of the electrochemical energy needed to develop the expected chemical reactions. The theoretical thermodynamic energy, on the other hand, is not a good comparison in this case as we work directly with a $NaHCO_3$ solution without using any gas flow, therefore not knowing the composition of the mixture from which the CO_2 that formed the salt was taken. Furthermore, thermodynamically speaking, if the CO_2 concentration of the gas used to produce the salt were 100%, the necessary work would be zero. Nagasawa, in his work, obtains a value in the order of 7-8 $\frac{MJ}{kg_{CO_2}}$, which turns out to be an abundant order of magnitude less than the value we obtained. This can be explained by a number of reasons:

- Time: the time taken for the tests in literature is 60 minutes, one third of ours. This is because we have tried to reach a pH value higher than what we obtained with tests of one hour. In fact, as can be seen in figure 5.8, the pH continues to rise over time, creating a plateau only towards the end of the experiment when the salt present in the solution was almost completely consumed.

- Current: Nagasawa's applied current was 177 mA, while our optimum was 255 mA, 50% more. We used a higher current because the output obtained was higher. Consistent with the theory, applying a greater current the power used is greater, but this aspect will be checked later thanks to our optimization.
- Stack: the cell used in literature is composed of 10 units in series for electrodialysis. In this way, the flow is better exploited over time and the losses, in percentage, due to the electrode chambers, in which H_2 and O_2 are produced, are less than our system consisting of only 2 units for electrodialysis. Furthermore, the electrochemical cell used in the literature has a gaseous fluid in chambers 1 and 2 - those in contact with the electrodes - for which the ohmic losses are negligible. It follows that the energy of our system, which uses a liquid fluid in those chambers, is greater.
- Final pH: thanks to the precautions described in the previous points, the final pH obtained in Nagasawa's work is both higher and achieved in a shorter time. This causes the system to be more efficient, leading to a lower required energy value per unit of CO_2.

Considering these aspects, it is possible to treat the data in such a way as to have a result that is better comparable to the literature data from an energy point of view. First of all, we will consider working in 60 minutes as well. In this way the final pH to be considered, according to figure 5.4, is equal to 12.67, obtaining an energy need (eq 5.6) equal to 61 $\frac{MJ}{kg_{CO_2}}$, our reference value for this paragraph. Furthermore, also considering that our system works with liquid in chambers 1 and 2, it is possible to subtract the resulting ohmic losses from the final voltage. To do this, it is considered that the ohmic loss ΔV is calculated with the following formula:

$$\Delta V[V] = I[A] * R[Ohm]$$

(5.7)

Where I is the current applied to the cell and R is the resistance due to the presence of the solution in the chamber. In particular, R can be calculated using the following formula:

$$R[Ohm] = \rho[Ohm * m] * \frac{l[m]}{S[m^2]}$$

(5.8)

Where ρ is the specific resistivity of the solution, in this case 0.8M $NaHCO_3$ and equal to 0.2299 $\frac{m}{S}$ or 0.2299 $Ohm * m$ (This value is taken experimentally with a conductivity-meter). S is the section, in this case the area of the chamber, equal to 10 cm^2 and l is the length of the section considered, in our case the thickness of the chamber, equal to 2 mm. From these values we obtain R (eq. 5.8) equal to 0.46 Ohm. Considering to always work with a current equal to 255 mA, a ΔV, considering the presence of two chambers, equal to 0.23 V is obtained (eq. 5.9). The new voltage to be considered in this case is therefore the difference between the previous one (6.84 V) minus the difference just obtained, resulting in 6.61 V. Applying again the formulas described in chapter 5.1 and considering a new time of 60 mins, an energy value (eq. 5.6) equal to 59 $\frac{MJ}{kg_{CO_2}}$ is obtained. This value is of an order of magnitude lower than the previous one obtained, thus becoming more comparable to the value obtained in the literature, although the differences remain evident, mostly due to the number of layers and a better optimization of the cell.

To obtain a more comparable value based on the same parameters used by Nagasawa, it is possible to consider the case of operation always in 60 minutes but with current equal to 170 mA. In this condition there is a pH equal to 12.44 and a voltage of 6.12 V, that became 5.89 V considering the losses due to the fluid in the chambers 1 and 2 as before. By repeating the same reasoning above, an energy value (eq. 5.6) equal to 89 $\frac{MJ}{kg_{CO_2}}$ is obtained. This result means that we have actually increased the efficiency of our system by increasing the current.

Ultimately, under the conditions present in this last analysis, it is still possible to consider subtracting the energy used by the two electrode compartments (chamber 1 and 2) for the electrolysis of water – so, the production of hydrogen. In the absence of a real value, we will consider the theoretical minimum necessary value equal to 1.23 V for electrolysis [41]. Considering that there are two membranes, the value of 2.46 V is subtracted from the 6.61 V (case of 255 mA, 60 mins and considering ohmic losses) calculated previously, obtaining a necessary energy (eq. 5.6) equal to 37 $\frac{MJ}{kg_{CO_2}}$, always in 60 mins. This value, however, must be compared to the value obtained by Nagasawa, who likewise did not consider the energy used by the two membranes. He estimates that the energy used for electrolysis is 20% of the total [40], while in our case it is 37%. The difference, as explained above, lies in the fact that in our case this slice of energy is proportionally heavier given the presence of only two chambers for electrodialysis, which optimize operation less. However, the energy value to be considered for the system is the one that also takes all these losses into account.

Finally, it is important to underline that once the $NaHCO_3$ present in the system is exhausted, it ceases to function, as there are no more CO_2 molecules to be released. In fact, the value of pH in time from a certain point tends to become very stable. So, we can consider to do the experiments considering to work in 90 mins in the following chapter. This value is the right compromise between the need of energy and the consumption of the reagent. Furthermore, this system does not consider the introduction of a gaseous CO_2 flow to be captured, but merely separates the one already presents in the sodium bicarbonate. These are the starting points of the next chapter, in which we will try to modify the system in such a way as to make up for these two shortcomings. In the end, considering the theoretical value of penalty for the capture obtained in paragraph 4.4, we can say that our system is not yet competitive as the real energy value obtained is at least one order of magnitude higher. In fact, considering our energy need of 61 $\frac{MJ}{kg_{CO_2}}$, we have an energy penalty of 1442% (eq. 3.3) and a second-law efficiency of 0.254% (eq. 4.14).

6. Continuous CO_2 capture

As will be analyzed in this chapter, the goal was to experiment with a solution to be able to work with the system described in the previous chapter continuously over time, in order to have a self-sustaining capture system. The principle of continuous work consists in introducing an external CO_2 flow that regenerates the system. As always, our system must meet the same requirements already described in paragraph 5. In fact, the use of high temperature operating principles and the use of toxic substances will be avoided, trying to make the system as advantageous as possible from the economic and energetic points of view. The chapter will present the set-up of the system, its composition and the tests carried out for its optimization. In particular, the system has been optimized so that it can be coupled with an existing electrochemical reduction system that will use our outlet CO_2 flow - as will be described in the next chapter. The CO_2 captured flow, therefore, has to be separated from the outlet flow of chamber 3 (liquid-gas mixture) and conveyed to the following system. Finally, after having optimized the system, its operation will be tested over time employing a gaseous fluid simulating an exhausted gas.

6.1 Operation

As previously introduced, the purpose of the system is to allow the electrodialysis system to work continuously and to capture the CO_2 from a gaseous mixture. In the first place, we tried to make the system able to work over time without discharging. In fact, in the system described in the previous chapter, once all the $NaHCO_3$ present in the circuit of chamber 3 had been consumed, the system was running out. Therefore, in this case a change has been made to the system set-up, in order to allow the regeneration of the fluid entering the chamber 3, in which the CO_2 is separated, measured and conveyed to another system. In this experimental setup a peristaltic pump MCP (Ismatec) was used as the one used previously broke the tubes beyond speeds of $10\,\frac{mL}{min}$. The new set-up can be seen in the figure 6.1.

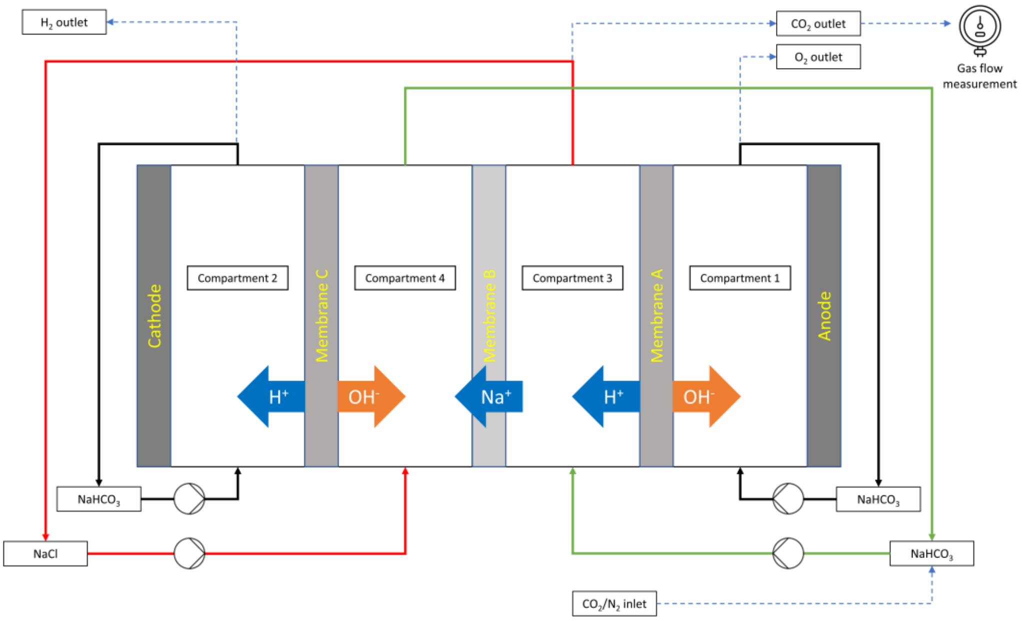

Figure 6.25: Scheme of the capture cell with regeneration of $NaHCO_3$ and injection of flue gas.

As can be seen from the figure, it was decided to connect the exit of chamber 4 to the entrance to chamber 3. In this way, in inlet to chamber 3 a gaseous mixture containing CO_2 (flue gas simulated with N_2 and CO_2, controlled with a mass flow meter) was put that can regenerate the solvent according to the following reaction:

$$NaOH + CO_2 \rightarrow NaHCO_3$$

The CO_2 involved in the reaction is the one captured from the system. In this way, at the inlet of chamber 3 there is always $NaHCO_3$ which no longer runs out but is regenerated as long as there is an external flow of CO_2. Similarly, the flow out of chamber 3 is sent to the inlet of chamber 4, so as not to have an imbalance in the quantity of circulating fluid and so as to be able to capture and concentrate the gaseous CO_2 emitted by the chamber without colliding with the CO_2 flow entering the same chamber. To do this, before entering chamber 4, a simple liquid gas phase separator was created, in which the mixture coming from chamber 3 can be separated from the CO_2 produced, and therefore captured, simply through a vent located in the upper end of the separator. The rest of the system has remained unchanged and, as in the previous case, there is always the production of H_2 in chamber 2 and of O_2 in chamber 1. Hydrogen can be used in the final mixture as a reusable product, while oxygen released in environment can contribute to the reduction of the greenhouse effect. Also the components and the instrumentations utilized have remained the same as those used in the previous chapter. The tests presented in this chapter consist in applying a current to the cell set as described above. Thanks to the applied power, the reactions described in the previous chapter are carried out, which work continuously thanks to the regeneration obtained with the incoming flow of CO_2. Consequently, the flow of CO_2 released after the phase separation system is measured with the flow meter. Given the simultaneous production of O_2 and H_2 they were also measured. The following paragraph will provide the results of the optimization made on the working parameters.

6.2 Optimization

The purpose of the optimizations in this paragraph was to increase the captured CO_2 outlet flow, in order to subsequently couple this system with the reduction one. All experiments were performed in ambient conditions and lasted 90 minutes. Moreover, all tests were carried out at least twice in order to guarantee the repeatability of the results.

The following parameters have been optimized: current, pump speed and the inlet regeneration flow. In this first series, the incoming flow is pure CO_2.

- Current effects

The effects of varying the applied current were explored first. The voltage and flow of CO_2 captured over time were evaluated. Still considering to work with an electrode area equal to 0.001 m^2, currents equal to 0.25 A, 0.5 A, 0.75 A, 1 A were applied. We can see the voltage behavior in figure 6.2a and the average CO_2 outflow – in 90 mins - in figure 6.2b. All tests were carried out with an inlet CO_2 flow of 20 $\frac{mL}{min}$ and a pump speed of 1 $\frac{mL}{min}$.

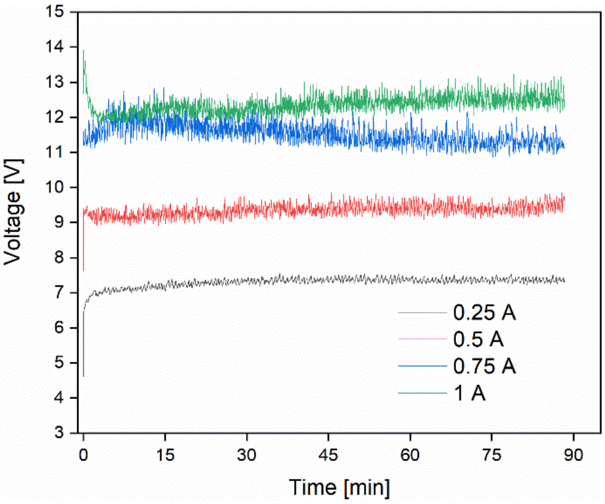

Figure 6.26a: Effect of current on voltage in time

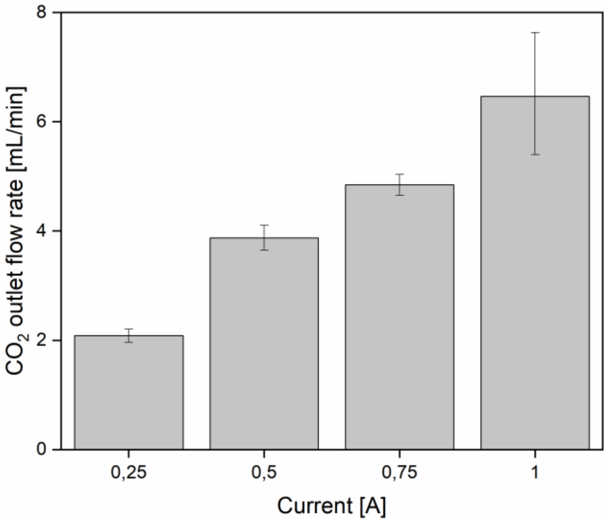

Figure 6.2b: Effect of current on CO_2 outlet flow rate

As expected, in figure 6.2a we can observe that the voltages turn out to be constant over time, a sign that the experiments are stable, regardless of the current. Furthermore, it drops with the descent of the applied current, as per the physical law. In particular, as can be seen in Figure 6.2b, for low currents the average output flux is lower since the extent of reactions that occur is fewer. In addition, the trend is not linear. Given these results, we will work with 1 A.

- Pump flow rate effects

The pump flow rate controls the circulation of fluids in the pump, allowing both the electrodialysis phase and the regeneration phase of the sorbent, leading to continuous reactions that are constant over time. In figure 6.3 it is possible to observe the optimization made on this parameter, analyzing the pump speed such as to have 0.25, 1, 3 and 5 $\frac{mL}{min}$ of pump flow, in order to have a higher average CO_2 output. All measurements were made by applying a 1 A of current and introducing a CO_2 flow equal to 20 $\frac{mL}{min}$.

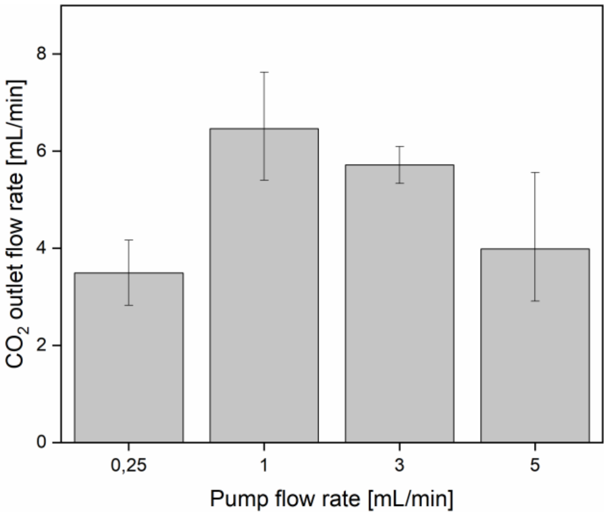

Figure 6.27: Pump flow rate effect on CO_2 outlet flow rate

As can be seen from the figure, a maximum output flow is obtained with a pump flow of 1 $\frac{mL}{min}$. This happens because probably the speed is such as to allow the cell to exploit the fluid inside it with sufficient time, thanks to the type of fluid dynamic motion formed. In fact, with a higher flow it seems that the cell does not have time to develop a consistent number of reactions, probably due to a too turbulent flow. While, with too low velocities the fluid exchange available for new reactions seems to be insufficient.

- CO_2 inlet flow rate effect

Finally, the amount of incoming CO_2 was optimized, analyzing flows equal to 0, 5, 10 and 20 $\frac{mL}{min}$. In this regard, both the average quantity of CO_2 in output and the percentage captured were measured. These values can be observed in figure 6.4, which presents the CO_2 output values on the ordinates and the percentage value of CO_2 captured above each column. This last parameter is calculated with the following formula:

$$percentage\ of\ capture = \frac{average\ captured\ flow\ rate\ \left[\frac{mL}{min}\right]}{average\ inlet\ flow\ rate\ \left[\frac{mL}{min}\right]} \tag{6. 1}$$

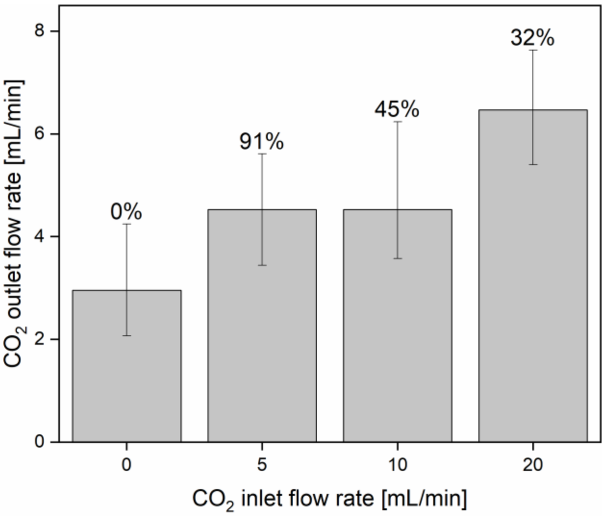

Figure 6.28: Effect of CO_2 inlet flow rate on CO_2 outlet flow rate and percentage of capture

First of all, it is important to underline that initially the CO_2 released is the one present in the starting $NaHCO_3$ solution, which is why even with zero CO_2 input flow the quantity captured is not zero. This quantity is in any case the lowest among those obtained, a sign that the reaction is running out and in the other cases, in which CO_2 is introduced, the solution is actually regenerated. Considering the percentage of capture it is observed that for incoming CO_2 flows equal to 10 $\frac{mL}{min}$ and 5 $\frac{mL}{min}$ there are respectively 45% and 91% of capture (eq. 6.1), while for 20 $\frac{mL}{min}$ there is only 32%. However, it is necessary to remember that in our case the quantity of absolute CO_2 produced that will be used in the coupled capture/reduction system is important, which is why we decided to work with an inlet flow of 20 $\frac{mL}{min}$, to the detriment of the percentage captured. The average CO_2 outflow is greater by increasing the incoming CO_2 as probably, even if the capture is lower in percentage, a greater flow is able to mix better with the solution, regenerating a greater quantity.

6.2.1 Interpolation

At the end of this optimization, the parameters considered ideal for the system are therefore current equal to 1 A, flow imposed by the pump equal to 1 $\frac{mL}{min}$ and CO_2 inlet flow equal to 20 $\frac{mL}{min}$. To better represent the results obtained, all the tests were grouped and represented in a MATLAB interpolation graph, as shown in figure 6.5. It shows the parameters optimized as a function of the amount of CO_2 output, our target, in the form of a curve. The curve is the result of the interpolation of the experimental data - the blue points. Furthermore, it considers to always work at a current equal to 1 A, since as noted above, if the current is increased, the output flux increases.

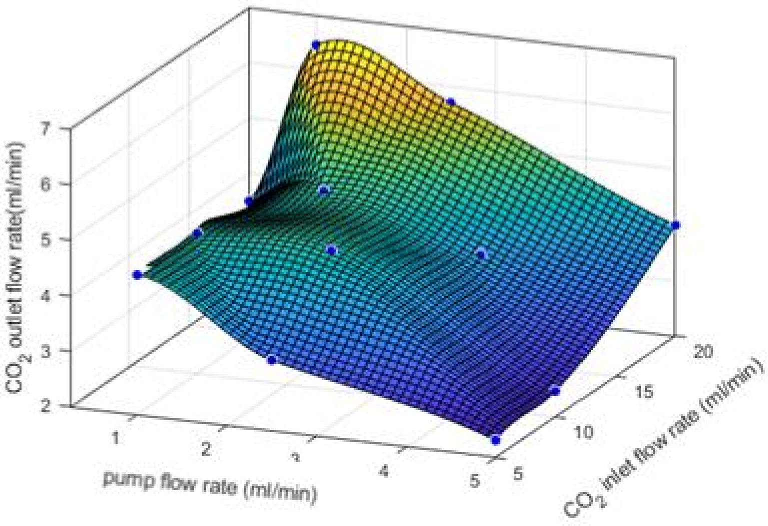

Figure 6.29: interpolation of the optimization results with MATLAB

As previously introduced, it is possible to observe the behavior of the pump speed and the incoming CO_2 flow. It is observed that the zone that tends to the maximum, the yellow one, coincides with the zone in which we have chosen our work point, which maximizes the flow of CO_2 captured at the outlet.

6.2.2 Typical test

This paragraph shows the results over time - 1.30 hours - of a typical test, carried out with the optimized parameters found previously: constant current equal to 1 A, constant flow applied by the pump equal to 1 $\frac{mL}{min}$ and pure CO_2 introduced equal to 20 $\frac{mL}{min}$. In figure 6.6a it is possible to observe the trend of CO_2, H_2 and O_2 productions over time, together with the voltage. In figure 6.6b, on the other hand, it is possible to observe the increase in production of the same gases over time, obtaining the total quantity released by the system at the final instant of time.

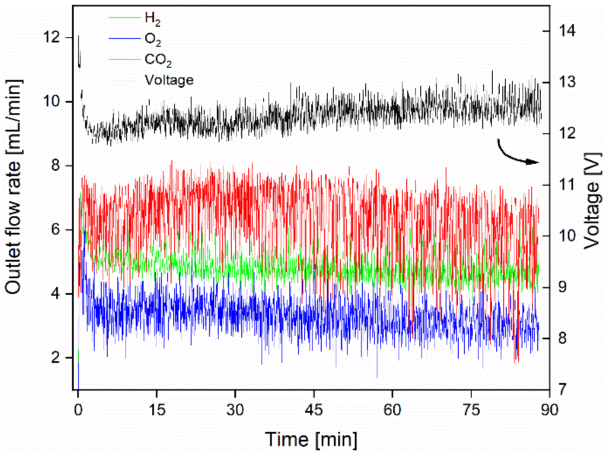

Figure 6.30a: CO_2, H_2, O_2 outlet flow rate and voltage in typical test

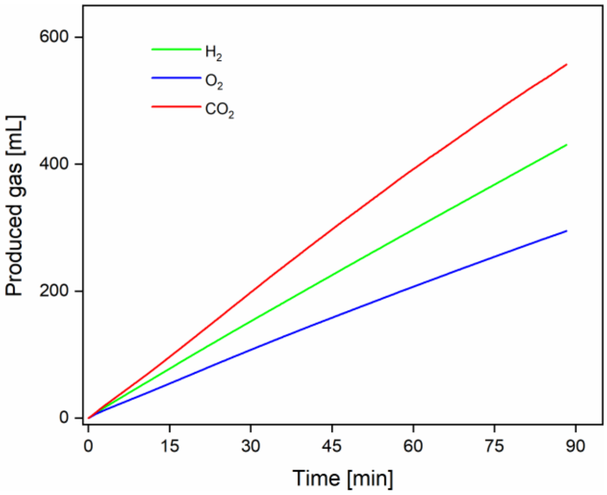

Figure 6.6b: CO_2, H_2 and O_2 produced in time

From figure 6.6a we can see the stability of the optimized test in 90 minutes. In fact, the voltage – with an average value of 12.4 V - rises a little, due to the mixing of the solutions, without presenting peaks. The same happens for gases, which remain stable over time. Thanks to this result it will be possible to couple the reduction system. The curves of the gases produced, in figure 6.6b, are sufficiently linear and monotonous, demonstrating that the system works in a constant and correct manner over time. As regards the two energetically useful products - CO_2 and H_2 - we can say that for CO_2 in a typical test the quantity captured is equal to 32-33%, given by the ratio between the final captured value

- 584 mL - and the total flow introduced over time – 20 $\frac{mL}{min}$ per 90 mins. Since we have observed that CO_2 regenerates the solvent, we can consider excluding the amount of CO_2 supplied by $NaHCO_3$ as at the end of the experiment this chemical, having been regenerated, will be present in the same quantity. While for hydrogen we can compare our value with respect to the theoretical production – in number of moles per second, that in these conditions can be calculated with the following formula, deriving from Nernst equation [42]:

$$n_{H_2}\left[\frac{mol_{H_2}}{s}\right] = \frac{I[A]}{Z_{H_2}[-] * F\left[\frac{C}{mol}\right]}$$

(6. 2)

In which I is the current - equal to 1A, Z_{H_2} is the number of electrons involved in the reaction - 2 for hydrogen - and F is the faradic constant, equal to 96485 $\frac{C}{mol}$. With our values, the theoretical production would therefore be 5.18E-6 $\frac{mol}{s}$ (eq. 6.2), equal to 684.6 mL in 90 minutes. From graph 7.5b we can see that our value is equal to 430 mL, which leads to a theoretical capture efficiency:

$$\text{theoretical capture efficiency } \eta = \frac{captured\ quantity\ [mL]}{theoretical\ capturable\ quantity[mL]}$$

(6. 3)

Substituting the values, we obtain a result of 63%. This means that there are faradic losses, which if decreased can lead to better efficiency. The best efficiency is necessary since, as seen in the previous chapter, each H^+ ion produced corresponds to a released CO_2 molecule. This means that given the presence of two H^+ ions inside the hydrogen molecule, theoretically 1369.2 mL of CO_2 could be released in an hour and a half. This is the maximum production value. From the experimental value obtained, 584 mL, we obtain a theoretical capture efficiency of 43% (eq. 6.3). This is due to the fact that there are faradic losses and ionic losses across the membranes involved. The efficiency value is similar to the one obtained by Nagasawa, so the system works correctly. In the end, if we could guarantee 100% efficiency, the optimal regeneration CO_2 flow would be 15.2 $\frac{mL}{min}$. Thus, maximum capture efficiency can be achieved while not capturing all of the incoming flow, which can be in excess.

From the energetic point of view, it is possible to repeat the same arguments made in the previous chapter. The difference is that in this case it is not necessary to go through the pH of the solution to calculate the amount of CO_2 produced, but it is sufficient to use the value obtained from the gas flow meter. First of all, using the values obtained in this stability test as a reference, the energy used in the process results in 66.96 kJ (eq. 5.5).

Considering the greenhouse gas captured, it is possible to obtain the energy required per unit of CO_2 produced, that is 58.4 $\frac{MJ}{kg_{CO_2}}$ (eq. 5.6). Neglecting the potential drop due to the presence of liquid in chambers 1 and 2 - equal to 0.92 V calculated as in the previous chapter (eq. 5.7) - an energy value equal to 54.1 $\frac{MJ}{kg_{CO_2}}$ is obtained (eq. 5.6). This value, therefore, is similar that obtained in the previous chapter (61 $\frac{MJ}{kg_{CO_2}}$), without a continuous loop. This means that our system appears to be functioning correctly. Furthermore, by optimizing the previous system, this will also benefit from the same improvements. Considering to neglect the energy necessary for the electrolysis of the water in chambers 1 and 2 - always 2.46 V, an energy value equal to 42.5 $\frac{MJ}{kg_{CO_2}}$ is obtained (eq. 5.6). In this case the energy required for electrolysis represents only 21% of the total energy used, similarly to Nagasawa (20%) [40].

6.2.3 Stability test

This section shows the result of a typical test, carried out with optimized parameters (current equal to 1 A, pump flow rate 1 $\frac{mL}{min}$ and CO2 inlet flow rate 20 $\frac{mL}{min}$), for a time of 8 hours, in order to verify the stability of the capture system over time. Figure 6.7 shows the results achieved in terms of voltage, outlet flow rate and the composition of the latter.

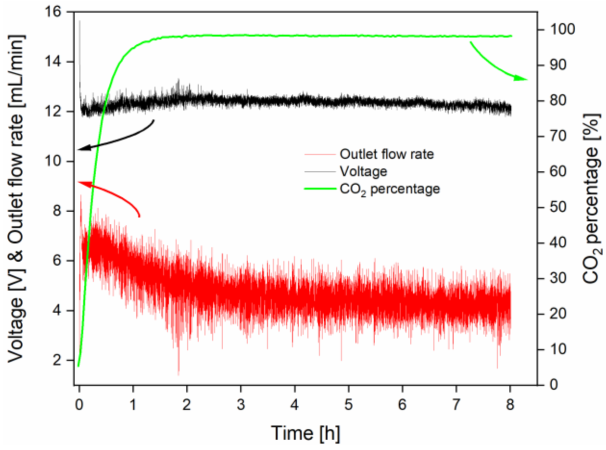

Figure 6.7: Stability test

From this, we can observe that the system works correctly and constantly for at least 8 hours. In fact, the voltage remains constant for all the time after a short initial settling phase, due to the hydraulic mixing of the chemicals flowing in the chambers 3 and 4, caused by the crossing of the outlets in the external tanks. As regards the flow of CO_2, as already mentioned above, at the beginning the captured CO_2 is that supplied by the electrodialysis of the $NaHCO_3$ solution, while subsequently this solution is regenerated and the captured CO_2 is part of the incoming one. This situation is maintained over time, a sign that the system works and the solution is regenerated, otherwise the CO_2 flow would decrease over time, while instead it becomes constant. Ultimately, after 1.30 hours the CO_2 percentage of the outflow is 98% and remains constant over time. This means that before coupling the system with the reduction system it is necessary to wait this time to be sure of having pure CO_2 at its entrance. This time is due to the fact that from the start of the experiment it takes some time before the whole system is 'clean' of the air present. Finally, it is important to underline that the purity of the outflow is not 100% as there are minimal losses between the chambers, so there are traces of other elements. This test provides us the information that the system is able to work in a constant way for a long time.

6.3 Flue gas simulation

After optimizing the capture system and observing its operation over time, it is necessary to simulate the actual capture from exhaust gases. To do this, we have added nitrogen in the regeneration gas flow introduced into the system, which up to now has always been made up of pure CO_2. Thanks to this, it was possible to simulate the behavior of the system with the introduction of exhaust gas, composed, net of particulates, pollutants and unreacted oxygen, of the nitrogen in the air and the CO_2 produced. Therefore, in this paragraph we will analyze different CO_2/N_2 ratios (0%/0%, 100%/0%, 0%/100%, 50%/50%, 16%/84%) to better frame the behavior. In each of these situations the absolute quantity of CO_2, when present, is equal to 20 $\frac{mL}{min}$, while the quantity of N_2 is adjusted where necessary. The applied current is 1A and the applied pump flow is 5 $\frac{mL}{min}$. In figure 6.8 it is possible to observe the output of the CO_2 captured in the different cases. They are 90 minutes long and have been replicated at least twice to ensure repeatability.

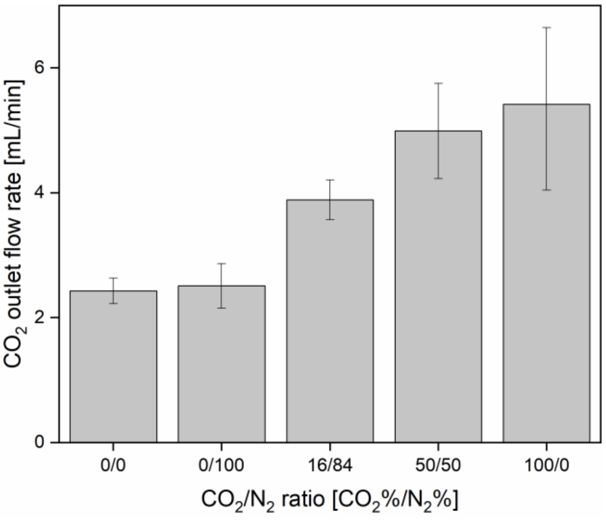

Figure 6.8: CO_2 outlet flow rate depending on CO_2/N_2 inlet ratio

The test carried out with CO_2 equal to 100% and null N_2 is the same previous case, which in this case serves as a reference. In this regard, tests were also carried out with zero flow, which as before have a non-null output flow, given by the electrodialysis reaction of the $NaHCO_3$ present. To confirm this behavior, testing the case with pure nitrogen inlet flow gives the same result. This is because nitrogen does not participate in any reaction and is not soluble in water [43]. Therefore, the two cases with CO_2/N_2 ratio equal to 0%/0% and 0%/100% have the same result, implying that the system correctly does not capture nitrogen. It is however good to remember that the presence of bubbling of a gas can help the mixing of the solutions. The capture from exhaust gas was simulated with concentrations equal to 50% CO_2 and 50% N_2 and 16% CO_2 and 84% N_2 in input. In particular, this latter ratio optimally simulates the capture from exhaust gases, as already observed in chapter 4. We can say that they do not differ substantially from the case of pure CO_2 inlet flow, a sign that the capture also works with an inlet gas mix, which can simulate capture from after combustion. The differences that are observed are probably due to the fact that, especially for the case with 84% of N_2, the CO_2 in the inlet is too dissolved in the gaseous flow itself, failing to effectively react with the sodium hydroxide present.

Even in the case of simulation of exhaust gas capture it is important to consider the energy required. In this regard, the situation is assessed that the CO_2/N_2 ratio is 16%/84%. In this context, we have an average outflow of 3.9 $\frac{mL}{min}$ - observable in figure 6.8. In 90 minutes, this corresponds to an amount of 350 mL of CO_2 captured. Considering to work at 1 A, the resulting voltage is the same as the typical test, equal to 12.4 V. From these values, a necessary energy of 97.6 $\frac{MJ}{kg_{CO_2}}$ is obtained (eq. 5.6). The value obtained is inclusive of all losses that could be separated, but which in any case are present at the moment. It is higher than that obtained in paragraph 6.2.2 (58.4 $\frac{MJ}{kg_{CO_2}}$) since, as previously mentioned, using a gas mixture at the inlet there is a smaller quantity of CO_2 captured due to the difficulties in mixing. Following the same reasoning as in paragraph 6.2.2 we have a theoretical capture efficiency equal to 25.6% (eq. 6.3), while the quantity captured on the total input is 19.4% (eq. 6.1). An energy penalty of 2307% is calculated (eq. 3.3). Also this value is higher than that obtained in the electrodialysis system because the quantity of capture CO2 is lower considering to use the same energy quantity. The same happen for the second-law efficiency value, that is 0.16% (eq. 4.14).

7. CO_2 reduction

In this last chapter the aim is to finally couple the two electrochemical systems, namely the capture and reduction ones. The reduction process consists in the direct production of CO starting from the captured CO_2 molecules. In addition to the CO, a substantial amount of H_2 will also be produced, which will make up the final, readily reusable, syngas mixture. A coupled system of this type, not yet present in the literature, allows numerous advantages:

- The ability to work with systems based on the same physical principle allows systems to be coupled using the same energy supply.
- It allows to work under the same ambient temperature and pressure conditions for both systems
- Possibility of by-passing the compression and temporary storage phases of CO_2, allowing to have a product with added value immediately available.

Afterwards, we will observe the functioning of the electroreduction cell, the coupling with the capture cell and the related set-up, the experimental values obtained and the final results.

7.1 Electroreduction cell

The reduction system, like the capture system, consists of an electrochemical cell to which a potential difference is applied, and the current flows. In particular, our system consists of a two-chamber system, named A and C. A is the anodic chamber, in which the water oxidation reaction takes place, which allows the formation of H^+ ions and the release of oxygen molecules. Subsequently, there is the passage of protons from chamber A to C through a Nafion cathodic membrane, attracted by the negative pole, the cathode – also called working electrode. The remaining OH^- ions react at the anode – also called counter electrode - further by reforming water and releasing oxygen and electrons:

$$2H_2O \rightleftarrows 2H^+ + 2OH^-$$

$$2OH^- \rightleftarrows H_2O + \frac{1}{2}O_2 + 2e^-$$

The passage of electrons is allowed by an external connection. In this system there is also the presence of a reference electrode, used to fix the potential of the working electrode with respect to a certain reference value. The anodic electrode, as for the capture cell, is a platinum foil. Chamber C is the cathode chamber in which the electro-reduction reactions take place. In this chamber there is the simultaneous presence of protons, electrons and CO_2 molecules. As the aim is to reduce the CO_2 into short-chain carbon molecules, such as carbon monoxide (CO) and formic acid (HCOOH), it is necessary to be selective towards this reaction - CO_2 reduction reaction - rather than on the production of hydrogen (for this purpose there are water electrolysers, which are electrochemical systems suitable for this [44]). Then, a zinc oxide (ZnO) catalyst was used [45]. The reactions that arise are therefore:

$$2H^+ + 2e^- \rightleftarrows H_2$$

$$CO_2 + 2H^+ + 2e^- \rightleftarrows CO + H_2O$$

$$CO_2 + 2H^+ + 2e^- \rightleftarrows HCOOH$$

The electrolyte used, both as catholyte and anolyte, is a 2M $KHCO_3$ solution, which allows both the ionic movement and the presence of CO_2 inside the cell. In fact, the solution is kept in constant saturation of CO_2, so as to allow the catalyst to always have the molecule to be reduced. In the anolyte the presence of CO_2 allows the acid-base balance of the cell. Both the electrolytes are kept in movement by a recirculating pump. In this type of cells it is difficult to be very selective towards the reduction of CO_2 due to problems related to the phenomenon of mass transport [46]. To overcome this problem, a gaseous CO_2 flow is sent to the face of the cathode not exposed to electrolyte, so that the CO_2 can go directly into contact with the catalyst, through a diffusion process [47].

This is allowed through a gas diffusion layer (GDL) on which the catalyst is deposited, which is impermeable to liquids, but permeable to gases. The GDL is deposited onto a special nanostructured carbon electrode, that is conductive.

In figure 7.1 we can see the diagram of the cell used in our. It presents the two chambers A and C, the path of electrolytic substances, CO_2 and reaction products inside the cell. The gaseous reaction products, CO and H_2, are able to permeate through the cathode GDL and exit in the purely gaseous phase with the unreacted CO_2, as said before. This flow, together with the hydrogen produced in the capture cell, will form the final syngas. The liquid products, formic acid, come out of the cell in aqueous solution, which will be separated at the end of the process. In particular, to the left of chamber C there is an area - closed from the external environment - where the necessary external CO_2 can flow. Furthermore, it shows the gray cathode membrane - which divides the two chambers - in the center of the cell and the three electrodes – CAT, AN and REF. For both we observe in the center the presence of the conductive material, the GDL with zinc oxide catalyst - in yellow - for the cathode and the platinum sheet - in black - for the anode. Finally, externally to the system, connecting the anode and cathode, there is the external circuit, with the potentiostat, mentioned above.

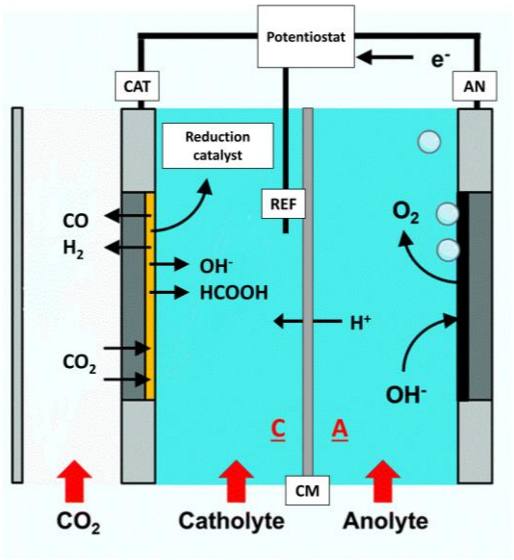

Figure 7.31: Reduction cell (adapted from [48]).

7.1.1 Parameters

As previously mentioned, the catalyst employed is ZnO. This was experimentally employed previously, in the work of Zeng et Al. [45]. The important aspects to characterize an electroreduction cell are the faradic efficiency, the amount of reacted substance, the applied current and the resulting voltage, and the test time:

- The faradic efficiency FE consists in the measurement of the reaction products, necessary for the classification of the selectivity of the cell and therefore of the catalytic material. According to the applied current there is a certain maximum number of electrons that can participate in the reactions. The FE therefore consists in the measurement of each of the reaction products on the maximum number of electrons participating in the reaction: the higher the FE for that product, the greater the selectivity towards it. Theoretically speaking, the sum of the faradic efficiencies of a test should be 100%, however often there are difficulties in gas identification and we consider a range of 90%-110% for the total FE as correct.

To calculate the faradic efficiency of a product, the following formula is used [49]:

$$FE[-] = \frac{z[-] * F[\frac{C}{mol}] * N[mol]}{Q[C]} = \frac{z * F * N}{\int_0^t I(t)dt}$$

(7. 1)

Where z is the number of electrons involved in the specific reaction, F the Faraday constant, N the number of moles of product measured and Q the charge available in the time interval. This last value corresponds to the integration of the current over the time of the measurement. The material we use should have 75% of FE for CO and 5% for HCOOH and the remaining destined for the hydrogen evolution reaction [45]. To identify the gases present in the product mixture, the output flow is sent to a gas chromatograph (GC), which returns the gas concentrations present.

- The quantity of reacted substance is the value that tells how much substance introduced into the system has reacted:

$$Reacted\ percentage\ [-] = \frac{outlet\ reacted\ product[mol]}{inlet\ substance[mol]}$$

(7. 2)

This value, especially in the case of capture-reduction coupling, gives an idea of how well the system is coupled. Obviously, we need to know the inlet quantity of the substance. In our case, neglecting HCOOH as a product, it is possible to simplify eq. 7.2 in the eq. 7.3, considering that the reduction of CO_2 produces only CO (since H_2 is produced by the electrolysis of water):

$$Reacted\ percentage\ [-] = \frac{CO\ outlet\ concentration[ppm]}{CO_2\ outlet\ concentration[ppm]}$$

(7. 3)

- These types of tests are carried out at constant potential on the cathode V_{CAT} (it is expressed as V vs reversible hydrogen electrode (RHE) [50]), therefore, once the potential applied is known, the resulting current I is ascertained through the use of a potentiostat. The applied potentials must be chosen in order to fix the desired selectivity of the catalyst. In fact, based on the potential applied a reaction can be more or less preferred because of its reaction potential [49]. It is important also to know the total potential over the reduction cell V_{TOT} in order to know the total energy used.
- The evaluation of the time t of the test is necessary to visualize the durability of the catalyst, before it degrades, and the stability of the overall operation of the cell for the necessary time.

7.1.2 Functioning test

Before coupling the system, the catalyst and the reduction cell were tested. The test was carried out by applying to the cathode a constant potential V_{CAT} equal to -1.2 V vs RHE, for a duration of about one hour. The input CO_2 flow equal to 25 $\frac{mL}{min}$. In the figure 7.2 it is possible to observe the results obtained over time:

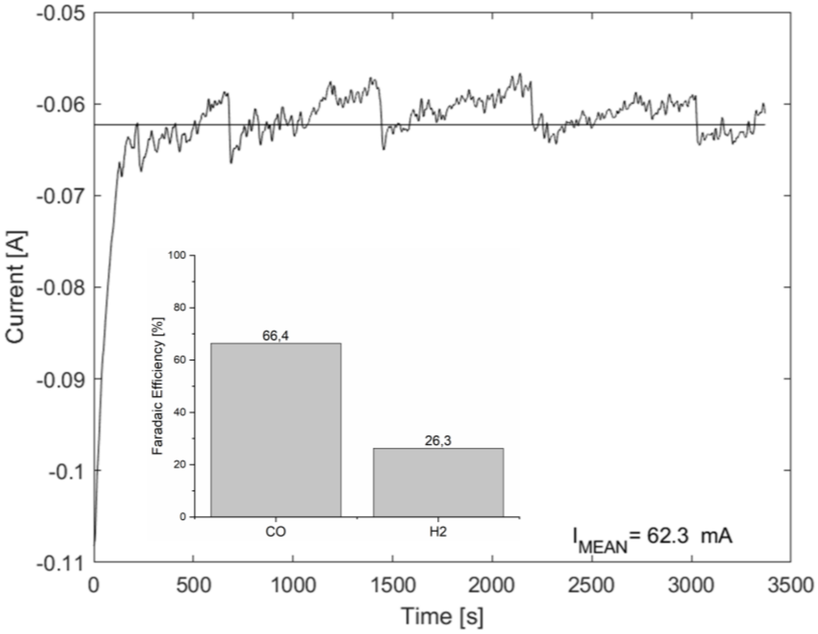

Figure 7.32: Electrochemical reduction cell test

In the graph we can see in black the resulting current over time, with an average value equal to -62.3 mA. In addition, the faradic efficiency of CO has an average value of 66.4%. Finally, the FE of hydrogen is on average equal to 26.3%. In this test the FE values obtained for CO are slightly lower than the values obtained by Zeng et Al., but in general the trend obtained reflects their work and is constant for the entire duration of the experiment. The quantity of reacted substance, in this case, turns out to be the 0.8% of the inlet CO_2.

7.2 Coupled system

After having tested the effective functioning of the reduction cell, we continued with the coupling of the latter with the capture system optimized in the previous chapter. The overall layout of the electro-capture and reduction system is shown in figure 7.3.

As can be seen from the figure, the capture system with an electrochemical cell is shown above, powered by an external energy supply. On the right are the CO_2 and N_2 cylinders that simulate the mixture of exhausted gases, which needs to be purified before being released into the environment. The concentrated CO_2 first passes into a gas-liquid phase separator to avoid damaging the following devices with any traces of liquid. Subsequently, before entering the reduction chamber, the quantity is measured through a mass flow meter. In the reduction chamber there are pumps for recirculation and the necessary potentiostat. There is a difference with respect to figure 7.1: in our coupled case, the catholyte is saturated only with the CO_2 coming from the capture system, which enters to the left of the GDL and subsequently spreads going to keep the solution saturated. In this way, the amount of CO_2 considered for the scales will be the same, i.e. the one arriving from the capture system. At the same time, the CO_2 passage channel is closed at the exit, in order to force all the CO_2 to diffuse and all the reaction products to exit with the cathodic solution, to avoid gaseous losses. Therefore, the gaseous flow in an outlet, a mixture of unreacted CO_2, CO and H_2, flows back into a phase separator before being analyzed by the gas chromatograph for the identification and quantitation of the substances present.

The capture cell, in the coupled configuration, works at 1A, with a pump speed equal to $1\ \frac{mL}{min}$ and with an input gaseous mixture composed of 50% CO_2 - equal to $20\ \frac{mL}{min}$ of carbon dioxide - and the 50% of N_2 firstly. Then, the real flue gas simulation, 16% CO_2 - equal to $20\ \frac{mL}{min}$ of carbon dioxide - and the 84% of N_2. Before starting the test, we waited for the capture cell to work stably (about 1.30 hours) and for the output to be pure CO_2.

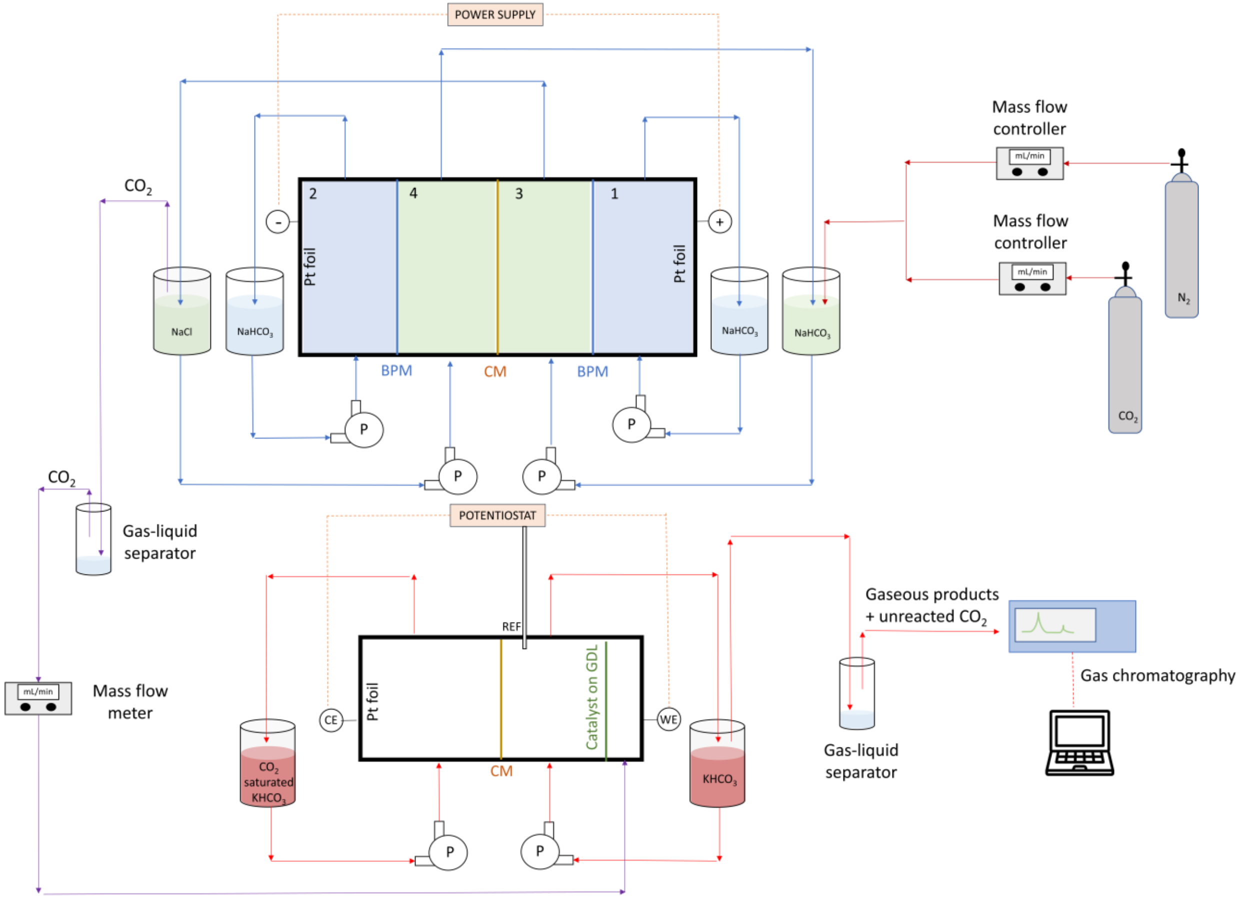

Figure 7.33: Coupled capture and reduction systems

- 50%/50% CO_2/N_2 ratio

In this case, a V_{CAT} of -1.2 V vs RHE was applied again for 90 minutes, the same time as the capture test. The CO_2 exiting the capture cell was directly fed into the reduction cell. Theoretically, the flow should have been 5.0 $\frac{mL}{min}$, as obtained above. However, due to problems related to low gas pressure, an average flow of 3.5 $\frac{mL}{min}$ was measured for the duration of the experiment. The resulting average current is equal to 47.9 mA, as shown in figure 7.4. Experimentally, FE values of 56.2% for CO and 40.9% for H_2 were obtained, with a traces of HCOOH (FE <5%). These values are different from the reference case as the incoming CO_2 flow is substantially lower (3.5 $\frac{mL}{min}$ instead of 25 $\frac{mL}{min}$) and cannot reach all the active sites made available by the catalyst for the CO production. Furthermore, also due to the low pressure, already mentioned, there is difficulty in the passage of CO_2 through the GDL. Nevertheless, the percentage of reacted substance is equal to 19%, that is higher than the value reported in the paragraph 7.1.2. This happen because in this case the inlet CO_2 flow is lower, but it is sufficient to guarantee a good number of reaction.

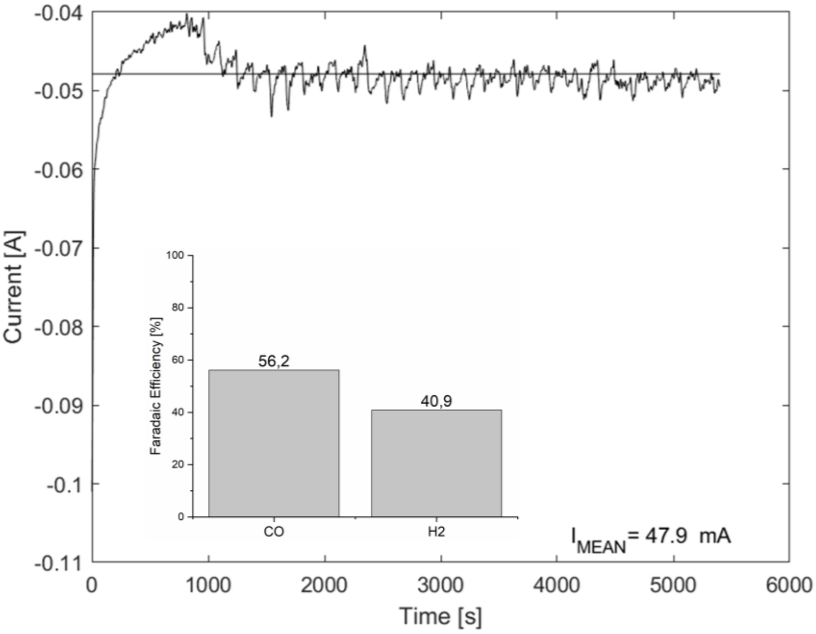

Figure 7.34: Current reduction cell of CO_2 50%/50% N_2 ratio

- 16%/84% CO_2/N_2 ratio

In this case we have simulated a flue gas. The flow captured should be 3.9 $\frac{mL}{min}$, but due to pressure problems, as in the previous case, the flow seen by the reduction system is equal to 1.6 $\frac{mL}{min}$. The voltage, like the coupling time, are the same as the previous case (1.2 V vs RHE for 90 mins). The resulting mean current is equal to 52.7 mA. We can see the current trend in the figure 7.5, that is constant for all the time, guaranteeing a constant working. The final FE for carbon monoxide and hydrogen were obtained, respectively, 36.8% and 58.9% (negligible traces of HCOOH, minor of 5%). Compared to the previous case, the effects of flow and low pressure manifest themselves in an even more consistent way, forcing the catalyst to work in a condition, far from our initial target, in which the FE of H_2 is greater than that of CO. The quantity of reacted substance is equal to 24%.

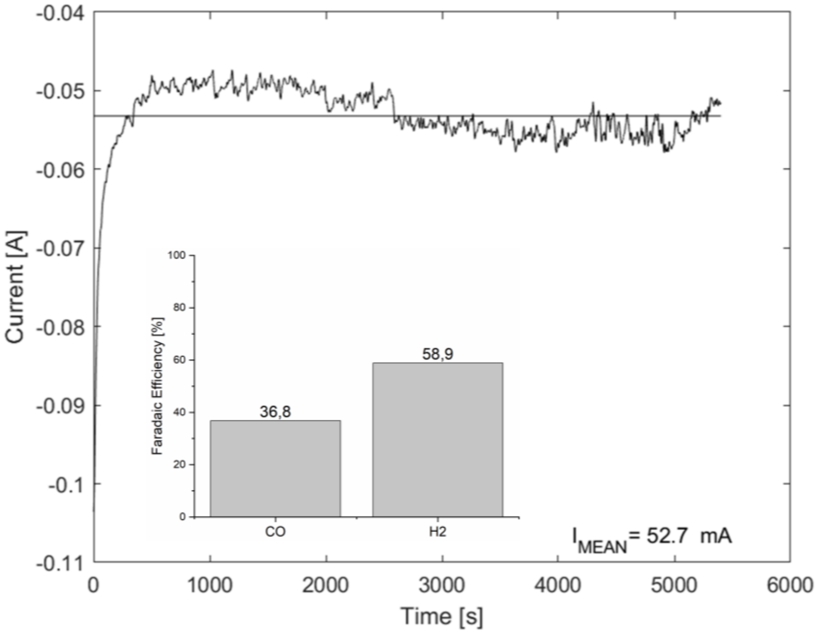

Figure 7.35: Current reduction cell of CO_2 16%/84% N_2 ratio

In conclusion, the coupling of the two solutions is working, but not yet working in an optimal way. In fact, the capture system works under its own potential, not allowing all the capturable flow to flow into the reduction chamber. In this regard, the flow of CO_2 captured in this configuration, equal to 1.6 $\frac{mL}{min}$, requires a specific energy (eq. 5.6), equal to 237.9 $\frac{MJ}{kg_{CO_2}}$, greater to be produced since the capture cell works under the same conditions described in paragraph 6.3. The production of hydrogen, on the other hand, coming from compartment 2 and being dependent on the current alone, is always equal to 430 mL in 90 minutes, equal to a flow of 4.8 $\frac{mL}{min}$. The reduction cell, in turn, does not work in optimal conditions due to the hydraulic problems described above. This means that the same energy is used to produce a greater quantity of hydrogen, at the expense of CO, than expected. For this purpose, the reduction cell working with a total average voltage V_{TOT} of 3.0 V and a current of 52.7 mA used 0.85 kJ to reduce 0.384 $\frac{mL}{min}$ of CO_2 - 24% of the input flow (eq. 7.2), which consists of 12.58 MJ per kg of CO_2 reacted. At the end of the process, at the outlet there are 6.4 $\frac{mL}{min}$ total of syngas mixture, composed of 78.3% H_2 (part from the capture cell plus part from the reduction cell), 2.2% CO (from the reduction cell) and 19.0% of CO_2 (captured and unreacted). The total is slightly lower that 100% due to traces of other chemicals, such as HCOOH. From an energy point of view, the overall system, in 90 minutes, used an amount of energy equal to 68.1 kJ, of which 98.7% for the capture phase and 1.3% for the reduction phase.

It is possible to calculate the efficiency power to fuel PtF of the reduction system if we consider the lower calorific value LHV of the CO and H_2 compounds of the mixture, which consist of the so-called 'added value':

$$\eta_{PtF}[-] = \frac{vol\ [L]\ * \rho \left[\frac{kg}{L}\right] * LHV \left[\frac{MJ}{kg}\right]}{E[MJ]} \tag{7.4}$$

Where vol is the volume of fuel - the reduction product in our case, ρ is the density (that is calculated consider to work at 0 °C and P_{atm}) and E is the energy used by the system. Substituting the values (eq. 7.4), we get a PtF efficiency of 44.4%. Always considering our final target, the production of syngas, it is possible to calculate the overall efficiency of the capture-reduction system only by considering this contribution as well: H_2 from capture cell as a usable product and the energy used as a cost. Thus, we obtain an overall efficiency value equal to 7.3% (eq. 7.4). This value is lower than that obtained previously due to the energy weight of the capture phase, but the beneficial environmental weight of CO_2 removal must also be considered.

Conclusions

After delving into the problem of global warming and analyzing the works from the scientific community, we have introduced strategies to mitigate the problem. Strategies that, from scientific evidence, can no longer be based only on the concept of reducing greenhouse gas emissions through the use of renewable sources. They must be based, for at least the current century, on the idea of mitigating emissions from fossil fuels. The latter cannot, at least instantaneously, be removed from the market for both economic and technical reasons. With this in mind, we tried to experiment with a first electrochemical coupled system for capturing and converting CO_2 into a product with added value, which can be used directly by industry. In the first instance, the thermodynamic theory was presented, through which the comparison values for the capture efficiencies from flue gas and the environment were calculated. Considering the capture of coal combustion gases from flue gas, the minimum necessary energy value is 0.155 $\frac{MJ}{kg_{CO_2}}$, leading to an energy penalty of 5%, compared to the energy produced by a power plant for each unit of CO_2 emitted. Experimentally, at the beginning, a capture system, already present in the literature and based on the principle of sodium bicarbonate electrodialysis was optimized. It is based on the concentration of only the CO_2 already included in the $NaHCO_3$ molecule and works with an energy equal to 61 $\frac{MJ}{kg_{CO_2}}$, equivalent to an efficiency of 0.254% with respect to the thermodynamic value and an energy penalty of 1442%. Subsequently, the setup was modified, verifying its continuous operation and with the introduction of a gas mixture to simulate the exhausted one to be purified. The system has been optimized again in order to have a sufficiently high and constant output flow to be able to couple this system with an electro-reduction system, for the direct reuse of the captured CO_2, in a final mixture called syngas. This capture system has been shown to work with an input mixture of 16% CO_2 and 84% N_2, with an output CO_2 flow of 3.9 $\frac{mL}{min}$. While, the N_2 was not captured and the system worked with a capture percentage - with respect to the flow introduced - of 19.4% and a capture efficiency of 25.6% - with respect to the theoretically captured quantity with the same amount of energy used. The system used 97.6 MJ per kg of CO_2 captured. Furthermore, it produces a significant amount of hydrogen - 4.8 $\frac{mL}{min}$, which flows directly into the final syngas. In general, the simulation of capture from exhaust gas worked, although it presented a deterioration compared to the capture system from sodium bicarbonate only due to the difficulty of reaction of the CO_2 - for the regeneration of $NaHCO_3$ - dissolved in a stream composed of majority of an inert substance. One solution could be to use a device for better dissolution of the exhaust gas in the solution to be regenerated. Furthermore, it might be interesting to test the system by working with $NaHCO_3$ in all compartments, to facilitate mixing and streamline the process. It is obviously necessary to reduce the energy used for this phase in order to both increase efficiency and be able to power the system with a renewable source. The energy penalty must also be lowered, otherwise it is illogical to use a capture system that consumes more energy than that produced by the plant that emits CO_2. To achieve this goal, it may be interesting to try to eliminate as much as possible the losses of this system, such as those due to the presence of liquid solutions, parasitic current losses, the mixing of solutions and the potential drop on the membranes. Subsequently, if the aim is only to capture the CO_2 and not to produce hydrogen, a system will have to be studied that can work with only two chambers and with a lower reaction potential. Finally, the fluid-dynamic seal of the system must also be improved, avoiding fluid leaks between the chambers of the flow cell used and trying to have as little head loss as possible, trying to raise the working pressure of the system.

When coupled with the reduction cell, the capture system provides a CO_2 inlet flow of 1.6 $\frac{mL}{min}$, leading to FE of 36.8% and 58.9% for CO and H_2, respectively, and reaction rate of 24%. The coupling proved to work, despite with lower performance with respect to the functioning of the reduction system alone (FE of 66% for CO and 26% for H_2 in the test under optimal conditions - 25 $\frac{mL}{min}$ of CO_2 in the inlet, with a reacted percentage equal to

0.8%). For this reason, some aspects of the cell itself need to be studied further. In fact, the faradic efficiency of carbon monoxide drops if the incoming amount of CO_2 lowers. This behavior, however, is not due to the lack of CO_2, which is present in sufficient quantity, but is due to the fact that it is unable to reach the reaction sites of the catalyst. An improvement of the diffusion system, through obligatory routes for inlet gas, could improve the capillarity. At the same time, as mentioned for the capture system, an increase in inlet flow pressure could help diffusion. In this regard, the reduction system forms a bottleneck on the coupled system: the coupling of the two systems ensures that the amount of CO_2 captured is less than the value obtained in the separate tests. This is due to a pressure problem, which at the outlet of the capture cell is too low so the flow is hindered by the reduction cell which acts as a cap. The resolution of this problem would also allow the reduction cell to work with a higher flow resulting in a better faradic efficiency. To solve the problem it may be interesting, as already mentioned, to work under pressure in the capture cell or to slightly compress the flow at the inlet of the reduction cell. Furthermore, since in many contexts CO_2 is not necessary in the final syngas, the goal is also to increase the number of reactions in the reduction cell, trying to use all the incoming CO_2. This can be possible either by increasing the performance of the catalyst, by increasing the active sites, or by increasing the area of the same and therefore the size of the cell.

In the final syngas, whose flux is equal to 6.4 $\frac{mL}{min}$, there is 78.3% of H_2, 2.2% of CO and 19% of CO_2. It is usable, but it is desirable to increase the amount of CO in the ways described above. From an energy point of view, the reduction system has a sufficient efficiency, equal to 44.4%, in the production of syngas. In this case, it is the capture system that appears to function as the bottleneck of the system as the overall efficiency of the system is only 7.3% due to the energy expended in the capture phase. It is therefore necessary to reduce the energy expenditure of the capture phase simultaneously with the increase in reduction reactions and fluid dynamics improvement, to obtain a syngas mixture with a lower H_2/CO ratio and with a better energy - and therefore economic - cost.

Ringraziamenti

Comunque, nel 2017, al primo anno, sono stato bocciato di Analisi 1, Chimica e due volte di Fisica 1. Quindi consegnare questa tesi – ovviamente l'ultimo giorno disponibile - è sicuramente già un traguardo. A tal proposito, desidero ringraziare il Prof. Pirri per l'opportunità concessami nello svolgere il mio lavoro di tesi presso dell'Istituto Italiano di Tecnologia di Torino, ambiente dinamico, multiculturale e all'avanguardia. Grazie al Prof. Santarelli, ad Alessio, a Nicolò, a Stefania, a tutti i collaboratori del centro, dove ho passato gli ultimi sei mesi, e, soprattutto, ad Adriano. Grazie per avermi seguito nel lavoro di tesi, di avermi aiutato nella sua stesura e di avermi accompagnato in questo ultimo capitolo del viaggio universitario. Ovviamente non siamo stati sempre così seri, quindi grazie anche per le imprecazioni, per le risate e per i litri di bicarbonato utilizzati. Non posso ovviamente non ringraziare papà Piero, mamma Sandra e tutta la mia famiglia, che mi hanno permesso di passare questi anni con tranquillità, sostenendomi e in tutto il percorso. Senza di voi questo non sarebbe sicuramente stato possibile. Grazie, in particolare, alla mia ragazza Erica, che mi ha supportato e che ha soprattutto sopportato tutti i miei scleri, le mie ansie, i miei pacchi all'ultimo ('fold' per gli amici) e i giorni passati a studiare. Grazie perché credi più te in me di quanto lo faccia io.

Come chi leggerà questi ringraziamenti ben sa, quando c'è da esagerare non mi tiro mai indietro. Quindi passiamo a ringraziare chi esagera con me. Grazie a Jacopo e Mattia, per esserci ogni giorno e per qualsiasi cosa. Festeggeremo sicuramente una mattina insieme dove piace a noi, ai Roc. Grazie a tutti i miei amici, ormai abituati ai miei fold per lo studio, per aver passato con me questi lunghi anni in cui assolutamente non abbiamo mangiato, bevuto, cantato 'Madonnina dai Riccioli d'Oro', degradato, insultato Strava, bucato gomme, insultato Strava, degradato, suonato la vuvuzela, imprecato perché a Gallipoli non c'erano i nomi delle vie, degradato e insultato Strava. Grazie per tutto questo, ma grazie soprattutto perché continueremo a partire da domani. Non vi ringrazio singolarmente perché moschini come siete va ancora a finire che se poi mi dimentico mi insultate. Ringrazio solo Strava, visto che l'ho nominato, per averci permesso di insultarlo ed essere un vero amico dal primo anno di superiori. Last but not least, come ama dire un nostro prof, grazie ai miei colleghi universitari per aver condiviso insieme questo viaggio ogni giorno, tra un prof e l'altro, tra una partita a carte e l'altra e tra un panino e l'altro.

Insomma, grazie un po' a tutti per aver condiviso con me questi anni! Ah, sempre Forza Toro!

Bibliography

1. Climate change, Wikipedia. Available online: https://en.wikipedia.org/wiki/Climate_change (accessed on 10/09/2021).
2. Manabe, S., Role of greenhouse gas in climate change**. *Tellus A: Dynamic Meteorology and Oceanography* **2019,** *71*, 1620078.
3. Lashof, D. A.; Ahuja, D. R., Relative contributions of greenhouse gas emissions to global warming. *Nature* **1990,** *344*, 529-531.
4. Climate Change 2013: Anthropogenic and natural radiative forcing, IPCC. Available online: https://www.ipcc.ch/report/ar5/wg1/ (accessed on 10/09/2021).
5. Global Climate Change Indicators, NCDC. Available online: https://www.ncdc.noaa.gov/monitoring-references/faq/indicators.php#warming-climate (accessed on 10/09/2021).
6. Carbon dioxide, Wikipedia. Available online: https://en.wikipedia.org/wiki/Carbon_dioxide (accessed on 10/09/2021).
7. Carbon dioxide in Earth's atmosphere, Wikipedia. Available online: https://en.wikipedia.org/wiki/Carbon_dioxide_in_Earth%27s_atmosphere (accessed on 10/09/2021).
8. Ballantyne, A. P.; Alden, C. B.; Miller, J. B.; Tans, P. P.; White, J. W. C., Increase in observed net carbon dioxide uptake by land and oceans during the past 50 years. *Nature* **2012,** *488*, 70-72.
9. CO2 emissions, Our World in Data. Available online: https://ourworldindata.org/co2-emissions#citation (accessed on 10/09/2021).
10. Davis, S. J.; Caldeira, K., Consumption-based accounting of CO2 emissions. *Proc Natl Acad Sci U S A* **2010,** *107*, 5687-5692.
11. The role of CCUS in low-carbon power systems, IEA. Available online: https://www.iea.org/reports/the-role-of-ccus-in-low-carbon-power-systems (accessed on 10/09/2021).
12. The Intergovernmental Panel on Climate Change, IPCC. Available online: https://www.ipcc.ch/ (accessed on 10/09/2021).
13. Representative Concentration Pathway, Wikipedia. Available online: https://en.wikipedia.org/wiki/Representative_Concentration_Pathway (accessed on 10/09/2021).
14. Scenari internazionali di emissione e assorbimenti di gas serra congruenti con l'Accordo di Parigi, ISPRA. Available online: https://www.isprambiente.gov.it/it/archivio/eventi/2018/05/gas-serra-inventario-emissioni (accessed on 10/09/2021).
15. Kyoto Protocol, Wikipedia. Available online: https://en.wikipedia.org/wiki/Kyoto_Protocol (accessed on 10/09/2021).
16. Paris Agreement, European Commission. Available online: https://ec.europa.eu/clima/policies/international/negotiations/paris (accessed on 10/09/2021).

17. 2030 climate & energy framework, European Commission. Available online: https://ec.europa.eu/clima/policies/strategies/2030_en (accessed on 10/09/2021).
18. Fuss, S.; Canadell, J. G.; Peters, G. P.; Tavoni, M.; Andrew, R. M.; Ciais, P.; Jackson, R. B.; Jones, C. D.; Kraxner, F.; Nakicenovic, N.; Le Quéré, C.; Raupach, M. R.; Sharifi, A.; Smith, P.; Yamagata, Y., Betting on negative emissions. *Nature Climate Change* **2014,** *4*, 850-853.
19. Tipping points in the climate system, Wikipedia. Available online: https://en.wikipedia.org/wiki/Tipping_points_in_the_climate_system (accessed on 10/09/2021).
20. Davis, S. J.; Socolow, R. H., Commitment accounting of CO 2 emissions. *Environmental Research Letters* **2014,** *9*, 084018.
21. Erickson, P.; Kartha, S.; Lazarus, M.; Tempest, K., Assessing carbon lock-in. *Environmental Research Letters* **2015,** *10*, 084023.
22. Energy Technology Perspectives 2020, IEA. Available online: https://www.iea.org/reports/energy-technology-perspectives-2020 (accessed on 10/09/2021).
23. Multiple Benefits of Energy Efficiency: Emissions savings, IEA. Available online: https://www.iea.org/reports/multiple-benefits-of-energy-efficiency/emissions-savings (accessed on 11/09/2021).
24. Amponsah, N. Y.; Troldborg, M.; Kington, B.; Aalders, I.; Hough, R. L., Greenhouse gas emissions from renewable energy sources: A review of lifecycle considerations. *Renewable and Sustainable Energy Reviews* **2014,** *39*, 461-475.
25. Climate change: using EU forests to offset carbon emissions, European Parliament. Available online: https://www.europarl.europa.eu/news/en/headlines/society/20170711STO79506/climate-change-using-eu-forests-to-offset-carbon-emissions (accessed on 10/09/2021).
26. Zhang, S.; Liu, L.; Zhang, L.; Zhuang, Y.; Du, J., An optimization model for carbon capture utilization and storage supply chain: A case study in Northeastern China. *Applied Energy* **2018,** *231*, 194-206.
27. CO_2 Mollier Chart, Chemicalogic. Available online: http://www.chemicalogic.com/Documents/co2_mollier_chart_met.pdf (accessed on 10/09/2021).
28. Zhang, Z. X.; Wang, G. X.; Massarotto, P.; Rudolph, V., Optimization of pipeline transport for CO2 sequestration. *Energy Conversion and Management* **2006,** *47*, 702-715.
29. Carbon capture and storage: Geological storage, Wikipedia. Available online: https://en.wikipedia.org/wiki/Carbon_capture_and_storage#Geological_storage (accessed on 10/09/2021).
30. Institute, E. *Good plant design and operation for onshore carbon capture installations and onshore pipelines*; 01 Sep 2010.
31. Sacco, A.; Speranza, R.; Savino, U.; Zeng, J.; Farkhondehfal, M. A.; Lamberti, A.; Chiodoni, A.; Pirri, C. F., An Integrated Device for the Solar-Driven Electrochemical Conversion of CO2 to CO. *ACS Sustainable Chemistry & Engineering* **2020,** *8*, 7563-7568.

32. Dye-sensitized solar cell, Wikipedia. Available online: https://en.wikipedia.org/wiki/Dye-sensitized_solar_cell (accessed on 11/09/2021).
33. Fiore, M.; Magi, V.; Viggiano, A., Internal combustion engines powered by syngas: A review. *Applied Energy* **2020,** *276*, 115415.
34. Selvatico, D.; Lanzini, A.; Santarelli, M., Low Temperature Fischer-Tropsch fuels from syngas: Kinetic modeling and process simulation of different plant configurations. *Fuel* **2016,** *186*, 544-560.
35. Sun, X.; Atiyeh, H. K.; Huhnke, R. L.; Tanner, R. S., Syngas fermentation process development for production of biofuels and chemicals: A review. *Bioresource Technology Reports* **2019,** *7*, 100279.
36. Brunner, D.; Kuhlmann, G.; Marshall, J.; Clément, V.; Fuhrer, O.; Broquet, G.; Löscher, A.; Meijer, Y., Accounting for the vertical distribution of emissions in atmospheric CO2 simulations. *Atmos. Chem. Phys.* **2019,** *19*, 4541-4559.
37. Bains, P.; Psarras, P.; Wilcox, J., CO2 capture from the industry sector. *Progress in Energy and Combustion Science* **2017,** *63*, 146-172.
38. Wilcox, J.; Psarras, P. C.; Liguori, S., Assessment of reasonable opportunities for direct air capture. *Environmental Research Letters* **2017,** *12*, 065001.
39. House, K. Z.; Baclig, A. C.; Ranjan, M.; van Nierop, E. A.; Wilcox, J.; Herzog, H. J., Economic and energetic analysis of capturing CO<sub>2</sub> from ambient air. *Proceedings of the National Academy of Sciences* **2011,** *108*, 20428.
40. Nagasawa, H.; Yamasaki, A.; Iizuka, A.; Kumagai, K.; Yanagisawa, Y., A new recovery process of carbon dioxide from alkaline carbonate solution via electrodialysis. *AIChE Journal* **2009,** *55*, 3286-3293.
41. Electrolysis of water, Wikipedia. Available online: https://en.wikipedia.org/wiki/Electrolysis_of_water (accessed on 01/10/2021).
42. Electrochemical and Thermodynamic Fundamentals. In *Membrane Science and Technology*, Strathmann, H., Ed. Elsevier: 2004; Vol. 9, pp 23-88.
43. Solubilità dei gas nei liquidi: Legge di Henry. Available online: https://www.chimica1956.it/generale/luc_71.htm (accessed on 01/10/2021).
44. Marshall, A.; Børresen, B.; Hagen, G.; Tsypkin, M.; Tunold, R., Hydrogen production by advanced proton exchange membrane (PEM) water electrolysers—Reduced energy consumption by improved electrocatalysis. *Energy* **2007,** *32*, 431-436.
45. Zeng, J.; Rino, T.; Bejtka, K.; Castellino, M.; Sacco, A.; Farkhondehfal, M. A.; Chiodoni, A.; Drago, F.; Pirri, C. F., Coupled Copper–Zinc Catalysts for Electrochemical Reduction of Carbon Dioxide. *ChemSusChem* **2020,** *13*, 4128-4139.
46. Sacco, A.; Zeng, J.; Bejtka, K.; Chiodoni, A., Modeling of gas bubble-induced mass transport in the electrochemical reduction of carbon dioxide on nanostructured electrodes. *Journal of Catalysis* **2019,** *372*, 39-48.
47. Malkhandi, S.; Yeo, B. S., Electrochemical conversion of carbon dioxide to high value chemicals using gas-diffusion electrodes. *Current Opinion in Chemical Engineering* **2019,** *26*, 112-121.

48. Burdyny, T.; Smith, W. A., CO2 reduction on gas-diffusion electrodes and why catalytic performance must be assessed at commercially-relevant conditions. *Energy & Environmental Science* **2019,** *12*, 1442-1453.
49. Sacco, A., Electrochemical impedance spectroscopy as a tool to investigate the electroreduction of carbon dioxide: A short review. *Journal of CO2 Utilization* **2018,** *27*, 22-31.
50. Reversible hydrogen electrode, Wikipedia. Available online: https://en.wikipedia.org/wiki/Reversible_hydrogen_electrode (accessed on 02/10/2021).